Roles of the Hippo pathway kinase Ndr2 in neural development and behavior

Thesis submitted to the Faculty of Natural Sciences
of Otto von Guericke University Magdeburg for the degree of

doctor rerum naturalium (Dr. rer. nat.)

Submitted on	January 28, 2019
Defended on	July 25, 2019
by	M.Sc. Deniz Ashan Madencioglu Kul

Supervisor	Prof. Dr. Oliver Stork
Reviewer	Prof. Dr. Gernot Riedel

DDC: 574.8

Abstract

Roles of the Hippo pathway kinase Ndr2 in neural development and behavior

M.Sc. Deniz Ashan Madencioglu Kul

The NDR (nuclear Dbf2-related) family members are highly conserved serine/threonine protein kinases, which function in many cellular processes extending from cytokinesis to neurite outgrowth. Over the last two decades, the significance of NDR kinases in neuronal cells from different species has been demonstrated. In humans, it has been observed that *NDR2*, one of four NDR kinases expressed in mammals, resides in a hot spot in the genome that is susceptible to deletions or duplications, resulting in several patients with phenotypes related to intellectual disabilities. Together with this, the important role of these kinases in dendritic and axonal branching led to the questioning of the function of Ndr2 *in vivo* and the impact on neuronal morphology and behavior. To answer these questions, several genetic mouse models were generated by either knocking-out or overexpressing Ndr2. Germline Ndr2-knockout mice displayed hippocampal morphological differences in the CA3 pyramidal neurons by displaying shorter first order apical dendrites. Behavioral tests revealed a disruption in the innate-fear response, yet no impairment in hippocampus-dependent behavior was eminent. Moreover, two different brain specific Ndr2-conditional knockout mouse lines went through behavioral phenotyping. The Ndr2-conditional knockout mouse generated with Emx1-Cre, displayed a slight anxiety-like behavior whereas the mice generated with CamKII-alpha-Cre, besides exhibiting an anxiety-like behavior, showed impairment in remote memory. Two transgenic mouse lines overexpressing Ndr2 in the same cell populations as the conditional knockout lines were also behaviorally tested. The transgenic mouse line overexpressing Ndr2 dependent on Emx1-Cre did not present an altered phenotype, yet the transgenic mice generated with CamKII-alpha-Cre exhibited a learning impairment and high exploratory behavior accompanied by mossy fiber terminal reduction in the ventral hippocampus. In summary, depending on the cell type and the timing of the expression during development, Ndr2 kinase plays an important role in neuronal branching and outgrowth *in vivo* and behavior.

Zusammenfassung

Die Rolle der Hippo-Pathway-Kinase Ndr2 in der neuronalen Entwicklung und im Verhalten

M.Sc. Deniz Ashan Madencioglu Kul

Bei den Mitgliedern der NDR-Familie (nuclear Dbf2-related Familie) handelt es sich um hochkonservierte Serin / Threonin-Protein-Kinasen, die in vielen zellulären Prozessen von der Zytokinese bis zum Auswachsen von Neuriten eine Rolle spielen. In den letzten zwei Jahrzehnten wurde die Bedeutung von NDR-Kinasen in neuronalen Zellen verschiedener Spezien gezeigt. Beim Menschen wurde beobachtet, dass sich NDR2, eine von vier NDR-Kinasen, die in Säugetieren exprimiert werden, an einem Hotspot im Genom befindet, der anfällig für Deletionen oder Duplikationen ist. In diesem Zusammenhang wurde bei Patienten Intelligenzminderungen beobachtet. Darüberhinaus sind diese Kinasen bei der dendritischen und axonalen Verzweigung von großer Bedeutung. Diese beiden Tatsachen gaben Anstoß zur Untersuchung der Funktion von NDR2 in der neuronalen Morphologie und im Verhalten. Um diese Fragen zu beantworten, wurden mehrere genetische Mausmodelle erzeugt, indem entweder NDR2 ausgeschaltet oder überexprimiert wurde. Keimbahn-Ndr2-Knockout-Mäuse wiesen morphologische Unterschiede im Hippokampus, in den CA3-Pyramidenzellen auf, sie hatten kürzere apikale Dendriten erster Ordnung. Verhaltenstests ergaben eine Störung der unkonditionierten Angstreaktion, jedoch war keine vom Hippokampus abhängige Beeinträchtigung des Verhaltens zu beobachten. Zwei verschiedene hirnspezifische Ndr2-bedingte Knockout-Mauslinien wurden einer Verhaltensphänotypisierung unterzogen. Der mit Emx1-Cre erzeugte Ndr2 Knockout resultierte in leicht ängstlichem Verhalten, während die mit CamKII-alpha-Cre erzeugten Knock-out Mäuse neben einem angstähnlichen Verhalten auch eine Beeinträchtigung des Remotegedächtnisses zeigten. Bei zwei transgenen Mauslinien, die Ndr2 in denselben Zellpopulationen wie die konditionalen Knockout-Linien überexprimieren, wurden ebenfalls Verhaltenstests durchgeführt. Die transgene Mauslinie, die Ndr2 in Abhängigkeit von Emx1-Cre überexprimierte, wies keine Beeinträchtigungen auf, jedoch zeigten die mit CamKII-alpha-Cre erzeugten transgenen Mäuse eine Lernbeeinträchtigung und ein hohes Explorationsverhalten, das von einer Reduktion der Mossy-Faserendigungen im ventralen Hippokampus begleitet wurde. Zusammenfassend kann gesagt werden, dass die Ndr2-Kinase in Abhängigkeit von Zelltyp und Zeitpunkt der Expression während der Entwicklung eine Rolle bei der neuronalen Verzweigung sowie beim Auswachsen in vivo, und beim Verhalten spielt.

Table of Contents

List of figures

List of tables

Abbreviations

(c)KO	(conditional) Knockout
°C	Degree Celsius
AA	Active avoidance
AAK1	AP-2 associated kinase-1
AEBSF	4-(2-aminoethyl)benzenesulfonyl fluoride hydrochloride
AGC	Protein kinase A (PKA)/PKG/PKC-like
AIS	Auto-inhibitory sequence
ANOVA	Analysis of variance
AS	Activation segment
ASD	Autism spectrum disorder
ASR	Acoustic startle response
B.P.	Behavioral paradigm
BLA	Basolateral amygdala
CA	*Cornu Ammonis*
camKII	Ca^{2+}/calmodulin-dependent protein kinase II
CEA	Central nucleus of amygdala
cm	Centimeter
CNS	Central nervous system
CNV	Copy number variation
CP	Caudoputamen
CRF	Corticotropin releasing factor
CS	Conditioned stimulus
dB	Decibel
DCO	Dorsal cochlear nucleus
DG	Dentate gyrus
DNA	Deoxyribonucleic acid
dNTP	Deoxynucleotide Triphosphate
E	East
ECM	Extracellular matrix
EDTA	Ethylenediaminetetraacetic acid
EGFP	Enhanced green fluorescent protein
Egr1	Early growth response protein 1

emx	Empty spiracles homeobox
EPM	Elevated plus maze
ERK	Extracellular signal-regulated kinase
ES	Embryonic stem
EtBr	Ethidium bromide
FAK	Focal adhesion kinase
FC	Fear conditioning
GABA(R)	gamma-aminobutyric acid (receptor)
h	Hour
HCA	Home cage activity
HD	Huntington's disease
HET	Heterozygous
HFS	High frequency stimulation
HM	Hydrophobic motif
HTT	Huntingtin
IIP	Infra/intrapyramidal
IP	Interposed nucleus
IPN	Interpeduncular nucleus
ISI	Inter-stimulus interval
ITI	Inter-trial interval
kHz	Kilohertz
L	Liter
L/D	Light/dark transition
LA	Lateral amygdala
Lats	Large tumor suppressor
LSD	Least Significant Difference
LTP	Long-term potentiation
µl	Microliter
mA	Milliampere
MA3	Medial accessory oculomotor nucleus
Mc	Magnocellular nucleus
MEK(MAP2K)	Mitogen-activated kinase kinase
MF	Mossy fiber
min	Minute

MOB	Mps-One Binder
mRt	Mesencephalic reticular form
ms	Millisecond
MST	Mammalian Ste20-like
MTN	Midline thalamic nuclei
N	North
NDR	Nuclear Dbf2-related
NF2	Neurofibromatosis type 2
NGF	Nerve growth factor
NOR	Novel object recognition
NTR	N-terminal regulatory domain
OF	Open field
PAG	Periaqueductal grey
PCR	Polymerase chain reaction
RGD	Arginylglycylaspartic acid
PKCδ	Protein kinase C delta
polyQ	Polyglutamine
PP2A	Protein phosphatase 2
PPI	Pre-pulse inhibition
PVDF	Polyvinylidene difluoride
RASSF	Ras-associated domain family
RN	Red nucleus
s	Second
S	South
S.E.M.	Standard error of the mean
SAX1	Sensory guidance
SDS-PAGE	Sodium dodecyl sulfate polyacrylamide gel electrophoresis
SI	Social interaction
SMA	S100/hMOB1 association domain
SNP	Single nucleotide polymorphism
SNR	Substantia nigra
SP	Suprapyramidal
STK38(L)	Serine/threonine kinase 38 (like)
SWR	Sharp wave ripples

TAZ	Transcriptional coactivator with PDZ-binding domain
TEAD	TEA domain proteins
TG	Transgenic
TOR	Target of rapamycin
Trc	Tricornered
TTX	Tetrodotoxin
vlPAG	Ventrolateral PAG
W	West
WCM	Water cross maze
WT	Wild type
YAP	Yes-associated protein
Zif268	Zinc finger protein

1 Introduction

NDR (nuclear Dbf2-related) kinases are a subclass of AGC (protein kinase A (PKA)/PKG/PKC-like) group of protein kinases, which are evolutionarily conserved, expressed from plants to humans. In *Drosophila melanogaster* NDR kinase members can be found as tricornered (Trc) and large tumor suppressor (Lats)/Warts, in *Caenorhabditis elegans* as sensory guidance-1 (SAX-1) and LATS, in *Saccharomyces pombe* as Sid2p and Orb6p. The human genome on the other hand encodes for four kinases; NDR1 (also known as serine/threonine kinase 38 or STK38), NDR2 (serine/threonine kinase 38 like or STK38L), LATS1, and LATS2. In non-neuronal cells NDR kinases have been described for their roles in cell proliferation and survival including promotion of cell cycle exit and apoptosis to control organ size (Pan 2010; Halder and Johnson 2011) that is regulated through the Hippo pathway. In addition, NDR kinases are also involved in cellular processes such as chromosome alignment (Chiba et al. 2009), centrosome duplication (Toji et al. 2004; Hergovich et al. 2007), cell polarity control (Verde, Wiley, and Nurse 1998; Geng et al. 2000; Hirata et al. 2002), cytoskeletal organization (Fang and Adler 2010), and autophagy (Joffre et al. 2015). In neuronal cells the functions of NDR kinases have been shown to include neurite growth and differentiation and will further be discussed in detail

1.1 NDR kinases

1.1.1 Structure of NDR kinases

The NDR kinases (Fig. 1.1, depicting Ndr2) are classified based on the sequence of the catalytic domain consisting of 12 subdomains (Millward, Cron, and Hemmings 1995) which are conserved from yeast to human. As being a subclass of the AGC kinases, NDR kinases contain an activation segment (AS) and a hydrophobic-motif (HM) regulatory-phosphorylation site. The hydrophobic motif is located at the C-terminus and contains a phosphorylation site important for the kinase activity. The activation segment resides at the subdomain VIII, which also has a phosphorylation site (Stegert et al. 2004). These kinases also contain two domains that are unique to the NDR kinases; the conserved N-terminal regulatory (NTR) domain and a 30-60 amino acid insert between subdomains VII and VIII (referred as the auto-inhibitory sequence (AIS)). The NTR domain, also known as the S100/hMOB1 association domain (SMA), is composed of a significant number of conserved basic hydrophobic residues that mediate the interaction between NDR kinases and MOB molecules (Bichsel et al. 2004). The

AIS is located near the C-terminal end of the kinase and is rich in basic amino acid residues creating a positively charged cluster, thus negatively regulating the NDR kinase activity.

Figure 1.1: Structure of NDR2 kinase in Homo sapiens.
The green spheres depict the key regulatory phosphorylation sites. The subdomain VIII contains the activation segment (AS) including the phosphorylation site Serine 282 (S282) that is shown in green. The catalytic subdomains that remain are in orange. The N-terminal regulatory domain (NTR) is shown in blue including the phosphorylation site Threonine 75 (T75). Subdomains VII and VIII are separated with an insert containing a putative auto-inhibitory sequence (AIS) shown in red. The hydrophobic motif (HM) is located at the C-terminal of the kinase harboring the phosphorylation site Threonine 442 (T442) that is shown in purple.

1.1.2 Regulation of NDR kinases and their role in Hippo pathway

NDR kinases are activated through the phosphorylation of Serine and Threonine residues on the activation segment (S282 for Ndr2) and hydrophobic motif (T442 for Ndr2) respectively. The phosphorylation of the residue on the NTR (T75 for Ndr2) is also required for the full kinase activity (Tamaskovic et al. 2003; Stegert et al. 2004). The Threonine residue on the hydrophobic motif is directly phosphorylated by upstream kinases such as mammalian Ste20-like (MST) kinases (MST1, MST2, and MST3) (Wu et al. 2003) and has been also suggested to be phosphorylated by the target of rapamycin (TOR) kinase (Koike-Kumagai et al. 2009). The Serine residue on the activation segment is auto-phosphorylated, supported by the phosphorylation of the threonine on the NTR domain through the binding of MOB1 (Mps-One Binder) (Tamaskovic et al. 2003; Stegert et al. 2004).

The Hippo pathway was initially discovered as a regulator of tissue growth and homeostasis (reviewed in: F.-X. Yu and Guan 2013; Fa-Xing Yu, Zhao, and Guan 2015) consisting of serine/threonine protein kinases MST1/2/3, LATS1/2, NDR1/2, adaptor proteins SAV1 and MOB1 as signal transducers, and transcriptional co-activators YAP (Yes-associated protein) and TAZ (transcriptional coactivator with PDZ-binding motif). When the Hippo pathway (Fig. 1.2) is turned on, MST1/2 is phosphorylated and form a complex with SAV1, which phosphorylates and activates the LATS1/2-MOB1 complex. This activated complex then phosphorylates YAP/TAZ resulting in either degradation or cytoplasmic retention leading to reduced nuclear YAP/TAZ levels and down regulation of the downstream targets of this pathway. During the off-state of the Hippo signaling pathway, unphosphorylated YAP/TAZ translocate to the nucleus and form a complex with TEA domain proteins 1-4 (TEAD1-4)

promoting gene expression involved in cell survival, proliferation, and migration (Bae and Luo 2018).

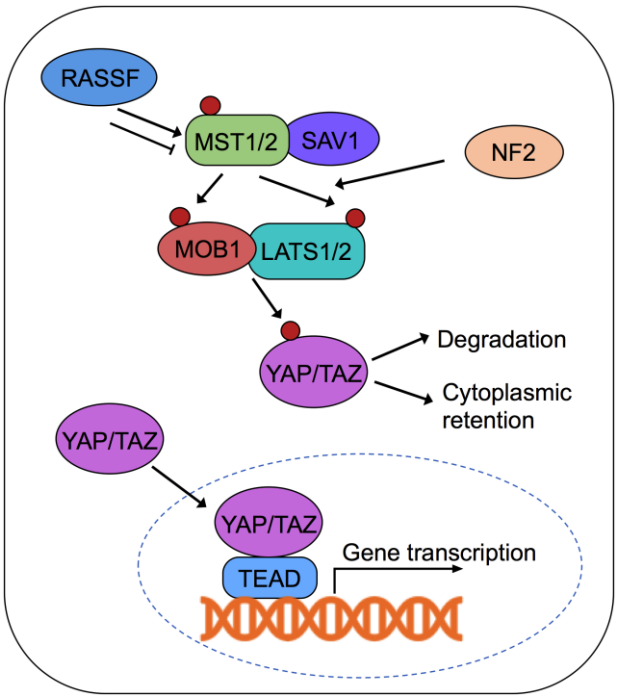

Figure 1.2: Mammalian Hippo pathway summary.
When the Hippo pathway is in the active state, MST1/2 is phosphorylated and forms a complex with SAV1. The complex phosphorylates and activates the LATS1/2-MOB1 complex. The activation of this complex phosphorylates YAP/TAZ, which results in degradation or cytoplasmic retention. If the pathway is in the inactive state, unphosphorylated YAP/TAZ translocate to the nucleus forming a complex with TEAD promoting gene transcription. Red spheres indicate phosphorylation. (Figure modified from Bae and Luo 2018)

The Hippo signaling pathway has been extensively shown to be activated through a number of intrinsic and extrinsic signals including stress signals, stiffness of the extracellular matrix (ECM), cell-cell contact, and cell polarity, modulating the phosphorylation of the MST and LATS kinases. For example, in mammals, the Neurofibromatosis type 2 (NF2) protein activates the pathway by directly binding to LATS and recruiting it to the plasma membrane where it is phosphorylated by the MST-SAV1 complex (Yin et al. 2013). Albeit the function of Ras-association domain family (RASSF) in Hippo pathway is still undergoing investigation, it has been shown that RASSF might be regulating the pathway both negatively and positively. RASSFs may negatively regulate the pathway by forming heterodimers with the MST kinases therefore inhibiting the activation or may positively regulate the pathway when co-expressed with Ras enhancing the MST1 kinase activity (Praskova et al. 2004). On the other hand, RASSF1A prevents MST1/2 dephosphorylation by protein phosphatase 2 (PP2A), promoting its phosphorylation and activation (Guo, Zhang, and Pfeifer 2011).

1.1.3 Functions of Ndr2 in neuronal cells

The importance of NDR kinases in neuronal cells in different species has been under investigation over the last two decades. In *Drosophila melanogaster* the NDR family kinase Trc (tricornered) has been shown to regulate dendritic tiling and branching (Emoto et al. 2004). Dendritic tiling is when dendrites of functionally homologous neurons cover receptive fields without dendritic overlap. These dendritic field patterns are crucial for the correct wiring of neural circuits. Trc-null mutants exhibited an over-branching phenotype. In class IV neurons, which has been shown to display dendritic tiling (Grueber, Jan, and Jan 2002; Sugimura et al. 2003), overlapping of dendritic branches resulted in an impaired dendritic tiling phenotype. Similarly, in *Ceanorhabditis elegans* SAX-1 and SAX-2 (regulator of SAX-1) has also been shown to regulate mechanosensory neurite tiling by controlling the neurite outgrowth (Gallegos and Bargmann 2004).

In canine, a mutation in the Ndr2 gene has been shown to cause retinal degeneration (Goldstein et al. 2010). Follow up studies of Ndr2 on retinal degeneration in canine further suggested that it controls cell division and morphogenesis in photoreceptors (Berta et al. 2011) and in mice Ndr2, and also Ndr1, play a role in cell proliferation and apoptosis, rod opsin mislocalization, and gene expression that is regulating retinal homeostasis (Léger et al. 2018).

In the mouse, it has been previously shown that Ndr2 mRNA expression increases in the amygdala six hours after fear-memory consolidation and is back at base line after 24 hours (Stork et al. 2004). In the same study, further investigation has demonstrated that Ndr2 co-localizes with actin filaments at growth cones in PC12 cells and in cultured cortical neurons at dendrites, spines, and outgrowing axons. The function of Ndr1/2 on neuronal branching and spine formation was shown in cultured rat hippocampal neurons as well as *in vivo* in mouse cortical neurons, in line with Trc-mutant *D. melanogaster*, to be a limiting factor in dendritic growth and is required for spine maturation (Ultanir et al. 2012). Moreover, AAK1 (AP-2 associated kinase-1) was identified as a regulator of dendritic branching and Rabin8 (Rab8 guanine nucleotide exchange factor) regulating the formation of mature dendritic spines, which are substrates of NDR1 and are phosphorylated by it.

Similarly, in cultured mouse hippocampal neurons, it has been indicated that through β1-integrin activation and its trafficking to the dendritic surface, Ndr2 controls dendritic and axonal growth (Rehberg et al. 2014). The phosphorylation of the cytoplasmic domain of β1-integrins

was shown to be indirectly through Ndr2. The involvement of β1-integrin activation through Ndr2 in outgrowing dendrites was demonstrated by the observation of a decrease in dendritic active β1-integrin labeling in cultured hippocampal neurons from Ndr2-deficient mice. Moreover, in these cultured hippocampal neurons, in the dendrite and soma, Ndr2 localization in early and recycling endosomes containing β1-integrins was demonstrated. Recently, it has been shown that Ndr2 regulates neurite outgrowth in PC12 cells and dendritic branching in hippocampal cultured neurons depending on the extracellular cues, which in these experiments were the coating substrates (Demiray et al. 2018). The branching impairment was observed on collagen IV coating and has been linked to the distribution of the α1 subunit on the surface, concluding that Ndr2 regulates the α1β1-integrin distribution and activity. Integrins are heterodimeric (consisting of α and β subunits) membrane receptors known to mediate cell attachment and spreading as well as transmitting extracellular information from the extracellular matrix (ECM) thus regulating intracellular signaling and the actin cytoskeleton rearrangement (Lilja and Ivaska 2018). Integrins are also shown to play a role in cell migration, neuronal outgrowth, and branching. For example, β1-integrin promotes axonal growth in newly differentiated neurons by binding to semaphorin 7A that activates FAK (focal adhesion kinase) and MAPK (mitogen-activated protein kinase) signaling (Carlstrom et al. 2011). During synapse formation and maturation, the importance of integrins have also been demonstrated. In cultured hippocampal neurons β1-integrin is shown to promote astrocyte-dependent excitatory synaptogenesis (Hama et al. 2004). In addition, integrins are crucial for synaptic plasticity, as in long term potentiation (LTP). Using RGD peptides (activate surface integrins) and integrin inhibitors it has been shown that, in acute hippocampal slices, an impairment in CA1-LTP stabilization is evident (Staubli, Vanderklish, and Lynch 1990; Stäubli, Chun, and Lynch 1998). Related to the functions of integrins in LTP, the role of integrins on behavior was also addressed. β1-integrin has been associated with working memory and spatial memory, α5 in spatial memory only, and α3 in working memory, spatial memory, and novel object recognition (summarized in Park and Goda 2016).

1.2 Ndr2 in human diseases

Variability in organisms is introduced mostly by genetic alterations. These genetic alterations may be a result of differences in the DNA nucleotide sequence or in the chromosomal structure. One of the most common changes in the genome is the single nucleotide polymorphism (SNP) observed in the population. Moreover, research over the last decades has shown that structural genetic variation, which mostly appears as copy number variation (CNV), modulates gene

expression and results in a disease phenotype. CNVs are deletions or multiplications in specific regions of the DNA in the genome that may occur *de novo* as well as be inherited. These regions can vary in size, from di- or tri-nucleotide repeats such as in Huntington's disease to thousands of nucleotides extending over many genes. The importance of CNVs as disease susceptibility variants has been studied and it has been demonstrated that specific CNVs may play a role in the immune response to HIV (human immunodeficiency virus) infections (Gonzalez et al. 2005), in autoimmune diseases (Fanciulli et al. 2007), and also in neurodevelopmental disorders such as autism spectrum disorder (ASD) (Sebat et al. 2007) and schizophrenia (Walsh et al. 2008).

The *NDR2* gene in the human genome is located on chromosome 12 (12p11.23, gene ID: 23012). There is no known disease directly associated with Ndr2 until now, yet there is some evidence pointing out that Ndr2 might be in a hotspot for CNVs resulting in disease. Open access databases, such as NCBI-ClinVar or DECIPHER (Firth et al. 2009), allows us to search for available patient data with CNVs including genes of interests. Using the DECIPHER database patients with deletion, duplication or triplication was screened and individuals having CNVs including the *NDR2* gene was summarized (Fig. 1.3). The hotspot includes at least four genes (*NDR2, ARNTL2*, *PPFIBP1,* and *SMCO2)* and can go up to containing 435 genes (protein coding and non-coding included). Patients with the CNVs at this hotspot display various phenotypes including developmental delay, intellectual disability, abnormal facial shape, autism, and seizures. Additionally, a sporadic rare genetic disorder namely Pallister-Killian syndrome (OMIM: #601803) caused by a mosaic isochromosome of 12p (Peltomäki et al. 1987) has been associated with numerous symptoms including intellectual disabilities, but also facial dysmorphia, hypotonia, pigmentary dysplasia, seizures, diaphragmatic hernia, and congenital heart defects (Pallister et al. 1977; Teschler-Nicola and Killian 1981; Schinzel 1991). The relation of *NDR2* with the neurodevelopmental symptoms observed in the patients having deletions and multiplications still need to be unveiled.

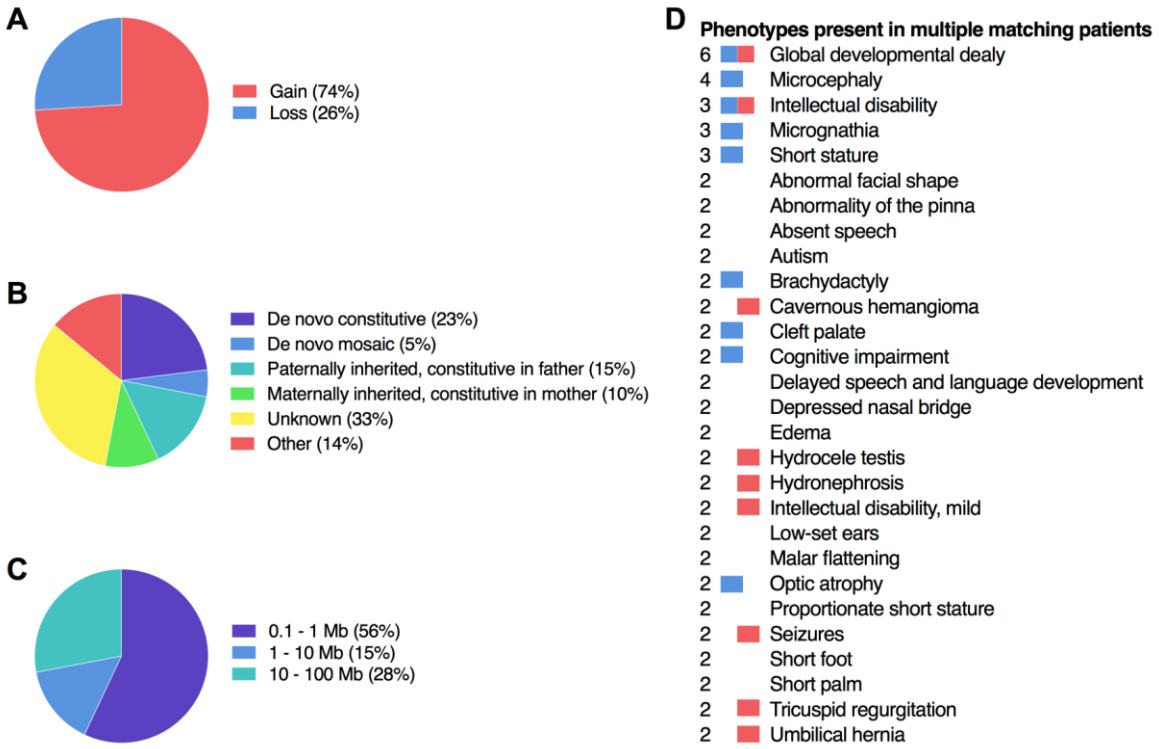

Figure 1.3: Summary of patient information with CNVs, including NDR2, collected from the DECIFER database.

39 patients were recorded in total. ***A.*** *The pie chart depicts the percentage of patients having deletions or multiplications in the genome containing the NDR2 gene.* ***B.*** *The inheritance of the mutations is illustrated including the percentage of patients in different categories.* ***C.*** *The size of the genetic modification that occurred in the genome is separated into three groups and the percentage of patients in these groups is graphed.* ***D.*** *Major phenotypes observed in the patients are listed including the number of patients displaying it. The list is comprised of phenotypes observed in at least two patients with deletions and multiplications. Blue boxes indicate the loss, the red boxes indicate the gain.*

1.3 Mouse models of CNVs

In order to understand human diseases and syndromes, animal models have been a valuable tool. With the development of genetic engineering technologies modifying or deleting specific genes, chromosomal loci, creating point mutations, and introducing CNVs has been possible. The models that have been created need to be translational to the human diseases replicating the relevant characteristics of the disease of interest. Mouse models have been used due to the ability of representing human diseases more accurate than models using *ex vivo* cell culture experiments and *in vivo* experiments with bacteria, invertebrates, and non-mammalian vertebrates. One reason for the mouse models to be more accurate than the other models is that over 90% of human and mice genomes share conserved synteny (the gene order has been conserved in both species) when divided into corresponding regions (Mouse Genome Sequencing Consortium et al. 2002). Furthermore, among ~30,000 protein-coding genes that

are present in mouse and human, 80% of these genes were identified to be ortholog to the human genome and less than 1% were not homologue to the human genome.

Mouse models have been widely used to understand the underlying mechanisms of neurodevelopmental and neurodegenerative disorders and eventually find a treatment. Different genetic approaches have been developed and used depending on the disease of interest by producing transgenic (introduction of a gene sequence into the genome) or knockout/-in (deleting or modifying endogenous genes) mouse lines. For example, one of the most common CNV diseases that has been modelled with genetically modified mice is Huntington's disease (HD). It is caused by a CAG trinucleotide repeat expansion in the *HTT* (huntingtin) gene, resulting in a toxic huntingtin protein with a polyglutamine (polyQ) sequence causing cellular dysfunction and neuronal death (The Huntington's Disease Collaborative Research Group, 1993). As the genetic approach can vary in order to reproduce the phenotype of HD, the resulting mouse models might show different phenotypes as well. For instance, the transgenic mouse line expressing human mHTT (mutant HTT) display an earlier and more severe phenotype when compared to the knockin mouse model with CAG repeats inserted into the endogenous Htt gene. In addition, the mouse model used for preclinical testing, such as the model expressing a truncated form of mHTT, showed a low prediction in therapeutic success in HD patients (reviewed in Ehrnhoefer et al. 2009). This points out to the fact that to proceed on with clinical trials, more than one mouse model must be generated and tested.

1.4 Mouse phenotyping

Model organisms, such as the mouse, are used to have a better understanding of a single gene and its function through comprehensive phenotyping (reviewed in Fuchs et al. 2011; Sukoff Rizzo and Crawley 2017). Behavioral phenotyping is composed of different tests that are performed to elicit any pleiotropic effects of the gene on the organism. The interaction of the central nervous system (CNS) with the external environment can be observed as an outward expression, in other words animal behavior. To investigate CNS dysfunctions behavioral phenotyping methods are essential.

Behavioral results can be influenced by several factors. One of the crucial factors is the genetic background of the mouse strain used for phenotyping, since genetic differences between mouse strains might shadow the effects of the genetic manipulation carried out. For example the mouse strain 129 has been shown to be poor in learning and memory tasks (Crawley et al. 1997)

whereas the C57BL strain show higher acoustic and tactile startle (Paylor and Crawley 1997). A germ line chimera mouse can be generated by using different mouse strains such that the embryonic stem (ES) cell is coming from the line 129 and the blastocyst from C57BL. To eliminate the mixed genetic background of such mice, it is suggested that they are backcrossed at least ten generations with the wild type strain of interest (breeding schemes shown and reviewed in Doetschman 2009).

Besides the genetic background, the age of the test subjects may play a role in the outcome of the results due to the developmental processes, thus age matched control mice should be tested concurrently, preferably littermate controls. Using littermate test subjects is crucial since environmental factors and home cage settings may significantly contribute to the phenotype. Maternal and/or paternal care, home cage environment and fighting, nearby construction noise, ultrasonic noise emitted from lights, and even caretaker handling may contribute to the behavioral phenotyping results. Animals from both sexes must be tested and analyzed due to the variability in behavioral phenotype in male and female subjects. Mice are nocturnal animals, being awake and active during the dark phase of the day. The light phase of the day the mouse is tested is important since circadian rhythm affects many biological and physiological processes influencing learning and memory and anxiety-like behavior (Albrecht et al. 2013; Krishnan and Lyons 2015). Another crucial point is that previous handling and experimental manipulations may influence the results. Therefore, a behavior test battery is generally planned and ordered from the experiment that is the least stressful and more vulnerable to handling to the most stressful and more resistant to handling. A behavior battery also ensures that the least possible number of test animals is used. Anxiety-related tests will be performed first, followed by learning and memory tests. Motor coordination and reflexes are tested last as they are considered to be more resistant to handling. Last but not least, the genetic background of the mouse strain needs to be considered when the age of the subject is determined. Strains known to have sensory degeneration, such as hearing loss in C57BL/6 mice, must be considered when tests relying on hearing will be carried out. (Bailey, Rustay, and Crawley 2006)

Mice can be tested with various behavioral tests, only the most frequently performed ones will be mentioned here (reviewed and summarized in Sukoff Rizzo and Crawley 2017). Innate nest building behavior and home cage activity, to assess the circadian rhythm, can be monitored. Anxiety-like behavior can be evaluated with an open filed test, light-dark transition test, elevated plus-maze or social interaction test. Depression-like behavior can be tested by applying

forced swimming test or tail suspension test. Conditioned anxiety and fear learning can be analyzed through active avoidance, contextual and cued fear conditioning. The Y-maze and T-maze tasks can be applied to evaluate working memory whereas Morris water maze or the radial arm maze can be used to assess reference memory, spatial memory, and working memory. Object memory tasks are used to determine object memory or novelty preference. Social memory, sociability, and olfactory function may also be tested by performing a social recognition task. Sensorimotor behavior and sensorimotor gaiting can be analyzed in hearing mice by the acoustic startle reflex and pre-pulse inhibition tests.

1.5 Hippocampus and its functions

The aforementioned behavioral tasks address learning and memory impairments and anxiety-like behavior. The function and connectivity of brain regions such as the hippocampus, amygdala, cortex, striatum, and midbrain play a significant role in expressing these cognitive and emotional states. The hippocampus is one of the most important brain structures that is involved in learning and memory and the alterations in its function may be tested with most of the behavioral tests mentioned above. The evidence of the relationship between hippocampus and learning and memory originates from one of the most studied human patient H.M., who underwent surgery due to severe epilepsy. The medial temporal lobe including parts of the hippocampi were removed bilaterally and the outcome of the procedure left the patient with anterograde and partial retrograde amnesia (Scoville and Milner 1957). The significance of hippocampus in learning and memory formation has been further studied in humans and other mammals and was confirmed. It has been shown that the hippocampus processes episodic memory, a type of long-term memory representing the relations between specific experiences and their context, and semantic memory that is general knowledge about the world. Studies in rodent models have suggested that hippocampus is important for remembering events in the spatial and temporal context (Eacott and Norman 2004; Butterly, Petroccione, and Smith 2012). Furthermore, it has been suggested that dorsal and ventral hippocampus have differential functions. The dorsal hippocampus functions more in spatial learning and memory as the ventral subregion is associated more in emotional processing and anxiety-like behaviors (Bannerman et al. 2004). The simple laminar organization of neurons and neuronal pathways in the hippocampus has enabled the usage of it as an experimental system to study synaptic plasticity. Synaptic plasticity, LTP, has been first identified in the hippocampus (Bliss and Lomo 1973) and has been further characterized using various techniques such as biochemical and molecular approaches and electrophysiology. Long-term potentiation is an enhancement of

excitatory synaptic transmission generated by high frequency afferent stimulation of the synapse.

Anatomically, hippocampus is a C-shaped structure located in the medial temporal lobe (in humans) at the floor of the lateral ventricle. The hippocampal formation consists of hippocampus proper, with three sub-regions of *Cornu Ammonis* (CA) 1-3 and the dentate gyrus. These structures are wired and form the "tri-synaptic loop/circuit". The major input is carried to the dentate gyrus (DG) through the perforant path, axons carrying sensory information from neurons in layer II of the entorhinal cortex. Axons of the perforant path make excitatory synaptic connections with the dendrites of granule cells in the dentate gyrus. Through the mossy fibers (axons of the granule cells), granule cells project to the proximal apical dendrites of CA3 pyramidal neurons. CA3 pyramidal neurons project through Schaffer collaterals to ipsilateral CA1 pyramidal cells and to contralateral CA3 and CA1 pyramidal cells through commissural connections. Moreover, CA3 pyramidal neurons get direct input from the entorhinal cortex layer II as well as the distal apical dendrites of CA1 pyramidal cells receive direct input from cells in layer III of the entorhinal cortex.

Previous research has demonstrated high levels of Ndr2 mRNA expression, via *in situ* hybridization, in the hippocampus, especially in the CA3 region (Stork et al. 2004). In terms of hippocampal circuits, CA3 circuits are suggested to be involved in memory encoding and recall (reviewed and summarized in Rebola, Carta, and Mulle 2017). The associative/commissural (A/C) loop, the interconnections between CA3 pyramidal cells, has been proposed to store associative memories and recall them through pattern completion. Moreover, DG granule cells project to CA3 pyramidal neurons through mossy fibers and make excitatory connections. This connection is suggested in encoding new activity patterns in CA3 through pattern separation. Cues for information retrieval from CA3 are provided by the direct connections from the entorhinal cortex to CA3. CA3 interneurons on the other hand, regulate the information flow between DG and CA3 depending on the presynaptic activity, so called the feedforward inhibition, and is proposed to influence the precision of memory. Furthermore, inhibitory loops (feedforward and feedback inhibition) in the CA3 regulate the oscillatory activity generation and are responsive to structural plasticity during learning.

1.6 Aims

Over the last two decades NDR kinases have been under investigation throughout species. Depending on the species and the NDR kinase, their functions vary in a wide range of cellular processes, from proliferation and survival to autophagy. More recently the NDR kinase function in neuronal cells started to unearth, yet the *in vivo* function of Ndr2 per se in neurons and its implication on behavior, such as on learning and memory and anxiety or fear responses, is still not clear. Also, considering the possible association of Ndr2 with various neurological phenotypes observed in humans due to CNVs, it is important and worthwhile to investigate Ndr2 in a model organism.

In order to study the function of Ndr2 *in vivo*, different Ndr2-mutant mouse models were generated in the Department of Genetics and Molecular Neurobiology, Otto von Guericke University Magdeburg. In the light of the previous findings on the function of Ndr2 *in vitro* on dendritic and axonal branching and neurite outgrowth and considering the expression pattern of Ndr2 in the brain, my first hypothesis was that knocking out Ndr2 would result in morphological deficits in the brain regions where Ndr2 is expressed. These morphological changes would then be manifested as less complex dendrical branching in Ndr2-knockout neurons. In order to verify or refute this hypothesis, an Ndr2 germ-line knockout mouse line was used to investigate the neuronal morphology changes.

My second hypothesis was that the possible morphological changes that would be observed in the Ndr2 germ-line knockout mouse line would in turn result in behavioral changes, especially in learning and memory. To provide an answer in this direction, mice were tested with a variety of behavioral tests resulting in a comprehensive behavioral phenotyping.

Continuing in the direction of the effects of the loss of Ndr2 expression in neurons, the function of Ndr2 on mouse behavior was investigated in a setting that excludes the possible secondary effects of other physiological systems on the central nervous system. For this purpose, two different brain specific conditional Ndr2-knockout mouse lines were used. The difference between these mouse lines was that the gene knockout was either introduced during embryonic development or postnatal.

Previously it has been shown at the Department of Genetics and Molecular Neurobiology that overexpressing Ndr2 in the brain at a postnatal time results in a reduction in mossy fiber

terminals and impairs mossy fiber dependent mouse behavior. Based on these previous findings, I have also investigated the behavioral effects of overexpressing Ndr2 from embryonic development onwards.

2 Materials and methods

2.1 Materials

2.1.1 Chemicals

Acrylamid 30%	Carl Roth, Karlsruhe, DE
Agarose	Peqlab, Erlangen, DE
dNTPs	Thermo Fisher Scientific, Waltham, MA, USA
EDTA	Carl Roth, Karlsruhe, DE
EtBr	Carl Roth, Karlsruhe, DE
Ethanol	Carl Roth, Karlsruhe, DE
Goat serum	Vector laboratories, Burlingame, USA
Halt Protease and Phosphatase Inhibitor Cocktail, EDTA-free (100X)	Thermo Fisher Scientific, Waltham, MA, USA
Shandon Immu-mount	Thermo Fisher Scientific, Waltham, MA, USA
Isoflurane	Nicholas Piramal limited, UK
Isopropanol	Carl Roth, Karlsruhe, DE
Ketamine – xylazine	Sigma-Aldrich, St. Louis, MO, USA
NaCl	Carl Roth, Karlsruhe, DE
PCR Direct Lysis Buffer	Peqlab, Erlangen, DE
PFA	Carl Roth, Karlsruhe, DE
PLL (Poly-L-Lysine)	Sigma-Aldrich, St. Louis, MO, USA
Proteinase K	Carl Roth, Karlsruhe, DE
PVDF membrane (Immobilon-FL)	Merck Millipore, Burlington, MA, USA
Syn-PER Synaptic Protein Extraction Reagent	Thermo Fisher Scientific, Waltham, MA, USA
Tablet Pierce protease inhibitor	Thermo Fisher Scientific, Waltham, MA, USA
Tris-HCl	Carl Roth, Karlsruhe, DE
Triton-X	Serva Electrophoresis, Heidelberg, DE

2.1.2 Enzymes and kits

Avidin/biotin blocking kit	Vector laboratories, Burlingame, USA
Bradford Assay	Bio-Rad Laboratories Inc., Hercules, CA, USA
Dream Taq-polymerase	Thermo Fisher Scientific, Waltham, MA, USA
Taq-polymerase	Qiagen, Hilden, DE

TaqMan copy number reference assay	Thermo Fisher Scientific, Waltham, MA, USA

2.1.3 DNA and protein standarts

Gene Ruler 100 bp Plus DNA Ladder	Thermo Fisher Scientific, Waltham, MA, USA
Gene Ruler 1 kb DNA Ladder	Thermo Fisher Scientific, Waltham, MA, USA
Paige Ruler Plus Prestained Protein Ladder	Thermo Fisher Scientific, Waltham, MA, USA

2.1.4 Primary antibodies

anti-actin(pan), mouse (1:10000, Merck Millipore, Burlington, MA, USA, MAB1501)
anti-alpha tubulin, mouse (1:10000, Sigma-Aldrich, St. Louis, MO, USA, T6199)
anti-β-galactosidase, chicken (1:500, abcam, Cambridge, UK, ab9361)
anti-GAPDH, rabbit (1:1500, Cell Signaling Technology, Danvers, MA, USA, #5174)
anti-Ndr1, goat (1:500, MyBioScource, San Diego, CA, USA, MBS422828)
anti-Ndr2, mouse (1:1000, OriGene Technologies Inc., Rockville, MD, USA, TA505176)
anti-Ndr2, mouse (1:1000, Pineda, Berlin, DE, described in Stork et al. 2004)
anti-PSD95, rabbit (1:1000, Cell Signaling Technology, Danvers, MA, USA, #3450)

2.1.5 Secondary antibodies

Biotinylated goat-anti-chicken IgY (1:250, Vector Laboratories, Burlingame, CA, USA)
Cy5-Streptavidin (1:750, Jackson ImmunoResearch Europe Ltd., Cambridgeshire, UK)
DAPI (1 µg/ml, Sigma-Aldrich, St. Louis, MO, USA)
IRDye 680RD donkey-anti-mouse (1:15000, LI-COR Inc., Lincoln, NE, USA)
IRDye 680RD donkey-anti-rabbit (1:10000, LI-COR Inc., Lincoln, NE, USA)
IRDye 680RD goat-anti-mouse (1:20000, LI-COR Inc., Lincoln, NE, USA)
IRDye 800CW donkey-anti-goat (1:15000, LI-COR Inc., Lincoln, NE, USA)
IRDye 800CW donkey-anti-mouse (1:10000, LI-COR Inc., Lincoln, NE, USA)
IRDye 800CW goat-anti-rabbit (1:15000, LI-COR Inc., Lincoln, NE, USA)

2.1.6 Animal care

Ssniff R/M-H V-1534	Ssniff Spezialdiäten, Soest, DE
Macrolon standard cages (type II long)	Techniplast, Hohenpeissenberg, DE

2.1.7 Solutions

10x PBS (Phosphate buffered saline)

Dissolve in 900 ml ddH_2O

- 11.5 g Na_2HPOxH_2O
- 2.0 g KH_2PO_4
- 80.0 g NaCl
- 2.0 g KCl

Adjust pH to 7.4 and add ddH_2O until final volume is 1 L.

4% Paraformaldehyde (PFA)

- Dissolve 40 g PFA in 700 ml ddH_2O
- Stir solution until clear at 70°C
- Add 500 µl 5 M NaOH
- Cool on ice and filter the solution
- Add 100 ml PBS and adjust pH to 7.4
- Fill the volume up to 1 L with ddH_2O

30% Sucrose

- Dissolve 30 g sucrose in 80 ml ddH_2O
- Add 10 ml 10x PBS (final concentration 1x)
- Complete the volume to 100 ml with ddH_2O

Poly-L-Lysine solution for coating glass slides

- Dilute PLL 1:10 in ddH_2O

Incubate glass slides for 5 min in solution at room temperature and air dry.

2.1.8 Equipment list

Cryostat, CM 1950	Leica, Nussloch, DE
DMI 6000 epifluorescence microscope	Leica, Nussloch, DE
Fridge/Freezer (KU 2407/GU4506)	Liebherr Hausgeräte, Ochsenhausen, DE
Glassware	Carl Roth, Karlsruhe, DE
Micro-Amp Fast Reaction Tubes	Life Technologies, Darmstadt, DE
Sanyo Ultra Low (-86°C)	Ewald Innovationstechnik, Bad Nenndorf, DE
Thermocycler, Veriti Thermal Cycler	Applied Biosystems, Darmstadt, DE

3-chamber social interaction box	Stoelting Co., Wood Dale, IL, USA
Elevated plus maze	Stoelting Co., Wood Dale, IL, USA
Home cage activity, 10-V2.1	Coulbourn Instr., Holliston, MA, USA
Open field	Stoelting Co., Wood Dale, IL, USA
PPI/ASR	Med Associates Inc., St. Albans, VT, USA
TSE Fear Conditioning System	TSE, Bad Homburg, DE
WCM	Custom made
Y-maze	Custom made

2.1.9 Software

Adobe Photoshop	Adobe Systems, San Jose, CA, USA
AnyMaze Behavior Tracking Software	Stoelting Co., Wood Dale, IL, USA
Fiji (ImageJ)	Open source
LAS AF software	Leica Microsystems, Nussloch, DE
Mendeley	Mendeley Ltd., London, UK
Microsoft Office	Mircosoft, Redmond, WA, USA
Neurolucida	MBF Bioscience, Williston, VT, USA
Prism	GraphPad, San Diego, CA, USA
TSE Fear Conditioning Software V08.03	TSE, Bad Homburg, DE

2.2 Methods

2.2.1 Mice

All mice were bred and maintained in the animal facility of Institute of Biology, Otto von Guericke University Magdeburg under standard laboratory conditions. The facility was kept on an inverted 12-hour dark/light cycle (lights off at 7 am with 30 min of dim phase), with regulated room temperature (21°C) and humidity (50-60%). Mice were weaned four weeks after birth and were group-housed 2-6 mice per cage with *ad libitum* food (Ssniff R/M-H V-1534, Ssniff Spezialdiäten, Soest, Germany) and water. After weaning tail biopsies (<0.3 cm) were taken for genotyping and earmarks were made for mouse identification in group-housed mice. Animals participating in behavioral experiments were single caged, with *ad libitum* food and water, 4-7 days prior to the experiments, which were performed in accordance with European regulations and approved by Landesverwaltungsamt Saxony-Anhalt (Permission numbers 42502-2-862 UniMD, 42502-2-1009 UniMD, and 42502-2-1284 UniMD). All experiments were performed during the active phase (lights off) of mice.

2.2.1.1 *Ndr2 constitutive-knockout mouse line*

Constitutive germ-line Ndr2-knockout mice (in lab abbreviation: 0NdrB) were generated using a gene-trap vector (supplied by the NIH Mutant Regional Resources Center (Stryke et al. 2003)) from the embryonic stem (ES) cell line E14TG2a ($Stk38l^{GT(RRT116)Byg}$, Bay Genomics). Using a sequence tag matching exon 9-7 on the Ndr2 gene the position of the insert was determined to be in intron 9 with the 5' rapid amplification of cDNA ends (5'RACE) (Fig. 2.1). After the verification of the insert and its position, the EC cells were injected into C57BL/6 blastocysts (Polygene) and one mouse line was acquired with a stable gene-trap insertion. Mice obtained from the stable line were further backcrossed with C57BL/6OlaHsd mice for at least ten generations. Experimental mice were obtained from heterozygous ($Ndr2^{+/-}$) male and female breeding pairs, giving littermate mice being Ndr2 wild type ($Ndr2^{+/+}$: WT) and knockout ($Ndr2^{-/-}$: KO).

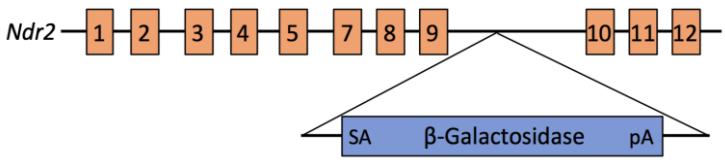

Figure 2.1: A scheme of the β-galactosidase insertion in intron 9 creating the constitutive knockout mouse line.

2.2.1.2 *Ndr2 conditional-knockout mouse line*

A conditional Ndr2-knockout mouse line (in lab abbreviation: 0NdrC) was generated on the C57BL/6 background by loxP site insertions into intron 5 and 6 of the Ndr2 gene (KOMP Repository, Davis, CA, USA), enabling the deletion of exon 6 when cre-recombinase is present (Fig. 2.2). The conditional mouse line was further bred to be homozygous for the loxP sites (lox/lox). Mice were further bred with cre-recombinase carrying driver lines to knockout Ndr2 in specific cells. In order to have littermate mice for the experimental studies, mice homozygous for loxP and heterozygous for the cre-recombinase (lox/lox, +/cre) were bred with mice homozygous for loxP and not carrying the cre-recombinase gene mice (lox/lox, +/+) to obtain littermate mice that were wild type (lox/lox, +/+: WT) and conditional Ndr2-knockout (lox/lox, +/cre: cKO).

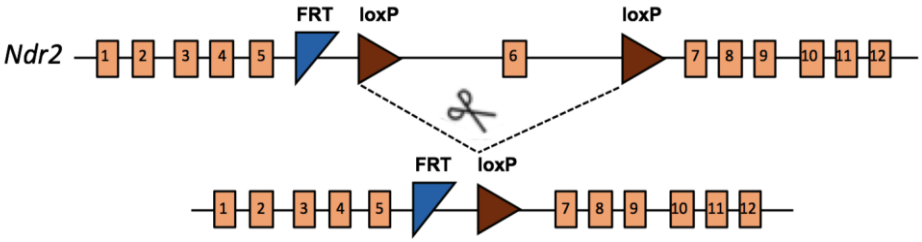

Figure 2.2: A scheme for cKO-mouse generation with loxP site insertions in intron 5 and 6, creating a cut in the gene when cre-recombinase is present.

2.2.1.3 Ndr2 conditionally overexpressing mouse line

Ndr2 transgenic mice (in lab abbreviation: Ndr89) were generated by cloning an EGFP::Ndr2 construct into the pCAGGS plasmid, kindly provided by Dr. K. Miyashita from Kyoto University, using restriction sites for SalI and SacII. The resulting plasmid containing the CAG and loxP sites were injected into the pronucleus of a zygote originated from CB6F2 mice by PolyGene and the transfected fertilized eggs were transferred to a pseudopregnant C57BL/6 mouse (Fig. 2.3). Offspring that carried the insertion were tested by PCR with primers amplifying a sequence fragment of the fusion protein EGFP::Ndr2: Forward: 5'-TCAAGATCCGCCACAACAT-3': and Reverse: 5'-CGTGCACAAACCAAAATCAG-3'. Samples were initially denatured at 95°C for 5 min and run for 35 cycles consisting of 15 s at 94°C, 30 s at 52°C, and 2 min at 72°C continued with a final extension stage at 72°C for 7 min. Tandem insertion was tested with polyA forward-primer (5'-ACGAGCCGGAAGCATAAAGTGTAAAG-3') and CAG reverse-primer (5'-GGGGGAGATGGGGAGAGTGAAG-3'). The number of copies inserted into the genome was analyzed with the TaqMan^{TM} copy number reference assay (mouse, TFRC, Thermo Fisher Scientific, Waltham, MA, USA) using heterozygous mice for the transgene. Samples ran for 40 cycles consisting of 15 s at 95°C and 60 s at 60°C with an initial step of 10 min at 95°C. The primers used in the assay were: Forward: 5'-CTTTGATGACTTCCCTGAGTCTGAT-3', Reverse: 5'-GGATTTGTAGTCGGGCTCTGT-3', and reporter: 5'-ATTCGGCACTGGCTGTAAG-3'. Experimental mice were obtained by breeding mice homozygous for the transgene (tg/tg) with mice heterozygous for the cre-recombinase (+/cre) giving littermate mice that are wild type (+/tg, +/+: WT) and transgenic (+/tg, +/cre: TG).

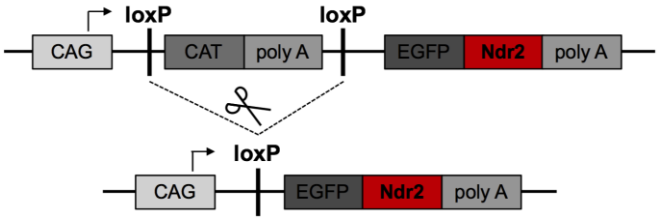

Figure 2.3: A scheme for TG mouse generation with transgene EGFP::Ndr2, and the generation of the overexpression when cre-recombinase is present.

2.2.1.4 Cre-recombinase driver mouse lines

Two different mouse lines were used that carry the cre-recombinase gene to conditional knockout or to overexpress the Ndr2 gene. The mouse line (Tg(camK2a-cre)159Kln) expressing cre-recombinase under the promoter of calcium/calmodulin-dependent protein kinase II alpha (CamKII-alpha) was purchased from the Jackson Laboratories (JAX® Bar Harbor, Maine, USA). Mice were bred (wild type (+/+) with heterozygous cre-mice (+/cre)) to obtain heterozygous (+/cre) mice to further be used in breeding with other Ndr2-mutant mouse lines.

The second mouse line (B6.129S2-Emx1$^{tm1(cre)Krj}$) expressing cre-recombinase under the promoter of empty spiracles homeobox 1 (Emx1) was purchased from the Jackson Laboratories (JAX® Bar Harbor, Maine, USA). Mice were bred (wild type (+/+) with homozygous cre-mice (cre/cre)) to obtain heterozygous (+/cre) mice to further be used in breeding with other Ndr2-mutant mouse lines.

2.2.2 Genotyping

Tail biopsies were used to determine the genotype of mice. Tail biopsies were lysed with 125 µl PCR Direct Lysis Buffer and 3.75 µl Proteinase K (stock: 10 mg/ml), incubated overnight at 55°C and heat inactivated at 85°C for 45 min. Samples, containing DNA that can be used for polymerase chain reaction (PCR), were kept in -20°C until further processing. Genotyping was done using the PCR method designed separately for individual mice line (Table 2.1 through 2.5). The PCR products were afterwards visualized on Agarose gels made with 1xTAE buffer.

Table 2.1: PCR protocol for the 0NdrB mouse line.

0NdrB	PCR Master Mix	4.8 µl ddH_2O 2.0 µl Q-solution 1.0 µl 10x Cl-Buffer (with $MgCl_2$) 0.5 µl dNTPs (2.5 mM) 0.5 µl Primer 0NdrB wt1: 5'CACTTGCCCACCTGCTCTCC3' 0.5 µl Primer 0NdrB wt2: 5'TTAAAACGGGGTCTCAAAACTCG3' 0.15 µl Primer 0NdrB ko: 5'ATCCCGGCGCTCTTACCAA3' 0.05 µl Taq-polymerase For each reaction tube: 9.5 µl Master mix 0.5 µl DNA sample
	PCR	94°C 3 min **94°C 15 s** **67°C 30 s** **40 cycles** **72°C 3 min** 72°C 7 min 4°C storage
	Agarose gel	1%, 7 µl/100 ml EtBr
	PCR products	wt: 1099 bp het: 1099 bp and 585 bp ko: 585 bp

Table 2.2: PCR protocol for the 0NdrC mouse line.

0NdrC	PCR Master Mix	4.45 µl ddH_2O 2.0 µl Q-solution 1.0 µl 10x Buffer 0.5 µl dNTPs (2.5 mM) 0.5 µl Primer FloxN5 1: 5'GGCGTGCTTGTTCCCTCTT3' 0.5 µl Primer FloxN5 2: 5'TTAACCCCGTGCACAAACCAA3' 0.05 µl Taq-polymerase For each reaction tube: 9.0 µl Master mix 1.0 µl DNA sample
	PCR	94°C 3 min **94°C 15 s** **67°C 30 s** **35 cycles** **72°C 3 min** 72°C 7 min 4°C storage
	Agarose gel	1%, 7 µl/100 ml EtBr
	PCR products	+/+ (wt): 1068 bp lox/lox: 1279 bp +/lox: 1068 bp and 1279 bp

Table 2.3: PCR protocol for the Ndr89 mouse line.

Ndr89	PCR Master Mix	6.15 µl ddH_2O 1.0 µl 10x Dream Taq Buffer 0.8 µl dNTPs (2.5 mM) 0.5 µl Primer Fag04 P8: 5'CGTGCACAAACCAAAATCAG3' 0.5 µl Primer EGFP 3: 5'TCAAGATCCGCCACAACAT3' 0.05 µl Dream Taq-polymerase <u>For each reaction tube:</u> 9.0 µl Master mix 1.0 µl DNA sample
	PCR	94°C 5 min **94°C 15 s** **58°C 30 s** **35 cycles** **72°C 90 s** 72°C 7 min 4°C storage
	Agarose gel	1%, 7 µl/100 ml EtBr
	PCR products	tg: 1003 bp

Table 2.4: PCR protocol for the Emx-Cre mouse line.

EmxCre	PCR Master Mix	5.05 µl ddH_2O 1.0 µl 10x Dream Taq Buffer 0.8 µl dNTPs (2.5 mM) 0.35 µl Primer oIMR 1084, mutant: 5'GCGGTCTGGCAGTAAAAACTATC3' 0.35 µl Primer oIMR 1085, mutant: 5'GTGAAACAGCATTGCTGTCACTT3' 0.07 µl Primer oIMR 4170, wt: 5'AAGGTGTGGTTCCAGAATCG3' 0.07 µl Primer oIMR 4171 wt: 5'CTCTCCACCAGAAGGCTGAG3' 0.05 µl Dream Taq-polymerase <u>For each reaction tube:</u> 9.0 µl Master mix 1.0 µl DNA sample
	PCR	94°C 3 min **94°C 30 s** **61°C 1 min** **35 cycles** **72°C 1 min** 72°C 2 min 4°C storage
	Agarose gel	1%, 7 µl/100 ml EtBr
	PCR products	Emx +/+ (wt): 378 bp Emx cre/cre: 102 bp Emx +/cre: 102 bp and 378 bp

Table 2.5: PCR protocol for the Cam-Cre mouse line.

CamCre	PCR Master Mix	6.15 µl ddH_2O 1.0 µl 10x Dream Taq Buffer 0.8 µl dNTPs (2.5 mM) 0.5 µl Primer Cre-tot 1: 5'ACGACCAAGTGACAGCAATG3' 0.5 µl Primer Cre-tot 2: 5'CTCGACCAGTTTAGTTACCC3' 0.05 µl Dream Taq-polymerase <u>For each reaction tube:</u> 9.0 µl Master mix 1.0 µl DNA sample
	PCR	94°C 5 min **94°C 30 s** **60°C 30 s** **30 cycles** **72°C 30 s** 72°C 6 min 4°C storage
	Agarose gel	2%, 7 µl/100 ml EtBr
	PCR products	Cre: 320 bp

2.2.3 Histological staining

Immunohistochemistry was done for β-galactosidase with tissue from constitutive Ndr2-knockout mice. Mice were anesthetized with a ketamine (80 mg/ml)-xylazine (6 mg/ml) mixture (1 mg/kg body weight) and were transcardially perfused using PBS (Phosphate-buffered saline) followed by 4% PFA in PBS. Brains were removed, kept in 4% PFA in PBS for 24 h at 4°C, in 30% Sucrose buffer in PBS for 48 h at 4°C, then snap frozen and stored at -20°C. 20 µm thick coronal sections were cut with a cryostat and were mounted immediately onto PLL (Poly-L-Lysine) coated glass slides. Sections were allowed to dry overnight at room temperature (RT) and were stored at 4°C. Slides were washed with PBS, permeabilized with 0.2% Triton-X in PBS at RT for 10 min and washed with PBS. Blocking was done at RT for 1 h with 5% goat serum in PBS. After washing with PBS, avidin-biotin blocking was done in avidin (1:5) and biotin (1:5) each 30 min. Slides were washed with PBS and primary antibody (1:500 chicken anti β-galactosidase, 2% goat serum, 0.2% Triton-X in PBS) incubation was performed over-night at 4°C. Slides were washed with PBS and afterwards secondary antibody (1:250 biotinylated goat-anti-chicken IgY, 2% BSA (bovine serum albumin), 0.1% Triton-X in PBS) incubation was done for 1 h at RT. Slides were washed with PBS, incubated with 1:750 Cy5-streptavidin in PBS at RT for 30 min, washed with PBS, incubated with 1:100 DAPI in PBS (stock 100 µg/ml), washed with PBS and covered with Immu-mount. Stained brain sections were further visualized with DMI 6000 epifluorescent microscope (Leica) at 10x

magnification, and images were captured and stitched using the software LAS AF software (Leica).

2.2.4 Synaptosome fractionation

Mice were deeply anesthetized with Isoflurane and decapitated. The hippocampi were extracted and were weighed immediately. On ice, tissue was homogenized using a tissue grinder with 10 ml/1 g of tissue of Syn-PER Synaptic Protein Extraction Reagent (mixed fresh with 100X Halt Protease and Phosphatase Inhibiton Cocktail, EDTA-free, final concentration 1X). The lysate was centrifuged at 4°C at 1200 g for 10 min. The pellet was discarded, and the supernatant was centrifuged at 15000 g for 20 minutes at 4°C. The supernatant was collected, containing the cytosolic fraction, and the pellet, containing the synaptosome fraction, was suspended with Syn-PER Reagent (1 ml/g of tissue sample). Protein concentration was determined using the Bradford Assay (Bio-Rad Laboratories Inc., Hercules, CA, USA) according to the manufacturer's instructions. The samples were kept at -20°C until further processed and were used for western blotting.

2.2.5 Western blotting

Mice were deeply anesthetized with Isoflurane and decapitated. Adult brain tissue was lysed on ice with laurylmaltoside lysis buffer (1% lauryl maltoside N-dodycyl-D-maltoside, 1% NP-40, 1 mM Na_3VO_4, 2mM EDTA, 50 mM Tris-HCl, 150 mM NaCl, 0.5% DOC, 1 mM AEBSF, 1 µM pepstain A, 1 mM NaF, 1 tablet Pierce protease inhibitor (Thermo Fisher Scientific, Waltham, MA, USA), using a tissue grinder, rotated at 4°C for 30 min then centrifuged for 30 min at 4°C at 16000 g. Protein concentration was determined using the Bradford Assay according to the manufacturer's instructions. Samples were separated on a 10% SDS-PAGE and transferred to a PVDF membrane (Immobilon-FL, Millipore, Germany). Membranes were incubated with primary antibodies, followed by secondary antibody incubation and were scanned with the Odyssey scanner (LI-COR).

2.2.6 Golgi-Cox staining

Mice were deeply anesthetized with Isoflurane and decapitated. Brains were removed and immediately incubated in 50 ml Golgi-Cox solution (Table 2.6) at room temperature for 14 days. Afterwards the brains were washed 3 times 2 min with dH_2O, dehydrated with ethanol in an ascending series (all at 4°C: 50% 3 h, 70% 10 min, 94% 24 h, 100% 2 times 24 h, at room temperature 100% ethanol-diethyl ether (1:1) 4 h), and were embedded in celloidin (2% 2 days, 4% 3 days, 8% 4 days).

Table 2.6: Preparation of the Golgi-Cox solutions.

Solution A: 5% K_2CrO_7 Solution B: 5% $HgCl_2$ Solution C: 5% K_2CrO_4	Solution D: Solution A + Solution B (1:1) Solution E: Solution C + dH_2O (1:2.5)
Golgi-Cox Solution: 100 ml Solution D is stirred with 140 ml of Solution E. The solution is kept in the dark for 5-14 days, in order to discard the precipitates that may occur.	

Brains were oriented in 8-10% celloidin and were stored in an open exsiccator for 24 h. The following day, the celloidin was dehydrated until it was half of its original volume in a closed exsiccator with drying agent Phosphorus Pentoxide (P_4O_{10}). Afterwards chloroform was added to the exsiccator for the celloidin to polymerize for 1-2 days. For complete polymerization the celloidin block was stored in 70% ethanol at 4°C for a few days. With a microtome, 150 µm thick horizontal sections were cut, collected in 70% alcohol and kept at 4°C. Collected sections were reduced and dried: washed 2 times 5 min with dH_2O, reduced in alkaline solution (NH_3:H_2O (1:1)) for 30-40 min, darkness increased with 0.5% Phenylenediamine 1 min and 5 min, washed with dH_2O 2 times 2 min, stabilized the impregnation with 1% DEKTOL (developer, Kodak) for 2 min, washed with dH_2O 2 times 1 min, fixed with 5% Tetenal (fixer, Kodak) for 5 min, washed with dH_2O 3 times 5 min, dehydrated with ethanol (50% 2 min, 70% 2 min, 96% 2 min), isopropanol:96% ethanol (2:1) 2 times 5 min, and finally in Xylol 2 times 5 min. Sections were embedded between two coverslips using Merkoglas.

Neurons were visualized under a light microscope using 100x magnification and single cells were traced live using the Neurolucida software. Dendritic branching was analyzed and Sholl analysis was performed with increasing 10-µm radii. The total length of dendritic branches in each circle was summed and the plotted.

2.2.7 Behavioral experiments

Behavioral experiments were conducted in a sequence from least stressful to the most, when these tests were performed with the same mice, in order to minimize the possible interference of the tests with the behavioral outcome. Anxiety tests were performed at the beginning and water cross maze was the last test. Unless stated otherwise, at least 24 h elapsed between tests.

2.2.7.1 Home cage activity

Activity in the home cage and the circadian rhythm changes were investigated using an infrared motion detection system mounted on top of the mouse cage cover, providing complete x-, y-,

and z-axis coverage (HCA 10-V2.1, Coulbourn Instr., Holliston, MA, USA). Activity was reported in 5 min bins.

2.2.7.2 Elevated plus maze

Mice were tested on a maze elevated 40 cm from ground level, consisting of two open (35 cm x 5 cm) and two closed arms (35 cm x 5 cm x 15 cm) under low light conditions (10 Lux). Mice were placed in the center of the maze to start the experiment and exploratory behavior was tracked and analyzed by AnyMaze software (Stoelting Co., Wood Dale, IL, USA) for 5 minutes. The apparatus was cleaned with 10% ethanol between each test mouse. (Rehberg et al. 2010)

2.2.7.3 Open field

Exploration and locomotor activity were tested in an open field apparatus (50 cm x 50 cm x 30 cm) under dark (red light, 3 Lux) and dim light (35 Lux) conditions. Each light condition was tested on separate days, with 24 h in between, for 20 min (Muller et al. 2014). Mice were tracked, and behavior was analyzed with the AnyMaze software (Stoelting Co., Wood Dale, IL, USA). Total distance covered in the apparatus and time spent in the corners (area 12.5 cm from the walls), rim (the area between the corners, 12.5 cm x 25 cm) and the center (inner square, 25cm x 25 cm) was analyzed. The distance covered in the maze was analyzed in 5 min bins and time spent in different areas was analyzed in a single 20 min bin. The apparatus was cleaned with 10% ethanol.

2.2.7.4 Light/dark transition test

Mice were tested in a Plexiglas box with two compartments (each 19 cm x 21 cm x 20 cm) separated with a 4 cm x 4 cm opening, one side dark (0 Lux) the other illuminated (110 Lux) enclosed in an isolating outer box equipped with a ventilation fan, light source, and a photobeam system for tracking the subject (TSE, Bad Homburg, Germany). Mice were placed in the lit compartment and were tracked for 5 min. The box was cleaned with 10% ethanol. (Muller et al. 2014)

2.2.7.5 Y-maze

Spontaneous alternation behavior (working memory) was tested in a Y-maze, with three arms separated by having 120° between them, under red light conditions (3 Lux) for 5 min. The starting arm was balanced among the test group (arms A, B or C) and the sequence of arm visits were manually recorded. When the mouse visited all three arms (A, B, and C) in a sequence without entering the previously visited arm, it was considered that the mouse performed a

correct alternation (e.g. if the sequence of visits was B → C → A, this was considered a correct alternation; yet, if the sequence was B → C → B, this was not) (Miedel et al. 2017). The correct alternations together with the total alternations made in the maze were calculated and an alternation index was calculated using the equation 2.1.

$$Alternation\ index\ (\%) = \frac{total\ number\ of\ correct\ alternations}{total\ number\ of\ all\ alternations} \times 100 \qquad (2.1)$$

2.2.7.6 Novel object recognition

An object recognition and novel object memory test was performed with mice in a Y-maze under red light conditions (3 Lux). The test consisted of two days, habituation and novel object test. For the habituation day, two identical objects (wooden blocks) were placed at the end corners of two test arms. Mice were placed in the starting arm, were tracked for 5 min and the time spent with objects were recorded with AnyMaze software (Stoelting Co., Wood Dale, IL, USA). The following day, one object was replaced with a novel object (Lego® block) and the object exploration was recorded for 5 min. The arm where the novel object was placed was randomized during the test. The maze and objects were cleaned with 10% ethanol.

2.2.7.7 Hot plate

To assess the pain threshold difference between mice, a hot plate test was done. Mice were placed on a heated plate at constant 55°C enclosed with a plastic cylinder (diameter: 11 cm). The latency to lick or shake the hind paws was recorded and mice were removed from the plate immediately afterwards. The maximum duration of the test was kept at 30 s in order to avoid tissue damage. (Bannon et al. 2000)

2.2.7.8 Active avoidance

Mice were tested in a clear Plexiglas box (36 cm x 21 cm x 20 cm) with two equal size compartments separated with an opening (4 cm x 4 cm) with steel shock grid as a floor and a photobeam system for tracking the subject, situated in an isolating box equipped with a ventilation fan, speaker, and light source (TSE, Bad Homburg, Germany). The total test duration was five days, each day consisting of the same sequence of testing. Each day started with a 3 min habituation phase followed by 50 conditioned stimuli (CS)-foot shock presentations. The CS (10 kHz, 65 dB) was presented for 5 s, afterwards a foot shock (0.40 mA for max. 10 s, followed by 0.60 mA for max. 5 s) was presented, which co-terminated when the mouse shuttled to the other compartment. If the mouse did not shuttle at the end of the 10 s of

foot shock, the shock intensity was increased to 0.60 mA and was presented for additional 5 s. The inter-stimulus interval (ISI) was set to 20 s. The total and correct shuttles were recorded. (Sparkman et al. 2005) The box and grid were cleaned with 10% ethanol.

2.2.7.9 Pavlovian cued-fear conditioning

Protocols used for the cued-fear conditioning were performed in a clear Plexiglas box (36 cm x 21 cm x 20 cm) with steel shock grid as a floor and a photobeam system for tracking the subject, in an isolating box equipped with a ventilation fan, speaker, and light source (TSE, Bad Homburg, Germany). (Laxmi, Stork, and Pape 2003) The box and grids were cleaned with 10% ethanol. Freezing behavior (complete immobility except of breathing) was recorded with the photobeam system throughout the experiment.

Cued-fear conditioning with cue and context retrieval

Mice were habituated to the box for 6 min 24 h before the training session. The training session consisted of a 2 min pre-training phase without any stimulus, three 9 s conditioned stimuli (CS+: 10 kHz, 80 dB) followed by a 1 s foot-shock (0.40 mA) with a 20 s ISI, and post-training phase without any stimulus. Next day cue retrieval was done by placing mice in the same isolation box with a clean mouse cage with wood chip bedding inside (neutral context) placed on the photobeam system. After a 2 min no-stimulus phase, four unconditioned stimuli (CS-: 10 s, 2.4 kHz, 80 dB, 20 s ISI) and four conditioned stimuli (CS+: 10 kHz, 80 dB, 20 s ISI) were presented, which followed by a 2 min resting phase. Context retrieval was performed the following day by placing the mice in the clear Plexiglas box with the grid floor (shock context) for 6 min.

Cued-fear conditioning with tone discrimination retrievals

Mice were habituated and trained using the same protocol described above, in “Classical cued-fear conditioning with cue and context retrieval”. 24 h after training mice were placed in the same isolation box with in the neutral context on the photobeam system and the first cue retrieval session was done by presenting four different tones including the CS+ (1.2, 2.4, 5, and 10 kHz, 80 dB, 10 s, 20 s ISI). A 2 min stimulus-free phase was presented before and after the tone presentation phase. 14 days after training the same cue retrieval protocol was performed in the neutral context. The following day, mice were tested for the context memory by being placed in the shock context for 6 min.

2.2.7.10 Water cross maze

Mice were tested in a cross maze (50 cm x 10 cm arm length, 30 cm deep) filled with 23°C water. A platform was present in one arm 1 cm below water and spatial cues were present on the wall and the room was dimly lit (10 Lux). Mice were tested in 6-8 cohorts (ITI 10-15 min), had 6 trials per day (lasting maximum 30 s each) for 5 days. Mice were placed in the water gently and were taken out of the water from the platform with a plastic skimmer. If the mice could not locate the platform in 30 s, they were guided to the platform with the help of the plastic skimmer. The water was mixed between each test mice to eliminate any trace, and the walls were cleaned with a squeegee. The maze was filled with fresh water before each experimental day. Mice were scored according to their performance (accuracy) during the trials; if the mouse left the starting arm and swam directly to the correct arm and went to the platform, the score "1" was given, otherwise "0". The latency to find the platform was recorded and if it took more than 30 s, 31 s was assigned for the calculations. If the mouse went to the last one-third part of the arm that is neither the starting arm nor the arm that contains the platform, the score "1" was given for the "wrong platform visit". The wrong platform visits were summed for each day. (Kleinknecht et al. 2012)

Place learning protocol

Mice were trained to learn the position of the platform using external spatial cues (allocentric strategy) over 5 days. The platform was placed in the "West" (W) arm during training, and mice started either from the "North" (N) or the "South" (S) arm pseudo-randomly (odd days: N-S-S-N-N-S, even days: S-N-N-S-S-N) and the opposite arm to the starting arm was blocked, South and North respectively. Mice who reached 83.3% or higher accuracy levels on the last day of training, were allowed to participate in the reversal-learning task conducted after a two-day break. The reversal-learning test followed the same protocol as the training except that the platform was relocated to the "East" arm and mice had to relearn the new position over 5 days.

Response learning protocol

With this protocol, mice had to learn the position of the platform over 5 days using a body-turn based strategy (egocentric strategy), in this case turning left to find the platform. Similar to the place learning protocol, mice started either from the "North" (N) or the "South" (S) arm pseudo-randomly (odd days: N-S-S-N-N-S, even days: S-N-N-S-S-N) and the opposite arm to the starting arm was blocked, South and North respectively. The position of the platform was

changed with respect to the starting arm to incite a left turn to find the platform: West if starting from South, East if starting from North.

2.2.7.11 Acoustic startle response and pre-pulse inhibition

Acoustic startle response (ASR) and pre-pulse inhibition (PPI) were performed in a sound-attenuating cubicle enclosing a motion sensor and speakers. Mice were placed in an acrylic holder, which was fixed on the motion sensor. Sound stimuli were presented by PHM-250 acoustic startle reflex equipment and responses were analyzed with SOF-825 software (Med Associates Inc., St. Albans, VT, USA). Both ASR and PPI were tested in the same session as individual test blocks respectively, with an initial 5 min acclimation period at the beginning of the session. During the experiment, constant white noise (65 dB) was played and inter-trial intervals were randomized (10-30 s).

After the 5 min acclimation period the ASR block began, consisting of 50 trials of 20 ms white noise pulses (1 ms rise) with different sound pressure levels (0, 80, 90, 100, and 110 dB) played in a pseudo-randomized order (Table 2.7). Each sound pressure level was presented ten times and the startle responses were recorded during 500 ms. Following the ASR block, the PPI block started that also consists of 50 pseudo-randomized trials of 4 ms white noise pre-pulses (1 ms rise) with 0, 70, 75, 80 or 85 dB sound pressure levels followed by a 20 ms white noise pulse (1 ms rise) with 110 dB sound pressure separated by 100 ms from the corresponding pre-pulse (Table 2.7). Each pre-pulse level was presented ten times and 450 ms of the response after the 110 dB pulse presentation was recorded. (Valsamis and Schmid 2011) The mouse holder was washed with soap water after each test.

Table 2.7: ASR and PPI experimental layout.

The letters represent the sound pressure level for the individual 50 trials. For the ASR: A: 0 dB, B: 80 dB, C: 90 dB, D: 100 dB, E: 110 dB. For the PPI: A: 70 dB, B: 75 dB, C: 80 dB, D: 85 dB, E: 0 dB

1 D	2 D	3 E	4 D	5 B	6 B	7 B	8 D	9 B	10 C
11 A	12 E	13 C	14 C	15 A	16 D	17 B	18 E	19 C	20 A
21 A	22 C	23 C	24 B	25 D	26 A	27 E	28 E	29 D	30 C
31 B	32 A	33 E	34 C	35 B	36 B	37 E	38 A	39 D	40 A
41 E	42 B	43 E	44 E	45 C	46 D	47 D	48 C	49 A	50 A

Quantification of the startle responses was done with the detected peak amplitudes. For the ASR block each pulse level was averaged within and normalized to 0 dB responses, as for the PPI block the percentage of PPI for each pre-pulse level was averaged. The percentage of PPI was calculated as in equation 2.2:

$$\%\ PPI = \frac{response\ to\ pulse\ alone - response\ to\ pre\text{-}pulse}{response\ to\ pulse\ alone} \times 100 \qquad (2.2)$$

2.2.7.12 3-chamber social interaction test

Social behavior and social memory were tested in a 3-chamber social interaction box (each compartment 20 cm x 40 cm), under red light conditions (3 Lux). Age matched male C57Bl/6BomTac (M&B Taconic, Germany) were used as interaction partners placed in wire tubes (diameter: 8 cm) enabling close contact. The test consisted of three stages, 5 min each. During the first stage (habituation) test mice freely explored the test box. Afterwards a partner mouse was placed in a tube and the interaction with the partner in the tube vis-à-vis an empty tube was scored (social test). During the last stage (new partner) a second partner mouse was placed in the previously empty tube and the interaction time with each partner was recorded. (Albrecht and Stork 2012) AnyMaze software (Stoelting Co., Wood Dale, IL, USA) was used for the tracking and the apparatus was cleaned with 10% ethanol.

2.2.8 Statistics

For statistical analysis and data presentation Prism (GraphPad Software, Inc.) was used. Experimental sample sizes were set according to Cohen's d=0.8. Before group comparisons were done, data were checked for normality using Shapiro-Wilk normality test and equal variance. Then, either Student's *t*-test or Mann-Whitney *U*-test was done. When it was required repeated measures 2-Way-ANOVA was performed. When applicable, post-hoc comparisons were done with Fisher's LSD test. p-values smaller than 0.05 were considered statistically significant. All data were presented as mean±S.E.M.

3 Results

3.1 Ndr2 knockout mouse lines

3.1.1 Ndr2-constitutive knockout mouse line (KO)

3.1.1.1 Verification of the knockout

Western blotting was performed with whole brain tissue collected from WT and KO mice using an Ndr2-antibody recognizing the C-terminus of the protein (Stork et al. 2004), where the phosphorylation site important for kinase activity resides. Since the KO mice were generated with a β-galactosidase cassette insertion into intron 9, the protein product would not contain the epitope of the antibody. Indeed, the KO brain samples did not display Ndr2 expression (Fig. 3.1)

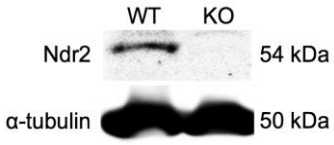

Figure 3.1: Ndr2 western blot for KO tissue.
An Ndr2 antibody that recognizes the C-terminus of the protein was used to detect the Ndr2 expression in WT and KO brain lysates. Ndr2 expression was not detected in the KO tissue

To confirm that Ndr1 kinase does not compensate for the loss of Ndr2 in the brain, western blotting was done against Ndr1 using brain, spleen, and thymus samples. In the brain, in neither of the genotypes (WT, HET, and KO) Ndr1 expression was observed, when compared to spleen and thymus samples from WT mice (Fig. 3.2)

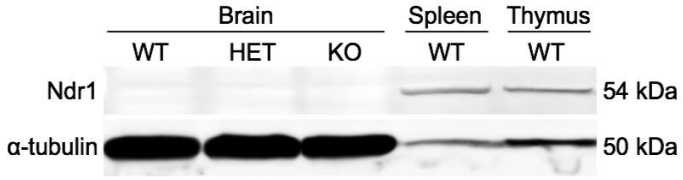

Figure 3.2: Ndr1 western blot.
Western blot with Ndr1 with brain, spleen, and thymus samples. Ndr1 expression in the wild type (WT), Ndr2-heterozygous (HET), and Ndr2-constitutive knockout (KO) brain lysates together with spleen and thymus lysates from WT mice are compared. In the brain Ndr1 is not detected when compared to the control organs spleen and thymus.

3.1.1.2 Ndr2 expression in the mouse brain

The constitutive Ndr2-knockout mice are generated with a gene-trap vector insertion into the *NDR2* gene containing a β-galactosidase cassette and as a result, the enzyme β-galactosidase is expressed under the Ndr2 promoter. In order to visualize the expression pattern of the Ndr2 protein indirectly in adult naïve mice, immunohistochemistry was conducted using an antibody against β-galactosidase. Positive staining was observed in a region and cell specific manner throughout the brain starting from cerebral cortex, striatum, thalamus, midbrain, and hindbrain until cerebellum. For example, expression could be observed in the caudoputamen (Fig. 3.3A), neocortex especially in the pyramidal layers 2/3 and 5 (Fig. 3.3B), and hippocampus in the pyramidal cells in the CA3 region (Fig. 3.3C and G). Stained cells are evident in the amygdala (Fig. 3.3D) but not as strong as observed in other regions. In the midbrain cells were strongly stained in the red nucleus (Fig.3.3H), substantia nigra, medial accessory oculomotor nucleus, and periaqueductal grey (Fig. 3.3E, and I). In the cerebellum the Purkinje cell are distinctly stained (Fig. 3.3F and J).

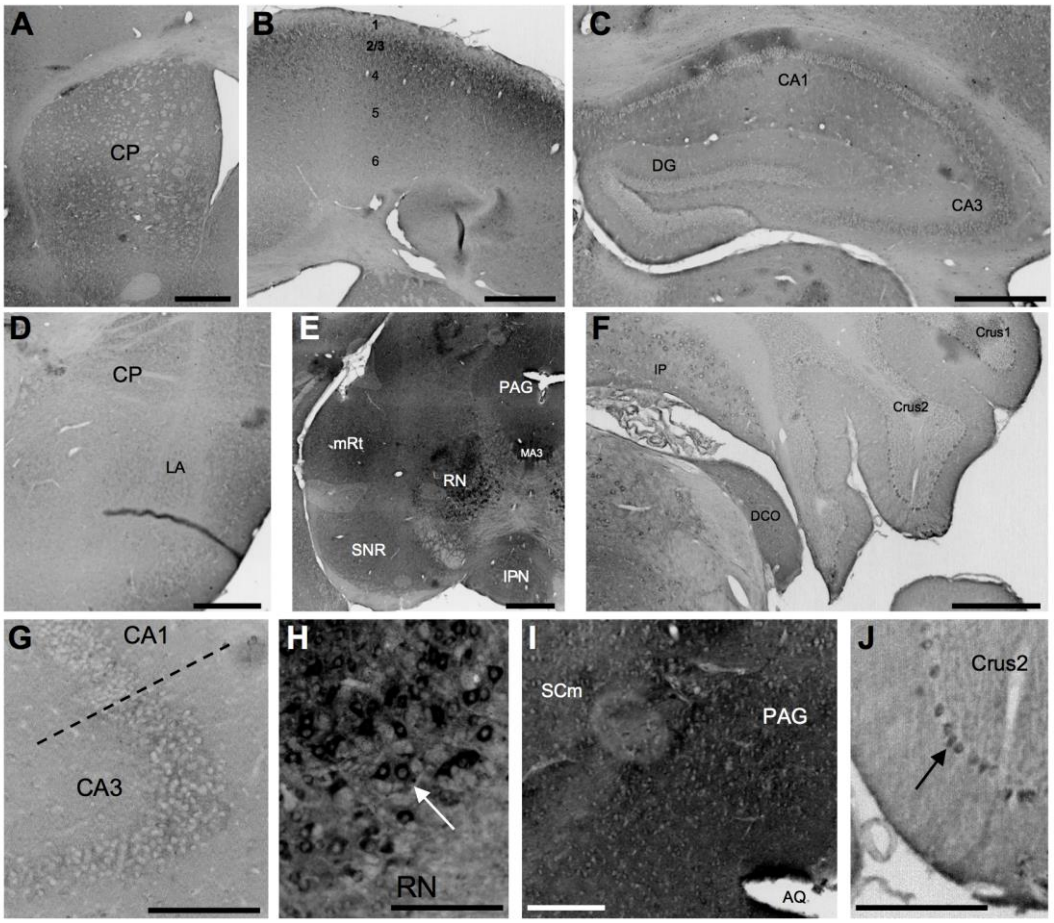

Figure 3.3: Expression of Ndr2 in the brain.

Immunohistochemistry performed with coronal brain sections from the KO mice, against β-galactosidase depicting the Ndr2 expression indirectly. ***A.*** *CP: caudoputamen.* ***B.*** *Cortical layers 1-6.* ***C.*** *Hippocampus subregions CA1, CA3 and DG.* ***D.*** *CP: caudoputamen, LA: lateral amygdala.* ***E.*** *Midbrain region. PAG: periaqueductal grey, mRt: mesencephalic reticular form. MA3: medial*

accessory oculomotor nucleus, RN: red nucleus, SNR: substantia nigra, IPN: interpeduncular nucleus. ***F.*** *Cerebellum. IP: interposed nucleus, DCO: dorsal cochlear nucleus, Crus1: crus1 ansiform lobule, Crus2: crus2 ansiform lobule.* ***G.*** *CA3 pyramidal neurons show distinct staining compared to CA1.* ***H.*** *Cytoplasmic staining was evident in the Red nucleus cells, shown with white arrow.* ***I.*** *Cells in the PAG show high levels of expression. AQ: cerebral aqueduct, SCm: superior colliculus.* ***J.*** *Purkinje cells are also Ndr2 rich indicated with the black arrow. Scale bar: A to F: 500 µm, G to I: 200 µm.*

3.1.1.3 Morphology of CA3 pyramidal neurons

The high expression levels of Ndr2 in the CA3 region of the hippocampus brought the question of the effects of Ndr2 on neuron morphology. Brains from adult littermate mice were stained using the Golgi-Cox method, and the dendrites of ventral CA3 pyramidal neurons were traced under a light microscope using Neurolucida software. The basal and apical dendrites were analyzed separately using Sholl analysis, describing the complexity of the dendritic branching. Concentric shells (with the soma being the center) 10 µm apart were drawn and the total lengths of the dendrites in each shell were summed for each genotype. The morphology of the basal dendrites did not differ between genotypes (N(WT)=5 mice, 14 neurons, N(KO)=4 mice, 14 neurons; Repeated measures 2-Way-ANOVA, F(1,26)=0.6454, p=0.4291), yet a shift in the dendritic complexity was observed in the apical dendrites of the KO mice (Fig. 3.4A). When the proximal apical dendrites (first 100 µm shell radius) were examined an increase in dendritic complexity was evident (Repeated measures 2-Way-ANOVA, F(1,26)=5.295, p=0.0297) and due to this shift the complexity of the distal apical dendrites was reduced (Repeated measures 2-Way-ANOVA, F(1,26)=5.731, p=0.0242). Furthermore, the length of the first order branch of the apical dendrite was significantly reduced in the KO neurons (Fig. 3.4B,C; (N(WT)=7 mice, 27 neurons, N(KO)=6 mice, 22 neurons; Student's *t*-test, t(47)=2.835, p=0.0067).

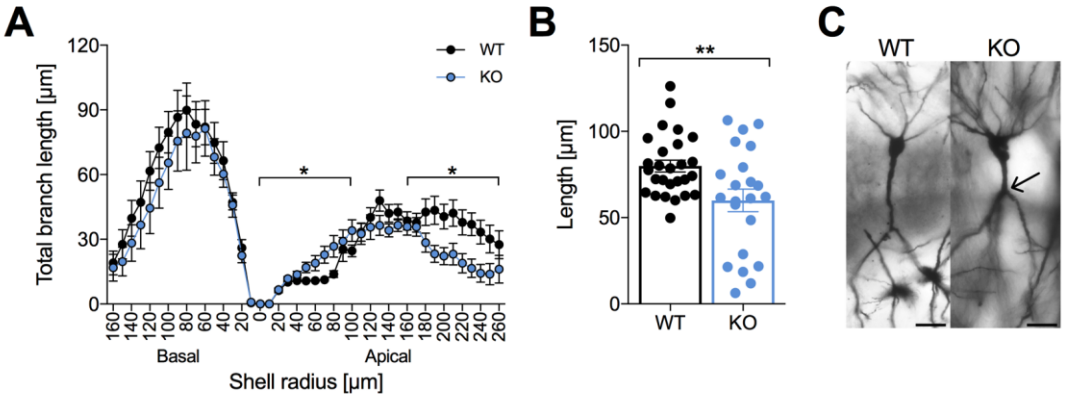

Figure 3.4: Tracing and analysis of CA3 pyramidal KO-neurons.
A. *Sholl analysis of the basal and apical dendrites of pyramidal neurons shows a shift in complexity in the apical dendrites (WT: N=5, n=14; KO: N=4, n=14).* ***B.*** *The first order branch length is compared for the apical dendrites and a reduction in the length is observed in the KO neurons (WT: N=7, n=27; KO: N=6, n=22).* ***C.*** *Representative images of CA3 pyramidal neurons from WT and KO hippocampus. Arrow indicates the premature branching point. Data presented as mean±S.E.M. *p<0.05, **p<0.01. Scale bar: 11 µm.*

3.1.1.4 PSD95 expression in the synaptosomes

Hippocampal tissue was isolated from WT and KO mice and synaptosome fractionation was done. The PSD95 expression levels were examined with the Western blot method. An expression difference in PSD95 at the synapses was not evident between genotypes (Fig. 3.5, N(WT)=3, N(KO)=4; Mann-Whitney *U* test, U=3, p=0.4000).

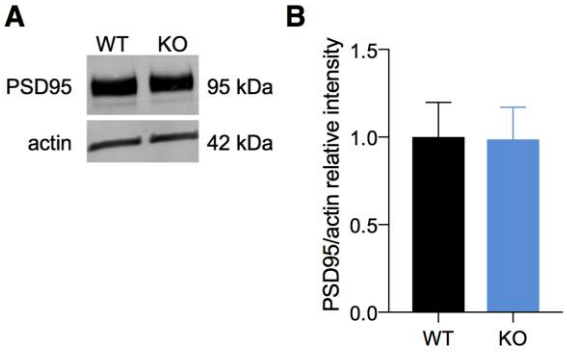

Figure 3.5: PSD95 expression in the synaptosomes in KO mice.
A. *Western blot image indicating the expression of PSD95 and actin in WT and KO hippocampus samples.* ***B.*** *No difference between genotypes was observed when the relative intensity of the bands was compared (N(WT)=3, N(KO)=4). Data shown as mean±S.E.M.*

3.1.1.5 Behavioral phenotyping of the KO mice

Adult (2-6 months old) littermate WT and KO male mice underwent behavioral tests to assess the outcome of the germline knockout of the *Ndr2* gene.

Initially, the **home cage activity** was monitored for five consecutive days. The circadian rhythm between genotypes was not significantly different (Fig. 3.6, N(WT)=8, N(KO)=11; Repeated measures 2-Way-ANOVA, F(1,17)=0.0842, p=0.7752). Mice were highly active during the dark phase of the light cycle and less active during the light phase.

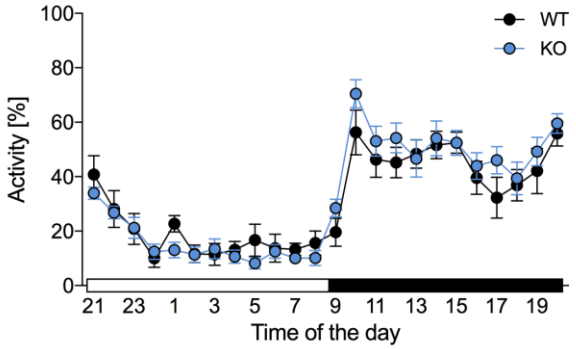

Figure 3.6: Home cage activity with KO mice.
The average activity over 24 hours is plotted and no difference is observed between genotypes (N(WT)=8, N(KO)=11). White bar on the x-axis represents the time when the lights are on, black bar represents when the lights are off. Data presented as mean±S.E.M.

Anxiety-like behavior together with exploration and activity was tested using different experimental setups. First a **light/dark transition test** was performed. Time spent in the dark and light compartments as well as the activity was compared and analyzed. Both genotypes spent more time in the dark compartment (Fig. 3.7-A; N(WT)=5, N(KO)=8; Dark and light compartments, Mann-Whitney *U* test, U=17, p=0.7242) and less in the lit compartment. Mice were also more active in the dark compartment (Fig. 3.7-B; Student's *t*-test, Dark: t(11)=1.404, p=0.1880; Light: t(11)=0.962, p=0.3567) in line with the time spent in the dark side of the box.

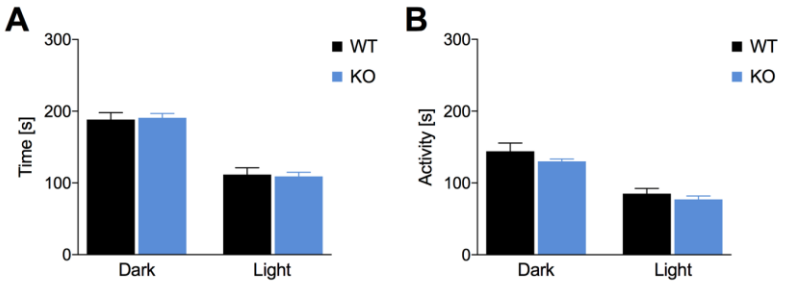

Figure 3.7: Light/dark transition test with KO mice.
*No difference between genotypes was observed neither in the **(A)** total time spent in both dark and light compartments nor in the **(B)** time mice were active in the compartment (N(WT)=5, N(KO)=8). Data presented as mean±S.E.M.*

Second, an **elevated plus maze** test was done. The time spent in the arms, the number of entries to the arms, and the total time immobile in the maze was analyzed and compared. Mice from both genotypes preferred to spend more time in the closed arm and less time in the open arm and the center (Fig. 3.8-A; N(WT)=8, N(KO)=11; Student's *t*-test, open arms: t(17)=0.07337, p=0.942; closed arms: t(17)=0.04176, p=0.9672; center: t(17)=0.01147, p=0.9909), and entered the open arms less than the closed arms (Fig. 3.8-B; Student's *t*-test, open arms: t(17)=0.03709, p=0.9708; closed arms: t(17)=0.02039, p=0.9839; center: t(17)=0.01336, p=0.9894). Immobility in the maze was also analyzed, yet no significant difference was observed between genotypes (Fig. 3.8-C; Student's *t*-test, t(17)=0.161, p=0.8740).

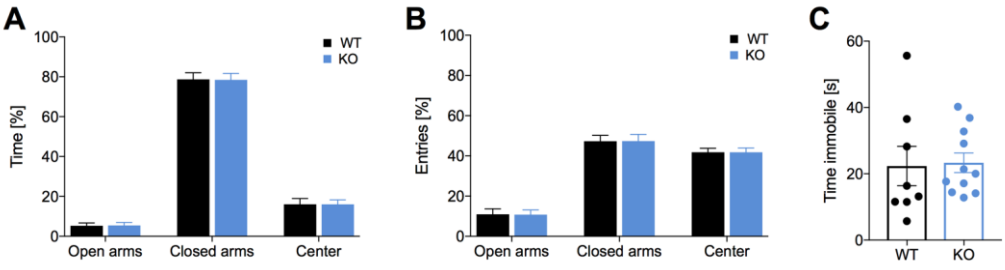

Figure 3.8: Elevated plus maze with KO mice.
*No difference between genotypes was detected in the **(A)** percentage of time spent in the open and closed arms as well as the center and in the **(B)** percentage of entries into the open and closed arms and the center (N(WT)=8, N(KO)=11). **C.** Total time immobile during the test in the whole apparatus is also did not differ between genotypes. Data presented as mean±S.E.M.*

Mice were subjected to a fear-conditioning paradigm and were tested in an elevated plus maze afterwards. Even though time spent in different compartments did not differ between genotypes (Fig. 3.9-A; N(WT)=7, N(KO)=7; Student's *t*-test, open arms: t(12)=0.7214, p=0.4845; closed arms: t(12)=0.9924, p=0.3406; center: t(12)=1.653, p=0.1242), entries to the center (Fig. 3.9-B; Student's *t*-test or Mann-Whitney *U* test, open arms: U=14, p=0.1958; closed arms: t(12)=0.3497, p=0.7326; center: t(12)=2.656, p=0.021) and immobility in the maze (Fig. 3.9-C; Student's *t*-test, t(12)=4.778, p=0.0004) significantly increased.

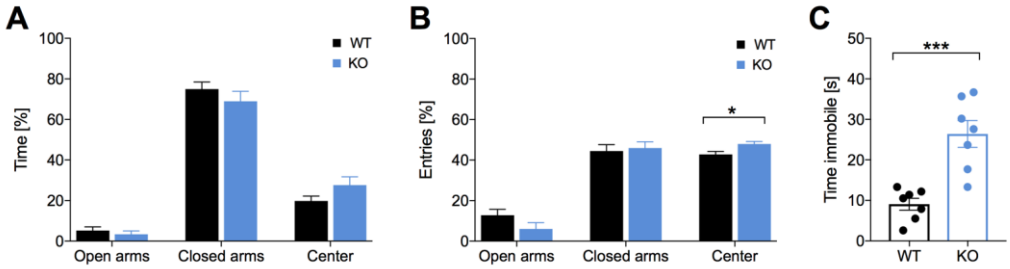

Figure 3.9: Elevated plus maze after fear-conditioning with KO mice.
A. *No difference between genotypes was detected in the percentage of time spent in the open and closed arms as well as the center of the apparatus (N(WT)=7, N(KO)=7).* ***B.*** *Percentage of entries into the open and closed arms and the center was compared and KO mice entered the center more than its littermate controls.* ***C.*** *Total time immobile during the test in the whole apparatus increased for the KO mice. Data presented as mean±S.E.M. *p<0.05, ***p<0.001.*

Last, mice were tested in an **open field** box for two days under different light conditions. Mice freely explored the apparatus and the total distance they covered as well as the time spent in different sections of the box was compared between genotypes. Maze exploration on the first day, when the test was done in the dark, decreased over time as the mice habituated to the environment however, exploration on the second day, tested in lit conditions, remained similar over time (Fig. 3.10-A) and no significant difference was observed between genotypes on both days (N(WT)=8, N(KO)=11; Repeated measures 2-Way-ANOVA, dark, F(1,17)=1.544, p=0.2309; light, F(1,17)=0.414, p=0.5285). Also time spent in the corners and the rim as well as the center of the open field arena was not different between genotypes for both days (Fig. 3.10-B; Student's *t*-test, dark: corners, t(17)=1.311, p=0.2072, rim, t(17)=0.9928, p=0.3347, center, t(17)=1.059, p=0.3043; light: corners, t(17)=0.9752, p=0.3431, rim, t(17)=0.9697, p=0.3458, center, t(17)=0.7903, p=0.4402). Mice in general preferred the corners and the rim to the center.

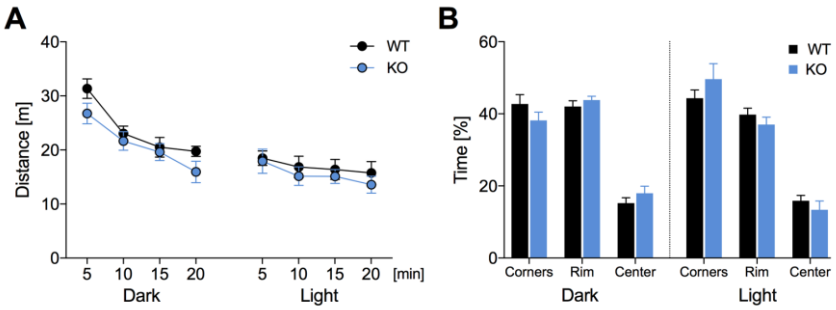

Figure 3.10: Open field with KO mice.

A. *Total distance covered in the arena over 20-minutes in dark and light conditions was not different between genotypes (N(WT)=8, N(KO)=11).* ***B.*** *Percentage of time spent in different areas of the arena (corners, rim, and center) was not different between groups. Data presented as mean±S.E.M.*

Naïve and trained (with cued-fear conditioning) mice were tested for their **acoustic startle response** and **pre-pulse inhibition**. Acoustic startle responses for different sound pressure levels were not different between genotypes neither with the naïve mice (Fig. 3.11-A; N(WT)=5, N(KO)=8; Repeated measures 2-Way-ANOVA, F(1,11)=0.2997, p=0.5950) nor with the previously trained mice (Fig. 3.11-C; N(WT)=9, N(KO)=10; Repeated measures 2-Way-ANOVA, F(1,17)=0.2847, p=0.6005). Pre-pulse inhibition also was not effected in the KO mice independent from being trained or not (Fig. 3.11-B, naïve: Repeated measures 2-Way-ANOVA, F(1,11)=0.2777, p=0.6087; Fig. 3.11-D, after FC: Repeated measures 2-Way-ANOVA, F(1,17)=0.5843, p=0.4551).

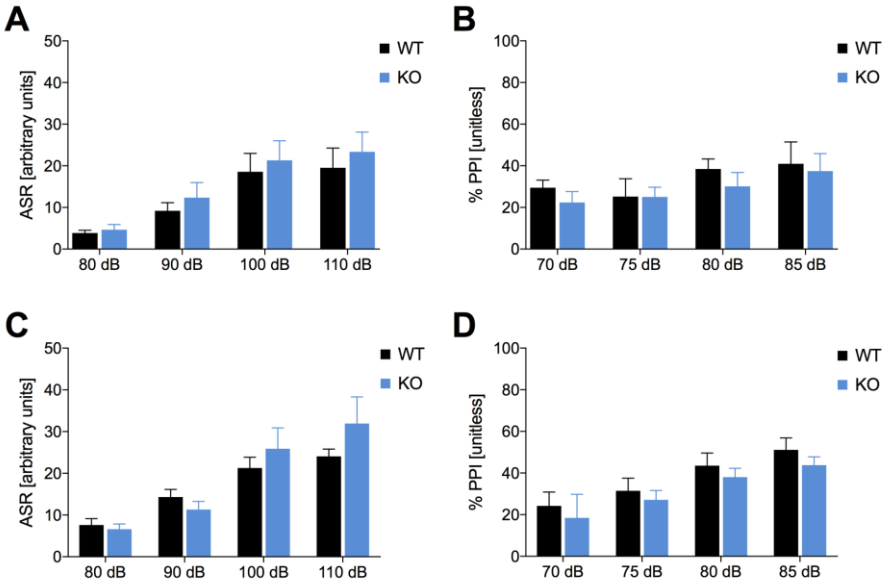

Figure 3.11: Acoustic startle response and pre-pulse inhibition with naïve and fear-conditioned KO mice.

Mice did not show a difference in ASR and PPI when tested in naïve state (N(WT)=5, N(KO)=8) ***(A,B)*** *or after fear-conditioning (N(WT)=9, N(KO)=10)* ***(C,D)****. Data presented as mean±S.E.M.*

In a **Y-maze**, mice freely explored three arms 120° apart from each other. Total spontaneous alternations performed was recorded together with the correct alternations done. As a measure for activity in the maze, total alternation count was compared between genotypes where no significant difference was eminent (Fig. 3.12-A; N(WT)=8, N(KO)=11; Student's *t*-test, t(17)=0.1986, p=0.8449). When the alternation index was calculated, representing the correct alternations performed during the task, KO mice did not perform different compared to their littermate WT mice (Fig. 3.12-B; Student's *t*-test, t(17)=1.525, p=0.1458).

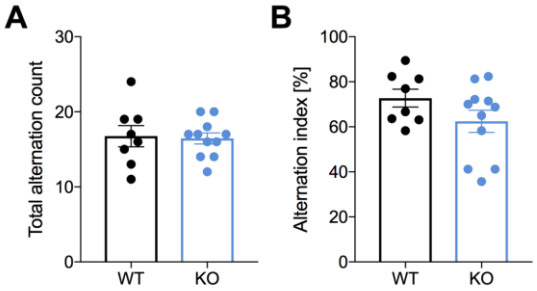

Figure 3.12: Y-maze spontaneous alternation test with KO mice.
Total number of alternations ***(A)*** *and correct alternation, represented as alternation index,* ***(B)*** *did not differ between genotypes (N(WT)=8, N(KO)=11). Data represented as mean±S.E.M*

Long-term **novel object memory** was tested in a Y-maze, with a 24-hour gap between sessions. Mice from both genotypes were habituated to two identical objects and did not show a preference toward either object (Fig. 3.13; N(WT)=8, N(KO)=11; Mann-Whitney *U* test, U=41, p=0.8404). 24 hours later, the time spent with the novel object increased compared to the familiar object, yet there was no significant difference between genotypes in the discrimination ratio (Fig. 3.13; Student's *t*-test, t(17)=0.3125, p=0.7584).

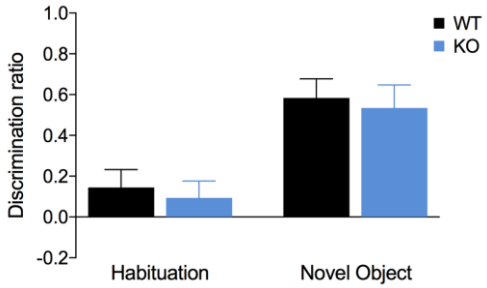

Figure 3.13: Novel object memory test with KO mice.
Object discrimination ratio was calculated for habituation and novel object recognition and no difference was observed between genotypes (N(WT)=8, N(KO)=11). Data presented as mean±S.E.M.

Spatial and reversal learning and memory were tested using the **water cross maze** using the place learning protocol. Mice were trained to find the platform using external spatial cues. The accuracy in finding the platform, the latency, and the wrong platform visits were recorded and

compared between genotypes. During the training session, even though in general WT and KO mice learned at the end of fifth day (Fig. 3.14A; N(WT)=10, N(KO)=10; Training: Repeated measures 2-Way-ANOVA, F(1,18)=1.873, p=0.1880), on the fourth day where WT mice made a learning jump above chance levels, the accuracy in finding the platform was significantly lower for the KO mice (Mann-Whitney *U* test, U=22, p=0.0256). The latency of finding the platform (Fig. 3.14B; Training: Repeated measures 2-Way-ANOVA, F(1,18)=0.000956, p=0.9757) and the wrong platform visits (Fig. 3.14C; Training: Repeated measures 2-Way-ANOVA, F(1,18)=2.452, p=0.1348) were not statistically different between genotypes during training. Mice who had 83.3% accuracy on the last day of training participated in the reversal-learning task. Regardless of the genotype, all mice relearned the position of the platform (Fig. 3.14A; N(WT)=7, N(KO)=7; Reversal: Repeated measures 2-Way-ANOVA, F(1,12)=0, p>0.9999), with similar latencies to find the platform (Fig. 3.14B; Reversal: Repeated measures 2-Way-ANOVA, F(1,12)=0.00323, p=0.9156) and wrong platform visits (Fig. 3.14C; Reversal: Repeated measures 2-Way-ANOVA, F(1,12)=0.2069, p=0.6573).

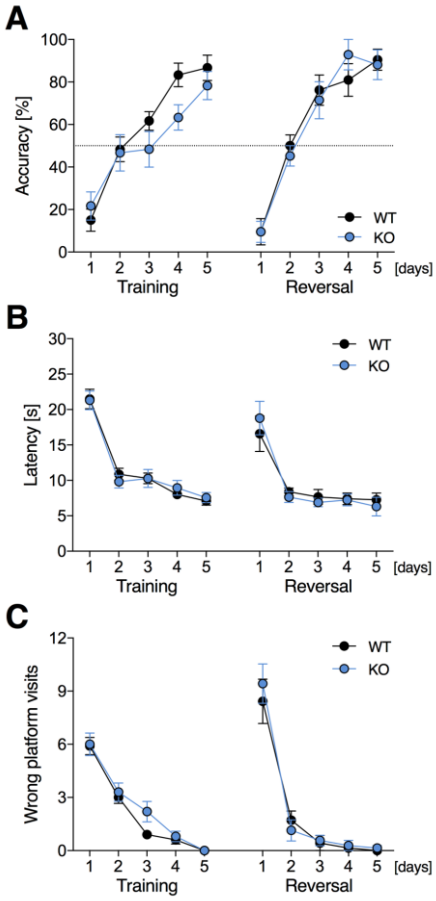

Figure 3.14: Water cross maze testing spatial and reversal learning with KO mice.
Mice were trained to find a hidden platform (N(WT)=10, N(KO)=10) and were tested to find the new position of the platform (N(WT)=7, N(KO)=7). No genotype difference was observed in the accuracy of finding the platform ***(A)****, latency in finding the platform* ***(B)****, and wrong platform visits* ***(C)****. Data presented as mean±S.E.M.*

WT and KO mice were trained in the **water cross maze** however using a response learning protocol where they had to find the platform based on a body-turn strategy (egocentric learning). Mice from both genotypes exhibited similar learning responses observed in the accuracy (Fig. 3.15A; N(WT)=8, N(KO)=9; Repeated measures 2-Way-ANOVA, F(1,17)=0.06716, p=0.7986), latency in finding the platform (Fig. 3.15C; Repeated measures 2-Way-ANOVA, F(1,17)=0.5579, p=0.4655), and wrong platform visits (Fig. 3.15D; Repeated measures 2-Way-ANOVA, F(1,17)=0.5791, p=0.4571). The distribution of the accuracy on the fifth day of training was also similar between genotypes whereas nearly half of the mice in each group were at the chance level or lower (Fig. 3.15B; Mann-Whitney *U* test, U=39.5, p=0.7244).

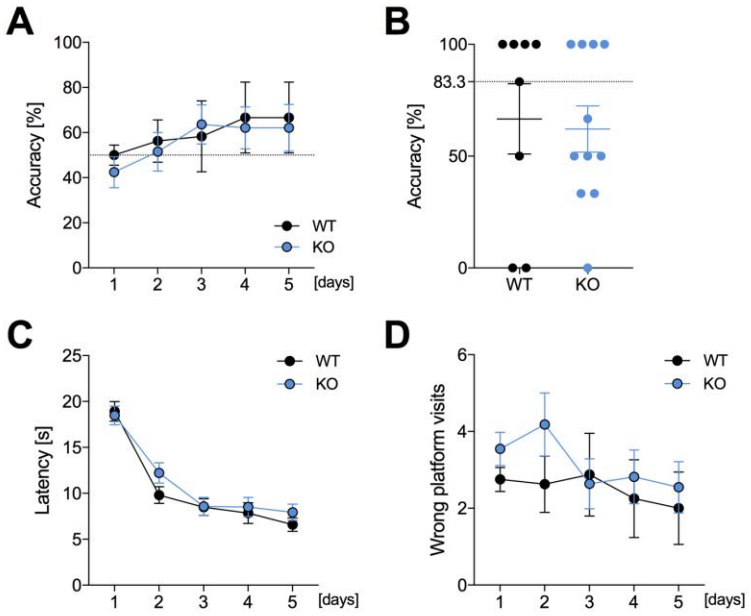

Figure 3.15: Water cross maze testing egocentric learning with KO mice.
*Mice were trained to find a hidden platform (N(WT)=8, N(KO)=9). No genotype difference was observed in the accuracy of finding the platform **(A)**, latency in finding the platform **(C)**, and wrong platform visits **(D)**. The accuracy of finding the platform on the fifth day also did not differ between genotypes **(B)**. Data presented as mean±S.E.M.*

A **hot plate** test was conducted to assess the pain threshold in mice. Mice were placed on a hot plate at 55°C and the latency to lick or shake the hind paws was recorded. Both WT and KO mice displayed similar latencies with no significant differences (Fig. 3.16; Student's *t*-test, t(13)=0.2474, p=0.8085).

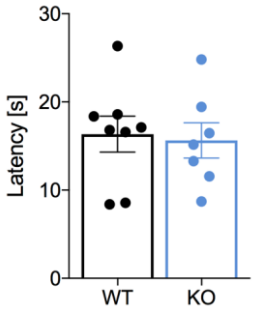

Figure 3.16: Hot plate test with KO mice.
Mice were placed on a hot plate to evaluate the pain sensitivity and no difference was observed between genotypes (N(WT)=8, N(KO)=7). Data presented as mean±S.E.M.

Mice were tested for associative learning using escapable and non-escapable conditioning tasks. As an escapable paradigm, an **active avoidance** test was performed where mice learned to avoid a foot shock by shuttling to the other compartment when a CS was presented. Data was analyzed over the course of five days and no significant difference in their correct runs between groups was observed (Fig. 3.17; N(WT)=5, N(KO)=8, Repeated measures 2-Way-ANOVA, F(1,11)=0.4862, p=0.5001).

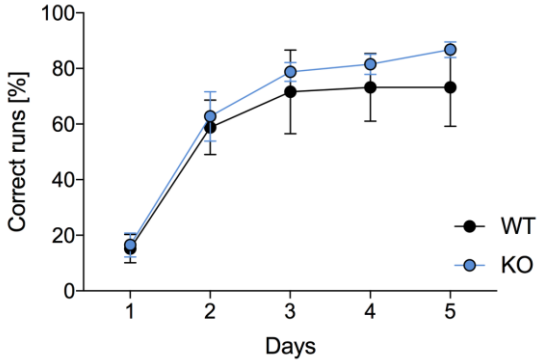

Figure 3.17: Active avoidance test with KO mice.
Mice were trained to avoid a foot-shock by shuttling to the other compartment and no significant difference was observed between genotypes (N(WT)=5, N(KO)=8). Data presented as mean±S.E.M.

Mice were **cued-fear conditioned** using a training protocol including 3 CS+-foot shock pairs. 24 h after training mice were introduced to a neutral context and were presented tones (1.2, 2.4, 5, and 10 kHz, 80 dB) including the CS+ (10 kHz, 80 dB). Mice were retested 14 days later in the same neutral context and tones. 24 h after the second neutral context retrieval, mice were reintroduced to the shock context. During the training session mice froze more post-training compared to pre-training (Fig. 3.18-A; N(WT)=8, N(KO)=11, Pre-training: Student's *t*-test, t(17)=1.065, p=0.3019, Post-training: Student's *t*-test, t(17)=2.16, p=0.0453). When individual freezing levels after each foot-shock during the training session was compared, a significant

difference was observed between genotypes where the KO mice showed an extreme high freezing behavior after the first foot shock (Fig. 3.18A; Repeated measures 2-Way-ANOVA, F(1,17)=15.39, p=0.0011, post-hoc Fisher's LSD) decreasing in time and coming to similar levels of the WT mice. The following day and 14 days later cue retrieval tests were done by presenting four tones, the CS+ and three CS-'s, and freezing levels were compared between genotypes. On both days mice froze less to the 1.2 and 2.4 kHz tones, and higher to the 5 and 10 kHz tones (Fig. 3.18B; Cue ret. D1: Repeated measures 2-Way-ANOVA, F(1,17)=2.316, p=0.1464; Cue ret. D2: Repeated measures 2-Way-ANOVA, F(1,17)=0.5741, p=0.4590) showing no impairment in the cue memory neither in long term memory (24 h after training) nor in remote memory. The freezing levels to the neutral context on both cue retrieval sessions was also investigated and there was no significant difference observed between genotypes (Fig. 3.18C; Neutral D1: Student's *t*-test, t(17)=0.494, p=0.6276, Neutral D14: Student's *t*-test, t(17)=1.432, p=0.1703). 24 after the last cue retrieval session, mice were placed back in the shock context and the freezing levels were recorded. Mice showed an increase in freezing behavior to the context yet there was no significant difference between genotypes (Fig. 3.18C; Shock D15: Student's *t*-test, t(17)=0.4778, p=0.6389).

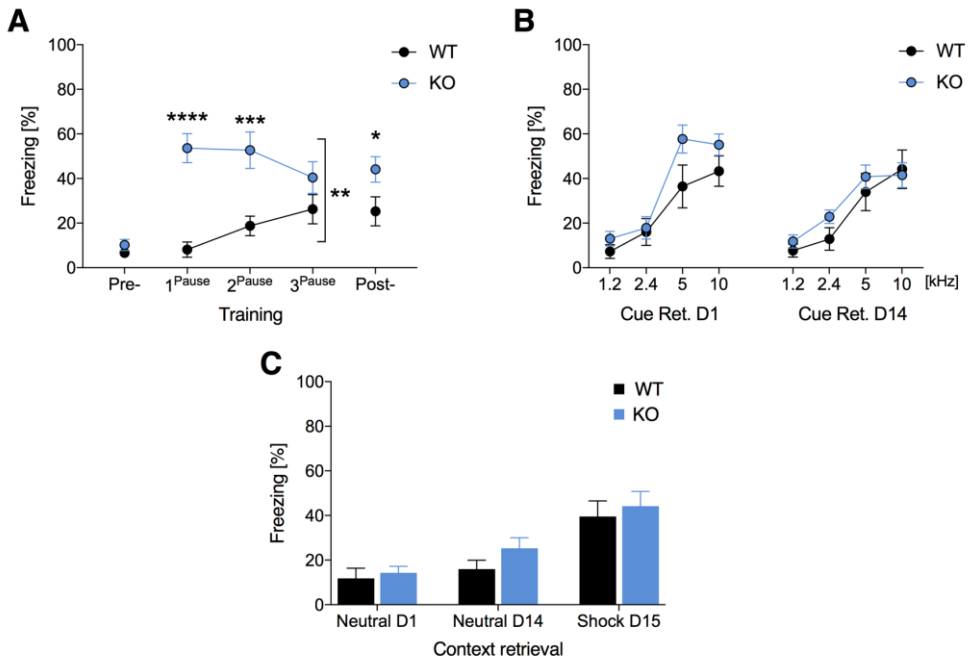

Figure 3.18: Cued-fear conditioning with KO mice.

(A) *Mice were trained by presenting 3 cues (CS+) terminating with a foot-shock. KO mice displayed higher freezing behavior during the pauses between the pairings and during the post-training (N(WT)=8, N(KO)=11). There was no genotypic difference during the cue retrievals; one day and two weeks after training* ***(B)*** *and during context retrievals* ***(C)****. Data presented as mean±S.E.M. *p<0.05, **p<0.01, ***p<0.001, ****p<0.0001.*

3.1.2 Ndr2 conditional-knockout mouse lines (cKO)

In addition to the constitutive Ndr2-knockout mouse line two conditional Ndr2-knockout mice lines underwent behavioral investigation, starting the gene knockout at different time points and cell types. The first conditional knockout mouse line was bred with the Emx1-Cre driver line as the second was with the CamKIIalpha-Cre.

3.1.2.1 Verification of the conditional-kncockout

Western blotting was performed with various areas of the brain (hippocampus, amygdala, pre-frontal cortex, and caudoputamen) collected from WT and cKO (cKO-camKII mouse used) mice using an Ndr2-antibody recognizing the N-terminus (OriGene). A major downregulation in the expression of Ndr2 was evident in the areas where camKIIalpha is highly expressed (Wang et al. 2013) (Fig. 3.19).

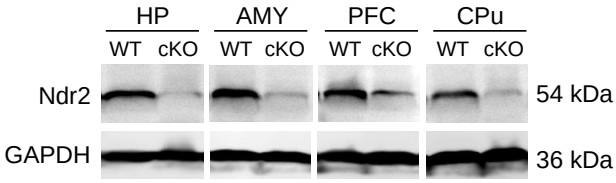

Figure 3.19: Ndr2 western blot for cKO tissue.
Western blot showing the loss of Ndr2 expression in various brain regions in the cKO mouse (cKO-camKII is shown in the figure). HP: hippocampus, AMY: amygdala, PFC: prefrontal cortex, CPu: caudoputamen.

3.1.2.2 cKO-emx

The knockout of the gene in mice generated with the Emx1-Cre driver line begins as early as e9.5 (embryonic) being more prominent at e17.5 and after birth. This model was used to investigate and compare the behavioral outcome of knocking out Ndr2 in a brain specific matter during the embryonic development.

3.1.2.2.1 Behavioral phenotyping of cKO-emx mice

Adult (2-6 months old) littermate WT and cKO-emx male mice were tested in behavioral tests to assess the outcome of the conditional-knockout of the *Ndr2* gene dependent on Emx1 expression.

The **home cage activity** was monitored for five consecutive days. The circadian rhythm between genotypes was not significantly different (Fig. 3.20, N(WT)=6, N(cKO-emx)=8; Repeated measures 2-Way-ANOVA, $F(1,12)=1.126$, $p=0.3095$). Mice were active during the dark phase compared to the light phase.

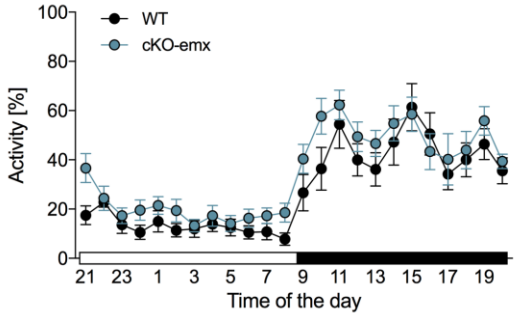

Figure 3.20: Home cage activity with cKO-emx mice.
The average activity over 24 hours is shown and no difference between genotypes was observed (N(WT)=6, N(cKO-emx)=8). White bar on the x-axis represents the time when the lights are on, black bar represents when the lights are off. Data presented as mean±S.E.M.

Next, anxiety-like behavior and exploration were tested. First a **light/dark transition test** was performed. Time spent in the dark and light compartments and the activity was compared and analyzed. Both genotypes spent more time in the dark compartment (Fig. 3.21A; N(WT)=6, N(cKO-emx)=8; Dark and light compartments, Mann-Whitney *U* test, U=13, p=0.1812) and less in the lit compartment. Mice were also more active in the dark compartment (Fig. 3.21B; Mann-Whitney *U* test, Dark: U=20, p=0.6620; Light: U=11, p=0.1079).

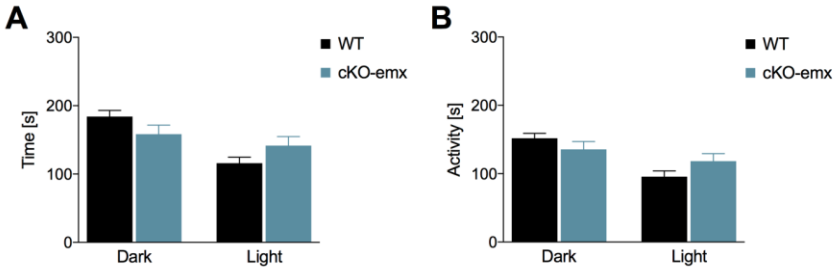

Figure 3.21: Light/dark transition test with cKO-emx mice.
*Mice did not show an anxiety like behavior and no difference was observed in the time spent in both compartments **(A)**, and the activity in the compartments **(B)** (N(WT)=6, N(cKO-emx)=8). Data presented as mean±S.E.M.*

Then, mice were tested in an **open field** box for two days under different light conditions. Mice freely explored the apparatus and the total distance they covered as well as the time spent in different sections of the box was compared between genotypes. Maze exploration on the first day, when the test was done in the dark, decreased over time as the mice habituated to the environment (Fig. 3.22A) and no significant difference was observed between genotypes (N(WT)=6, N(cKO-emx)=8; Repeated measures 2-Way-ANOVA, dark, F(1,12)=2.085, p=0.1743), whereas the following day under lit conditions the cKO mice showed significantly less exploration compared to the WT mice (Repeated measures 2-Way-ANOVA, light,

F(1,12)=5.326, p=0.0396). Time spent in the corners, rim as well as the center of the open field was not different between genotypes on the first day (Fig. 3.22B; Student's *t*-test, dark: corners, t(12)=0.1681, p=0.8693, rim, t(12)=0.1404, p=0.8907, center, t(12)=0.1217, p=0.9052), yet on the second day cKO-emx mice preferred the corners significantly more and the center significantly less compared to the WT mice (Student's *t*-test, light: corners, t(12)=2.498, p=0.0280, rim, t(12)=2.04, p=0.0639, center, t(12)=2.616, p=0.0225).

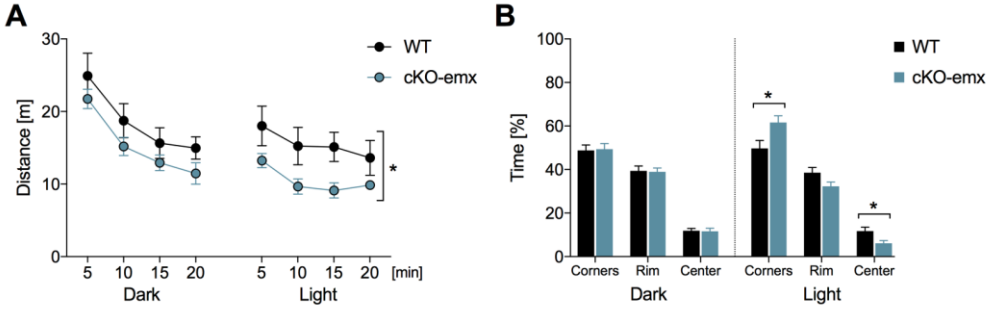

Figure 3.22: Open field test with cKO-emx mice.
A. *Total distance covered in the arena over 20-minutes in dark was not different between genotypes yet the cKO-emx mice explored the arena less under light conditions (N(WT)=6, N(cKO-emx)=8).* ***B.*** *Percentage of time spent in different areas of the arena (corners, rim, and center) was not different between groups in the dark but cKO-emx mice spent more time in the corners and less in the center under the light condition. Data presented as mean±S.E.M. *p<0.05.*

Mice were tested in an **elevated plus maze** 24 h after a fear-conditioning paradigm. Even though time spent in different compartments did not differ between genotypes (Fig. 3.23A; N(WT)=5, N(cKO-emx)=7; Student's *t*-test or Mann-Whitney *U* test, open arms:U=7.5, p=0.0985; closed arms: U=15, p=0.7551; center: t(10)=0.987, p=0.3469), entries to the open arms and closed arms were significantly different between genotypes (Fig. 3.23B; Student's *t*-test or Mann-Whitney *U* test, open arms: U=5.5, p=0.0303; closed arms: t(10)=2.623, p=0.0255; center: U=15, p=0.7222). Immobility in the maze was not significantly different between genotypes (Fig. 3.23C; Mann-Whitney *U* test, U=6, p=0.0732).

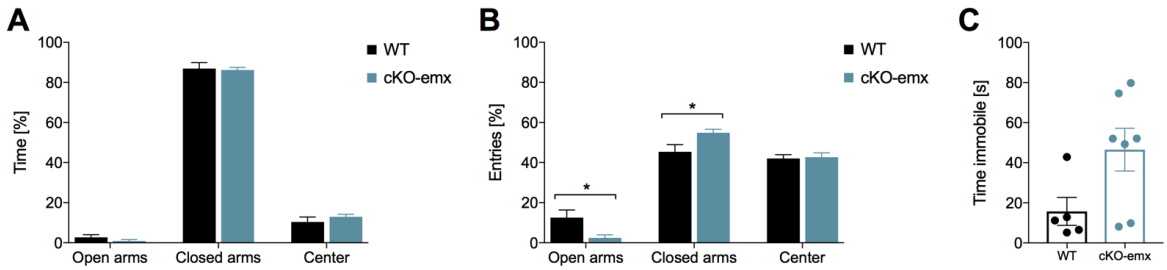

Figure 3.23: Elevated plus maze after fear conditioning with cKO-emx mice.
A. *Time spent in different areas of the maze was not different between genotypes (N(WT)=5, N(cKO-emx)=7).* ***B.*** *Percentage of entries on to the open arms was less for cKO-emx mice, more into the closed arm, and not different for the center.* ***C.*** *Time immobile during the 5-minute test was not different between genotypes. Data shown as mean±S.E.M. *p<0.05.*

Spatial and reversal learning and memory were tested using the **water cross maze** using the place learning protocol. Mice were trained to find the platform using external spatial cues. The accuracy in finding the platform, the latency, and the wrong platform visits were recorded and compared between genotypes. During the training session, in general WT and KO mice learned at the end of fifth day (Fig. 3.24A; N(WT)=5, N(cKO-emx)=8; Training: Repeated measures 2-Way-ANOVA, F(1,11)=0.303, p=0.5930). The latency of finding the platform (Fig. 3.24B; Training: Repeated measures 2-Way-ANOVA, F(1,11)=1.426, p=0.2575) and the wrong platform visits (Fig. 3.24C; Training: Repeated measures 2-Way-ANOVA, F(1,11)=1.146, p=0.3073) were not statistically different between genotypes during training. Mice who had 83.3% accuracy on the last day of training participated in the reversal-learning task. Regardless of the genotype, all mice relearned the position of the platform (Fig. 3.24A; N(WT)=2, N(cKO-emx)=3; Reversal: Repeated measures 2-Way-ANOVA, F(1,3)=0.8363, p=0.4279), with similar latencies to find the platform (Fig. 3.24B; Reversal: Repeated measures 2-Way-ANOVA, F(1,3)=5.095, p=0.1092) and wrong platform visits (Fig. 3.24C; Reversal: Repeated measures 2-Way-ANOVA, F(1,3)=0.2239, p=0.6684).

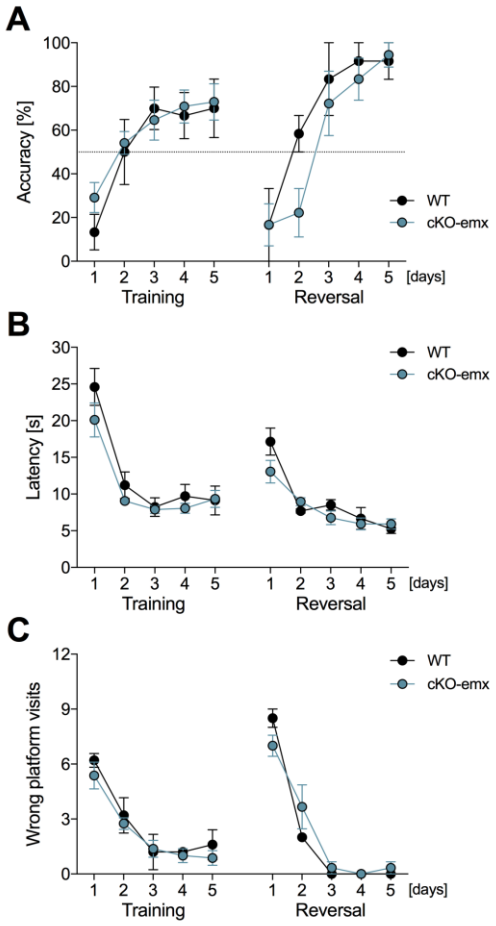

Figure 3.24: Water cross maze testing spatial learning with cKO-emx mice.
Mice were trained to find a hidden platform (N(WT)=5, N(cKO-emx)=8) and were tested to find the new position of the platform (N(WT)=2, N(cKO-emx)=3). No genotype difference was observed in the

*accuracy of finding the platform **(A)**, latency in finding the platform **(B)**, and wrong platform visits **(C)**. Data presented as mean±S.E.M.*

An **active avoidance** test was performed where mice learned to avoid a foot shock by shuttling to the other compartment when a CS was presented. Data was analyzed over the course of five days. No significant difference between genotypes was observed in the correct runs (Fig. 3.25; N(WT)=6, N(cKO-emx)=8, Repeated measures 2-Way-ANOVA, F(1,12)=0.06325, p=0.8057).

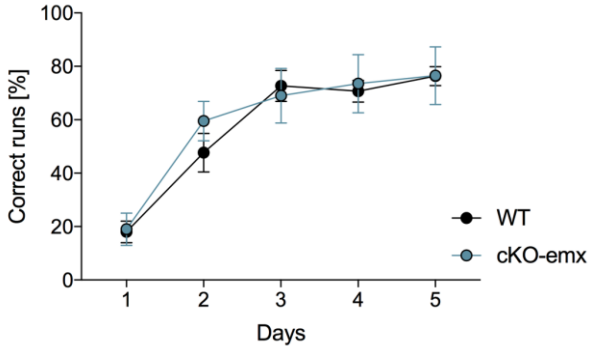

Figure 3.25: Active avoidance test with cKO-emx mice.
No difference in learning over the 5-day test was observed between genotypes (N(WT)=6, N(cKO-emx)=8). Data shown as mean±S.E.M.

Mice went through a **cued-fear conditioning** paradigm where they were trained with 3 cue-foot shock pairings. 24 h after training mice were introduced to a neutral context and were presented tones (1.2, 2.4, 5, and 10 kHz, 80 dB) including the CS+ (10 kHz, 80 dB). Mice were retested 14 days later in the same neutral context and tones. 24 h after the second neutral context retrieval, mice were reintroduced to the shock context. During the training session a higher freezing behavior was observed during the post-training compared to pre-training (Fig.3.26A; N(WT)=6, N(cKO-emx)=8, Pre-training: Mann-Whitney *U* test, U=23, p=0.9500, Post-training: Student's *t*-test, t(12)=0.03289, p=0.9743, Pause1-3: Repeated measures 2-Way-ANOVA, F(1,12)=0.02838, p=0.8690). The following day and 14 days later cue retrieval tests were done by presenting four tones, the CS+ and three CS-'s, and freezing levels were compared between genotypes yet no impairment in the cue memory neither in short term nor in remote memory was observed (Fig.3.26B; Cue ret. D1: Repeated measures 2-Way-ANOVA, F(1,12)=2.097, p=0.1732; Cue ret. D14: Repeated measures 2-Way-ANOVA, F(1,12)=3.769, p=0.0761). The freezing levels to the neutral context on both cue retrieval sessions was also investigated and there was no significant difference between genotypes (Fig.3.26C; Neutral D1: Mann-Whitney *U* test, U=21.5, p=0.7826, Neutral D14: Student's *t*-test, t(12)=0.7706,

p=0.4558). 24 after the last cue retrieval session, mice were placed back in the shock context and the freezing levels were recorded. Mice showed high freezing behavior to the context yet there was no significant difference between genotypes (Fig.3.26C; Shock D15: Student's *t*-test, t(12)=1.042, p=0.3182).

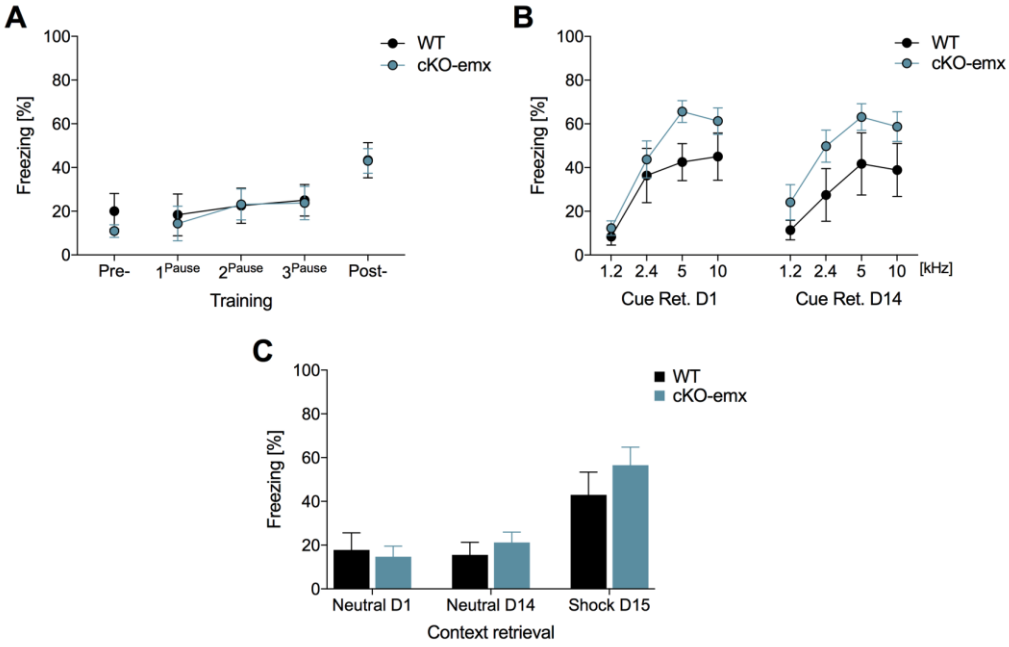

Figure 3.26: Cued-fear conditioning with cKO-emx mice.
(A) *Mice were trained by presenting 3 cues (CS+) terminating with a foot-shock and freezing levels was not different between genotypes (N(WT)=6, N(cKO-emx)=8). There was no genotypic difference during the cue retrievals at one day after training and two weeks later* ***(B)*** *and context retrievals* ***(C)****. Data presented as mean±S.E.M.*

3.1.2.3 cKO-camKII

The knockout of the gene in mice generated with the CamKIIalpha-Cre driver line begins around p20 (postnatal). This model was used to investigate and compare the behavioral outcome of knocking out Ndr2 in a brain specific matter bypassing the embryonic developmental stages.

3.1.2.3.1 Behavioral phenotyping of cKO-camKII mice

Adult (2-6 months old) littermate WT and cKO-camKII male mice underwent behavioral tests to assess the outcome of the conditional-knockout of the *Ndr2* gene dependent on the expression of CamKII-alpha.

Home cage activity was monitored for five consecutive days. The activity during the dark and light phase of the day between genotypes was significantly different between genotypes (Fig. 3.27, N(WT)=5, N(cKO-camKII)=6; Repeated measures 2-Way-ANOVA, F(1,9)=6.262,

p=0.0337). Even though mice from both genotypes were more active during the dark phase compared to the light phase, cKO mice less active compared to the WT mice.

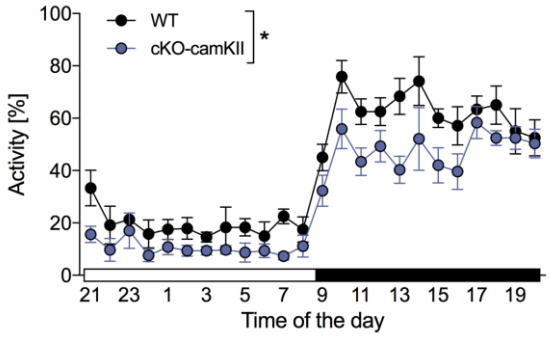

Figure 3.27: Home cage activity with cKO-camKII mice.
*The average activity over 24 hours is shown and the cKO-camKII mice were less active than their WT littermates (N(WT)=5, N(cKO-camKII)=6). White bar on the x-axis represents the time when the lights are on, black bar represents when the lights are off. Data presented as mean±S.E.M. *p<0.05.*

Anxiety-like behavior together with exploration and activity was tested using different experimental setups. First a **light/dark transition test** was performed. Time spent in the dark and light compartments and the activity was compared and analyzed. Both genotypes spent more time in the dark compartment (Fig. 3.28A; N(WT)=8, N(cKO-camKII)=9; Student's *t*-test; Dark, t(15)=1.780, p=0.0937; Light, t(15)=1.791, p=0.0935) and less in the lit compartment. Mice were also more active in the dark compartment (Fig. 3.28B; Student's *t*-test, Dark: t(15)=1.219, p=0.2416) however cKO mice were less active in the light compartment (Student's *t*-test, Light: t(15)=2.132, p=0.0500).

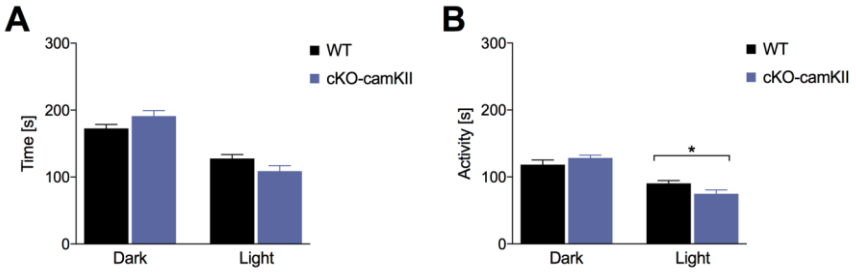

Figure 3.28: Light/dark transition test with cKO-camKII mice.
A. *No difference between genotypes was observed in the time spent in two compartments of the box (N(WT)=8, N(cKO-camKII)=9).* ***B.*** *The active time in the lit compartment was lower for the cKO-camKII mice yet the activity did not differ in the dark compartment. Data shown as mean±S.E.M. *p<0.05.*

Secondly, mice were tested in an **open field** for two days under different light conditions. Mice freely explored the apparatus and the total distance they covered as well as the time spent in different sections of the box was compared between genotypes. Maze exploration on the first day, when the test was done in the dark, decreased over time as the mice habituated to the environment however, exploration on the second day, tested in lit conditions, remained similar over time (Fig. 3.29A) and no significant difference was observed between genotypes on both days (N(WT)=10, N(cKO-camKII)=11; Repeated measures 2-Way-ANOVA, dark, $F(1,19)=0.1091$, $p=0.7448$; light, $F(1,19)=1.501$, $p=0.2354$). Time spent in the corners and the rim as well as the center of the open field arena was not different between genotypes on the first day (Fig. 3.29B; Student's *t*-test or Mann-Whitney *U* test, dark: corners, $U=37$, $p=0.2230$, rim, $t(19)=0.444$, $p=0.6621$, center, $U=31$, $p=0.0986$) yet on the second day, under light conditions, cKO mice spent significantly more time in the corners and less time in the center (Student's *t*-test; light: corners, $t(19)=2.434$, $p=0.0250$, rim, $t(19)=1.904$, $p=0.0723$, center, $t(19)=2.474$, $p=0.0230$).

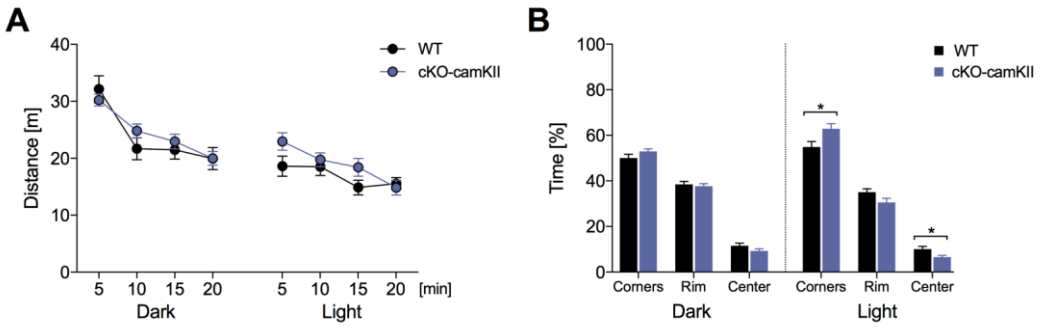

Figure 3.29: Open field test with cKO-camKII mice.
A. *Total distance covered in the apparatus over 20 days for dark and light conditions was not different between genotypes (N(WT)=10, N(cKO-camKII)=11).* ***B.*** *Time spent in different areas of the box was not different between genotypes under dark conditions but under light conditions cKO-camKII mice spent more time in the corners and less time in the center. Data shown as mean±S.E.M. *p<0.05.*

When mice were subjected to a fear conditioning paradigm and were tested in an **elevated plus maze** afterwards. Even though time spent in different compartments did not differ between genotypes (Fig. 3.30A; N(WT)=10, N(cKO-camKII)=11; Student's *t*-test or Mann-Whitney *U* test, open arms: $U=48$, $p=0.6363$; closed arms: $t(19)=1.789$, $p=0.0.0895$; center: $t(19)=1.972$, $p=0.0633$) together with the entries to the open and closed arms (Fig. 3.30B; Student's *t*-test, open arms: $t(19)=0.3782$, $p=0.7112$; closed arms: $t(19)=1.841$, $p=0.0813$), entries to the center was significantly less for the cKO mice (Student's *t*-test, center: $t(19)=3.777$, $p=0.0013$).

Immobility in the maze (Fig. 3.30C; Student's *t*-test, t(19)=0.2466, p=0.8079) was not different between genotypes.

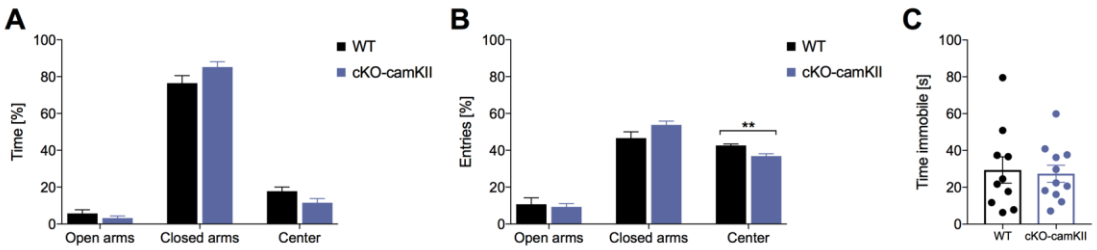

Figure 3.30: Elevated plus maze after cued-fear conditioning with cKO-camKII mice.
A. *Time spent in different areas of the maze was not different between genotypes (N(WT)=10, N(cKO-camKII)=11).* ***B.*** *Percentage of entries into the center was less for cKO-camKII mice and not different for the open and closed arms.* ***C.*** *Time immobile during the 5-minute test was not different between genotypes. Data shown as mean±S.E.M. *p<0.05.*

Mice were tested for associative learning using escapable and non-escapable conditioning tasks. As an escapable paradigm, an **active avoidance** test was performed where mice learned to avoid a foot shock by shuttling to the other compartment when a CS was presented. Data was analyzed over the course of five days and no significant difference in their correct runs between groups was observed (Fig. 3.31; N(WT)=5, N(cKO-camKII)=6, Repeated measures 2-Way-ANOVA, F(1,9)=0.3139, p=0.5890).

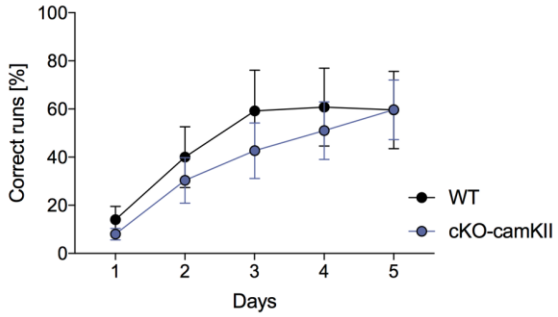

Figure 3.31: Active avoidance with cKO-camKII mice.
No difference was observed between genotypes in the learning of the paradigm (N(WT)=5, N(cKO-camKII)=6). Data shown as mean±S.E.M.

Mice were tested for **cued-fear conditioning** using a training protocol with 3-cue (CS+)-foot shock pairs with different memory retrieval tests. One group of mice were introduced to a neutral context and were presented tones (1.2, 2.4, 5, and 10 kHz, 80 dB) including the CS+ (10 kHz, 80 dB) 24 h after training. Mice were retested 14 days later in the same neutral context and with the same tones. 24 h after the second neutral context retrieval, mice were reintroduced to the shock context. During the training session no difference was observed between genotypes in freezing behavior (Fig. 3.32A; N(WT)=10, N(cKO-camKII)=11, Student's *t*-test or Mann-

Whitney *U* test; Pre-training: t(19)=0.1226, p=0.9037, Post-training: U=22, p=0.0184, Pause1-3: Repeated measures 2-Way-ANOVA, F(1,19)=0.6744, p=0.4217). The following day and 14 days later cue retrieval tests were done by presenting four tones, the CS+ and three CS-'s, and freezing levels were compared between genotypes. On day 1 mice from both genotypes froze less to the 1.2 and 2.4 kHz tones, higher to the 5 and 10 kHz tones (Fig. 3.32B; Repeated measures 2-Way-ANOVA, Cue ret. D1: F(1,19)=3.724, p=0.0687) showing no impairment in the long term cue memory. However, two weeks later cKO-camKII mice presented lower freezing behavior to 5 kHz and 10 kHz (CS+) (Repeated measures 2-Way-ANOVA, Cue ret. D14: F(1,19)=6.628, p=0.0186) indicating an impairment in the remote memory. The freezing levels to the neutral context on both cue retrieval sessions was also investigated and there was no significant difference observed between genotypes (Fig. 3.32C; Student's *t*-test or Mann-Whitney *U* test; Neutral D1: t(19)=0.06297, p=0.9505, Neutral D14: U=44, p=0.4568). 24 after the last cue retrieval session, mice were placed back in the shock context and the freezing levels were recorded. Mice showed an increase in freezing behavior to the shock context however, cKO mice froze significantly less to the context compared to the WT mice indicating a remote context memory deficiency (Fig. 3.32C; Shock D15: Student's *t*-test, t(19)=2.541, p=0.0199).

A second group of mice was tested for remote cue and context memory without having a cue reminder session 24 h after training. During the training session mice froze significantly higher post-training compared to pre-training (Fig. 3.32D; N(WT)=6, N(cKO-camKII)=8, Student's *t*-test; Pre-training: t(12)=0.8918, p=0.3900, Post-training: t(12)=1.003, p=0.3355, Pause1-3: Repeated measures 2-Way-ANOVA, F(1,12)=0.04082, p=0.8433). 14 days later a cue retrieval test was done by presenting four tones, the CS+ and three CS-'s, and freezing levels were compared between genotypes. Mice froze less to the 1.2 and 2.4 kHz tones, as higher to the 5 and 10 kHz tones (Fig. 3.32E; Cue ret. D14: Repeated measures 2-Way-ANOVA, F(1,12)=0.2183, p=0.6487) showing no impairment in remote memory. The freezing levels to the neutral context was also investigated and there was no significant difference observed between genotypes (Fig. 3.32F; Student's *t*-test; Neutral D14: t(12)=0.07974, p=0.9377). 24 after the cue retrieval session, mice were placed back in the shock context and the freezing levels were recorded. Mice showed an increase in freezing behavior to the context and there was no significant difference between genotypes (Fig. 3.32F; Shock D15: Student's *t*-test, t(12)=0.6346, p=0.5375).

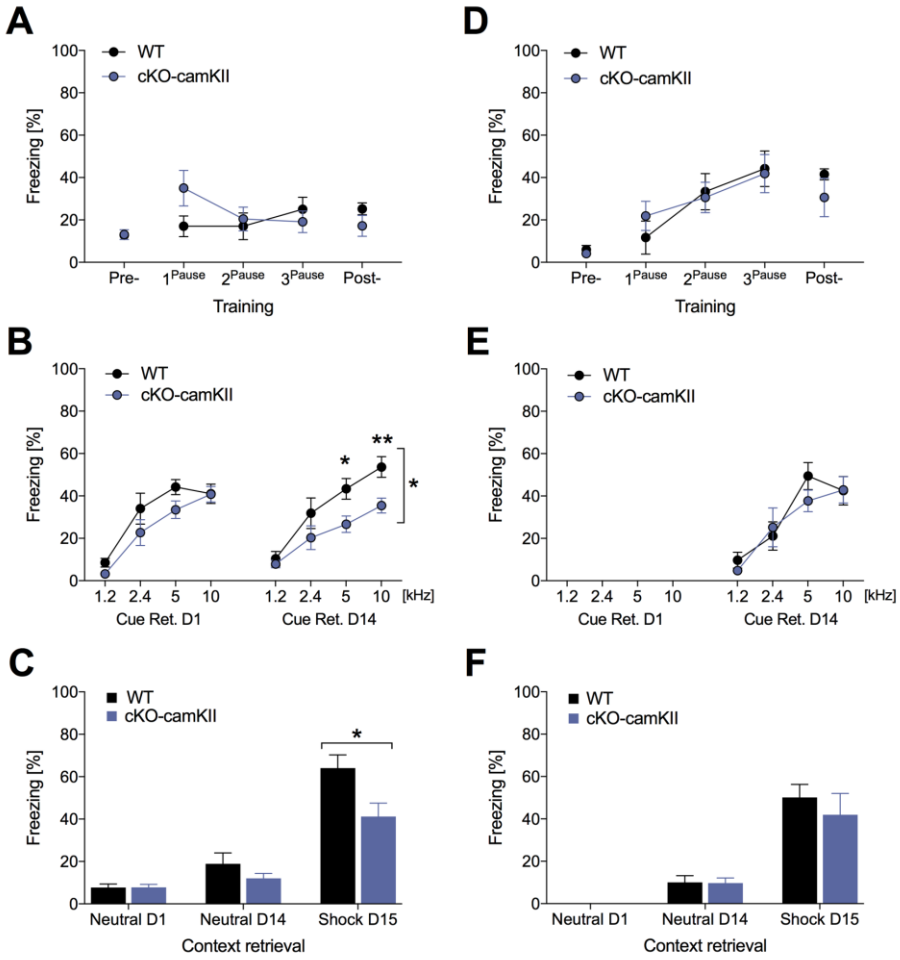

Figure 3.32: Cued-fear conditioning with cKO-camKII mice.

Two separate groups were tested with different retrieval protocols. ***A.*** *Mice were trained with 3 cue-foot-shock pairings and no difference was observed between genotypes (N(WT)=10, N(cKO-camKII)=11).* ***B.*** *One day and 14 days after training mice were tested for the cue memory in a neutral context. On the first retrieval day no difference was observed yet two weeks later cKO-camKII mice froze less to the cue tone (10 kHz).* ***C.*** *Freezing levels to the neutral contexts themselves was not different but freezing to the context was lower for the cKO-camKII mice.* ***D.*** *The second group of mice were trained with the same 3 cue-foot-shock pairings and no difference was observed between genotypes (N(WT)=6, N(cKO-camKII)=8).* ***E.*** *Mice were tested for the cue memory on 14 days after the training in the neutral context and no difference was observed.* ***F.*** *Neither in the neutral context nor in the shock context mice displayed a different freezing behavior. Data shown as mean±S.E.M. *p<0.05, **p<0.01.*

3.2 Ndr2-overexpressing mouse lines

3.2.1 Verification of the transgene expression

Western blotting was done with the subregions of the hippocampus (CA1, CA3, and DG) and cerebellum collected from WT and TG (TG-camKII mouse used) mice using an Ndr2-antibody recognizing the N-terminus (OriGene). The transgene expression could be confirmed due to the size shift as the Ndr2 protein is fused with EGFP presenting a band at ~85 kDa only in the TG samples (Fig. 3.33). Endogenous expression of Ndr2 in both WT and TG samples were evident.

The transgene expression was not observed in the cerebellum due to the expression specificity of camKII-alpha.

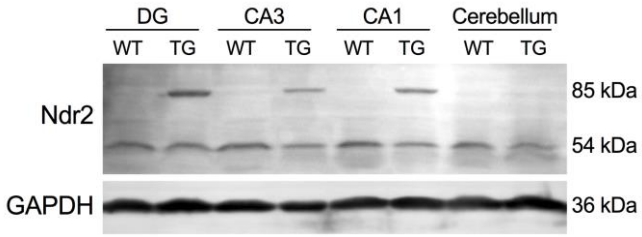

Figure 3.33: Western blot showing the overexpression of Ndr2 in the hippocampus and cerebellum. *The fusion protein could be detected at 85 kDa through the molecular weight shift and is separated from the endogenous Ndr2. The TG tissue sample from the cerebellum does not show a transgenic signal confirming the regional specificity of CamKII-alpha-cre mediated activation.*

3.2.2 TG-emx

This model was used to investigate and compare the behavioral outcome of overexpressing Ndr2 in a brain specific matter during the embryonic development. The overexpression of Ndr2 begins as early as e9.5 (embryonic) being more prominent at e17.5 and after birth.

3.2.2.1 Behavioral phenotyping of TG-emx mice

Adult (2-6 months old) male WT and TG-emx littermate mice underwent behavioral tests to assess the outcome of the conditional-overexpression of the *Ndr2* gene under the Emx1 promoter.

Home cage activity was monitored for five consecutive days. The circadian rhythm between genotypes was not significantly different (Fig. 3.34, N(WT)=7, N(TG-emx)=5; Repeated measures 2-Way-ANOVA, $F(1,10)=4.941$, $p=0.0504$). Mice were active during the dark phase and less active during the light phase.

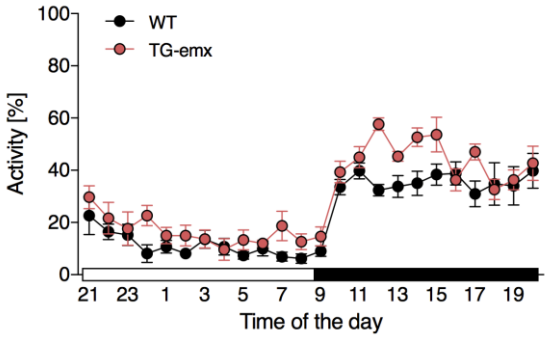

Figure 3.34: Home cage activity with TG-emx mice.
The average activity over 24 hours was not different between genotypes (N(WT)=7, N(TG-emx)=5). White bar on the x-axis represents the time when the lights are on, black bar represents when the lights are off. Data shown as mean±S.E.M.

An **elevated plus maze** test was done. The time spent in the arms, the number of entries to the arms, and the total time immobile in the maze was analyzed and compared. Mice from both genotypes preferred to spend more time in the closed arm and less time in the open arm and the center (Fig. 3.35A; N(WT)=6, N(TG-emx)=7; Student's *t*-test or Mann-Whitney *U* test, open arms: t(11)=0.09848, p=0.9233; closed arms: U=19, p=0.8357; center: t(11)=0.05392, p=0.9580), and entered the open arms less than the closed arms (Fig. 3.35B; Student's *t*-test, open arms: t(11)=1.451, p=0.1748; closed arms: t(11)=1.503, p=0.1610; center: t(11)=0.02106, p=0.9836). Immobility in the maze was also analyzed, yet no significant difference was observed between genotypes (Fig. 3.35C; Student's *t*-test, t(11)=0.4421, p=0.6670).

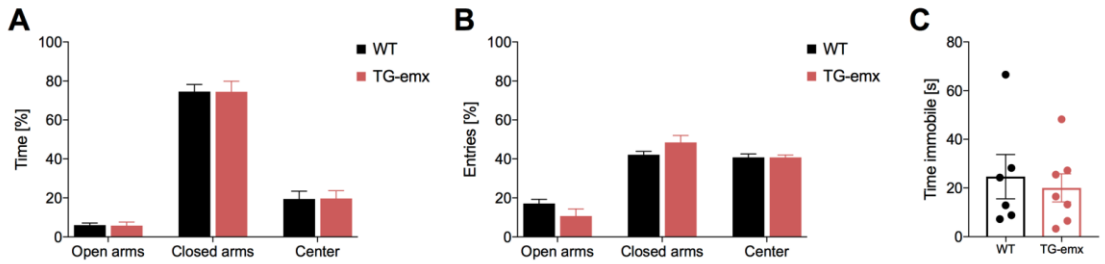

Figure 3.35: Elevated plus maze test with TG-emx mice.
Time spent in open and closed arms and the center ***(A)*** *and the percentage of entries to these areas of the maze* ***(B)*** *was not different between genotypes (N(WT)=6, N(TG-emx)=7).* ***C.*** *Time immobile during the 5-minute test was not different either between genotypes. Data shown as mean±S.E.M.*

Mice were tested in an **open field** box for two days under different light conditions. Mice freely explored the apparatus; the total distance they covered and the time spent in different sections of the box was compared between genotypes. Maze exploration on the first day, when the test was done in the dark, decreased over time as the mice habituated to the environment however, exploration on the second day, tested in lit conditions, remained similar over time (Fig. 3.36A) and no significant difference was observed between genotypes on both days (N(WT)=7, N(TG-emx)=6; Repeated measures 2-Way-ANOVA, dark, F(1,11)=1.443, p=0.2548; light, F(1,11)=2.075, p=0.1776). Also time spent in the corners and the rim as well as the center of the open field arena was not different between genotypes on the first day (Fig. 3.36B; Student's *t*-test, dark: corners, t(11)=0.03741, p=0.9708, rim, t(11)=0.799, p=0.4412, center, t(11)=0.6205, p=0.5476) yet TG mice preferred the rims less and the corners more on the second day (Student's *t*-test, light: corners, t(11)=2.109, p=0.0587, rim, t(11)=2.999, p=0.0121, center, t(11)=0.4827, p=0.6388).

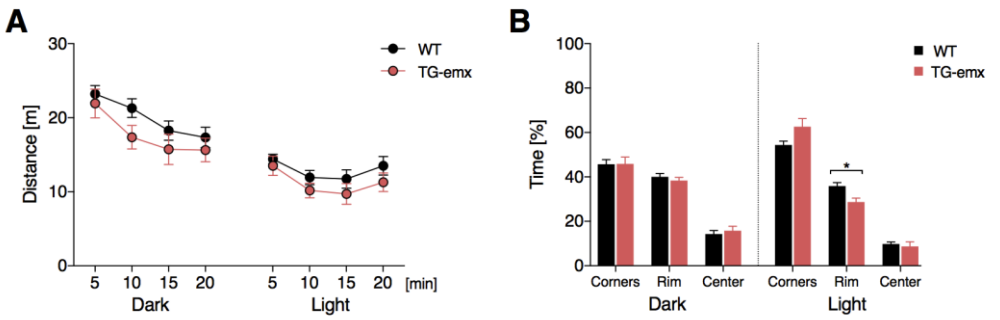

Figure 3.36: Open field test with TG-emx mice.
A. *Distance covered in the apparatus was not different between genotypes on both days under dark and light conditions (N(WT)=7, N(TG-emx)=6).* ***B.*** *Time spent in different areas of the arena was not different under dark conditions yet under light conditions TG-emx mice spent less time at the rim of the arena. Data shown as mean±S.E.M. *p<0.05.*

Sociability and social memory were tested using a **3-chamber social interaction test**. After mice were habituated to the apparatus and the chambers for 5 minutes, an interaction partner was put into one of the tubes and afterwards a second interaction partner was added to the empty tube and time spent with the partners was evaluated 5 minutes each. During habituation, mice did not show a preference toward any tube (N(WT)=6, N(TG-emx)=7, Fig. 3.37A,B Habituation: Student's *t*-test or Mann-Whitney *U* test, A- t(11)=0.4638, p=0.6518, B- tube1 t(11)=0.8094, p=0.4354, tube2 U=20, p=0.9452). In the social test mice from both genotypes spent more time with the interaction partner (Fig. 3.37A,B Social test: Student's *t*-test, A- t(11)=0.2047, p=0.8416, B- tube1 t(11)=0.9153, p=0.3796, tube2 t(11)=1.201, p=0.2550). At the last session of the test, when a second interaction partner was included, the attention of the test mice shifted toward the novel partner (Fig. 3.37A,B New partner: Student's *t*-test or Mann-Whitney *U* test, A- t(11)=0.06134, p=0.9522, B- tube1 U=12, p=0.2343, tube2 U=12, p=0.2343).

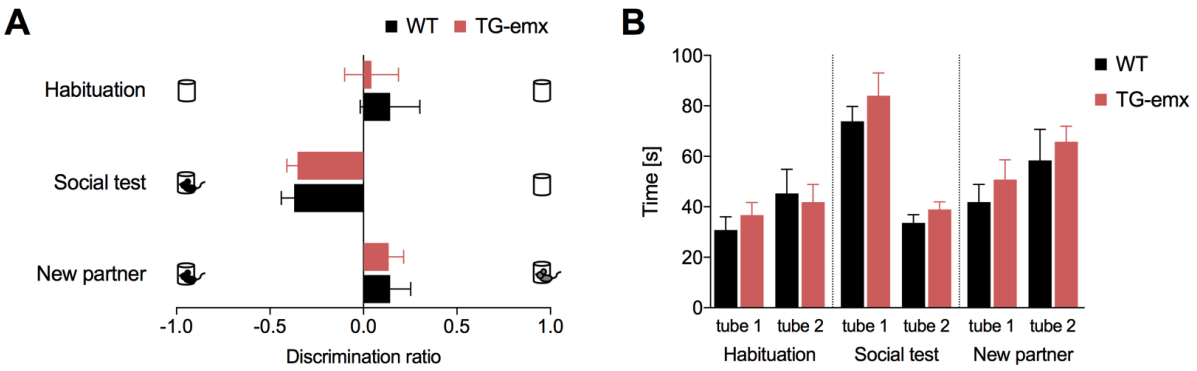

Figure 3.37: 3-chamber social interaction test with TG-emx mice.

A. *Discrimination ratio was calculated for three stages of the test and no difference was observed between genotypes (N(WT)=6, N(TG-emx)=7). During habituation mice did not show a preference to the empty holders while during the social test mice from both genotypes preferred to interact with the stranger mouse. When a second unfamiliar partner was introduced the attention of the test mice shifted to the newer one.* ***B.*** *Total time spent with the tubes with or without social partners was not different between genotypes. "tube 1" indicated the first social partner, "tube 2" the unfamiliar second social partner. Data shown as mean±S.E.M.*

Spatial and reversal learning and memory were tested using the **water cross maze** using the place learning protocol. Mice were trained to find the platform using external spatial cues. The accuracy in finding the platform, the latency, and the wrong platform visits were recorded and compared between genotypes. During the training session, in general WT and TG-emx mice learned at the end of fifth day (Fig. 3.38A; N(WT)=6, N(TG-emx)=7; Training: Repeated measures 2-Way-ANOVA, $F(1,11)=0.2714$, $p=0.6127$). The latency of finding the platform (Fig. 3.38B; Training: Repeated measures 2-Way-ANOVA, $F(1,11)=0.03388$, $p=0.8573$) and the wrong platform visits (Fig. 3.38C; Training: Repeated measures 2-Way-ANOVA, $F(1,11)=1.992$, $p=0.1858$) were not statistically different between genotypes during training. Mice who had 83.3% accuracy on the last day of training participated in the reversal-learning task. Regardless of the genotype, all mice relearned the position of the platform (Fig. 3.38A; N(WT)=5, N(TG-emx)=6; Reversal: Repeated measures 2-Way-ANOVA, $F(1,9)=0.8948$, $p=0.3689$), with similar latencies to find the platform (Fig. 3.38B; Reversal: Repeated measures 2-Way-ANOVA, $F(1,9)=0.1024$, $p=0.7563$) and wrong platform visits (Fig. 3.38C; Reversal: Repeated measures 2-Way-ANOVA, $F(1,9)=0.01792$, $p=0.8965$).

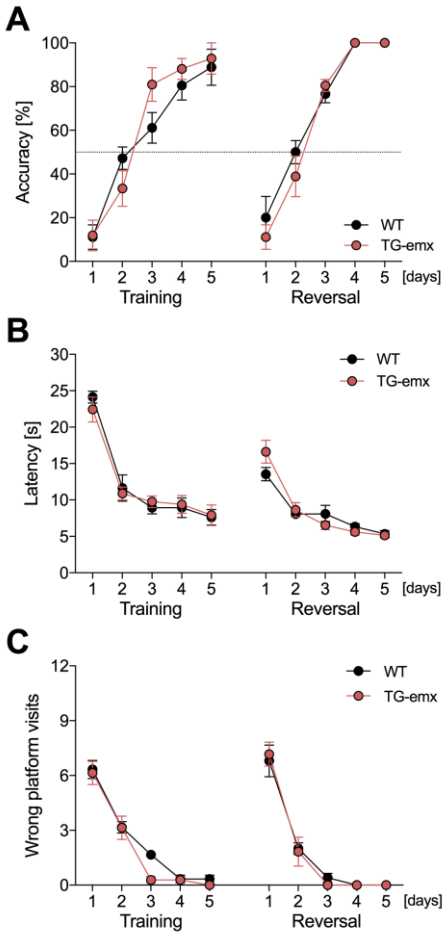

Figure 3.38: Water cross maze testing spatial learning with TG-emx mice.
Mice were trained to find a hidden platform (N(WT)=6, N(TG-emx)=7) and were tested to find the new position of the platform (N(WT)=5, N(TG-emx)=6). No genotype difference was observed in the accuracy of finding the platform ***(A)****, latency in finding the platform* ***(B)****, and wrong platform visits* ***(C)****. Data presented as mean±S.E.M.*

Mice were tested in an **active avoidance** test where mice learned to avoid a foot shock by shuttling to the other compartment when a cue was presented. Correct runs were analyzed over the course of five days and no significant difference between genotypes was observed (Fig. 3.39; N(WT)=7, N(TG-emx)=6, Repeated measures 2-Way-ANOVA, F(1,11)=0.3029, p=0.5931).

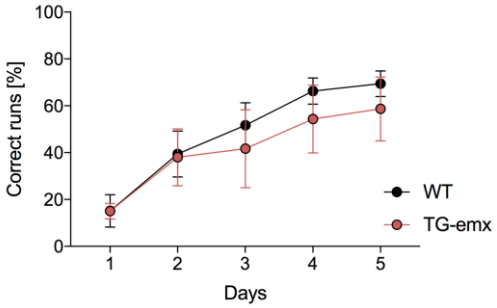

Figure 3.39: Active avoidance test with TG-emx mice.
No difference between genotypes was observed in the learning paradigm (N(WT)=7, N(TG-emx)=6). Data shown as mean±S.E.M.

For non-escapable conditioning, **cued-fear conditioning** was done with cue and context retrieval sessions. WT and TG mice were trained with a tone-foot shock pairing and were tested for cue and contextual memory 24 and 48 hours after the training sessions respectively. Freezing behavior during the test was used as a measurement of learning. Mice showed elevated freezing levels after receiving three foot shocks paired to a tone (CS+, 10 kHz, 80 dB) compared to pre-training (Fig. 3.40A; N(WT)=6, N(TG-emx)=7, Student's *t*-test, Pre-training: t(11)=0.3479, p=0.7345, Post-training: t(11)=0.9338, p=0.3705, Pause1-3: Repeated measures 2-Way-ANOVA, F(1,11)=0.09004, p=0.7697). No significant difference was observed between genotypes in the shock context retrieval and neutral context (Fig. 3.40B; Student's *t*-test, Neutral context: t(11)=1.327, p=0.2114, Shock context:, t(11)=0.6105, p=0.5539). There was also no significant difference between genotypes when CS- and CS+ were presented (Fig. 3.40C; Student's *t*-test, CS-: t(11)=1.363, p=0.19998, CS+: t(11)=0.08637, p=0.9327). An elevation in freezing was observed when mice were exposed to the shock context and the CS+.

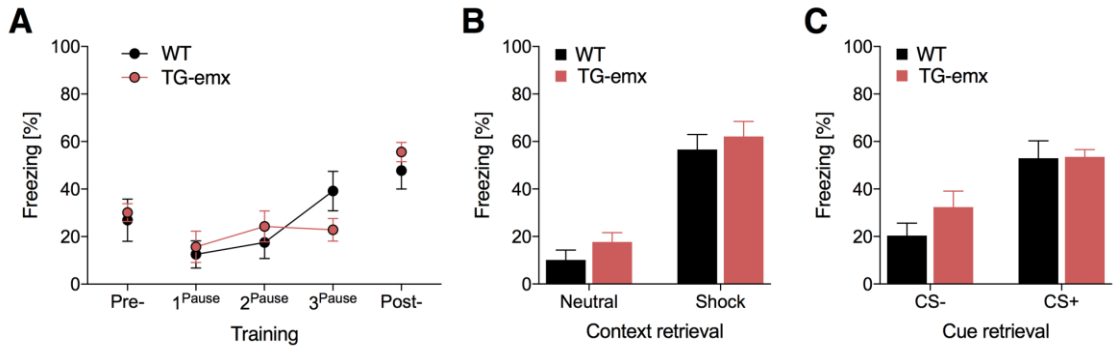

Figure 3.40: Cued-fear conditioning with TG-emx mice.
A. *Mice were trained with 3 cue-foot shock pairings and no difference was observed in the freezing behavior between genotypes (N(WT)=6, N(TG-emx)=7).* ***B.*** *24 and 48 hours after the training mice were exposed to a neutral context and the shock context respectively and a difference between genotypes was not evident for both contexts.* ***C.*** *In the neutral context, mice were presented with a CS- (2.4 kHz) and CS+ (10 kHz) tone and freezing levels were not different between genotypes. Data shown as mean±S.E.M.*

3.2.3 TG-camKII

This model was used to investigate and compare the behavioral outcome of overexpressing Ndr2 in a brain specific matter after embryonic development. The overexpression of Ndr2 begins around p20.

3.2.3.1 Behavioral phenotyping of TG-camKII mice

Adult (2-6 months old) littermate WT and TG-camKII male mice underwent behavioral tests to assess the outcome of the conditional-overexpression of the *Ndr2* gene under the CamKIIalpha promoter.

Home cage activity was monitored for five consecutive days. The circadian rhythm between genotypes was not significantly different (Fig. 3.41, N(WT)=10, N(TG-camKII)=8; Repeated measures 2-Way-ANOVA, F(1,16)=1.048, p=0.3212). Mice were active during the dark phase and less active during the light phase.

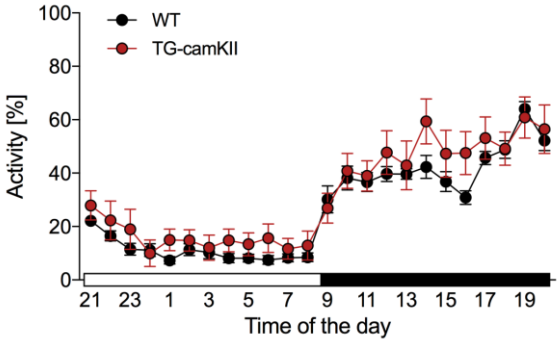

Figure 3.41: Home cage activity with TG-camKII mice.
The average activity over 24 hours was not different between genotypes (N(WT)=10, N(TG-camKII)=8). White bar on the x-axis represents the time when the lights are on, black bar represents when the lights are off. Data shown as mean±S.E.M.

Spatial and reversal learning and memory were tested using the **water cross maze** using the place learning protocol. Mice were trained to find the platform using external spatial cues. The accuracy in finding the platform, the latency, and the wrong platform visits were recorded and compared between genotypes. During the training session, in general WT and TG-camKII mice learned at the end of fifth day (Fig. 3.42A; N(WT)=15, N(TG-camKII)=12; Training: Repeated measures 2-Way-ANOVA, F(1,25)=0.4722, p=0.4983). The latency of finding the platform (Fig. 3.42B; Training: Repeated measures 2-Way-ANOVA, F(1,25)=1.098, p=0.3047) and the wrong platform visits (Fig. 3.42C; Training: Repeated measures 2-Way-ANOVA, F(1,25)=0.043, p=0.8374) were not statistically different between genotypes during training. Mice who had 83.3% accuracy on the last day of training participated in the reversal-learning task. Regardless of the genotype, all mice relearned the position of the platform (Fig. 3.42A; N(WT)=8, N(TG-camKII)=8; Reversal: Repeated measures 2-Way-ANOVA, F(1,14)=0.5631, p=0.4655). The latency in finding the platform was significantly higher for the TG mice (Fig. 3.42B; Reversal: Repeated measures 2-Way-ANOVA, F(1,14)=4.096, p=0.0625). Wrong

platform visits also was not significantly different between genotypes (Fig. 3.42C; Reversal: Repeated measures 2-Way-ANOVA, F(1,14)=0.164, p=0.6916).

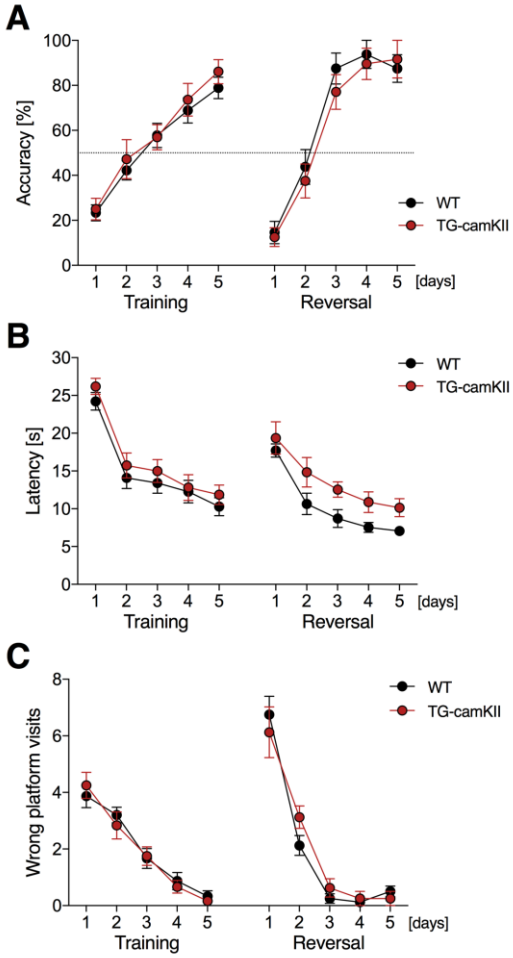

Figure 3.42: Water cross maze testing spatial and reversal learning with TG-camKII mice. *Mice were trained to find a hidden platform (N(WT)=15, N(TG-camKII)=12) and were tested to find the new position of the platform (N(WT)=8, N(TG-camKII)=8). No genotype difference was observed in the accuracy of finding the platform* ***(A)****, latency in finding the platform* ***(B)****, and wrong platform visits* ***(C)****. Data presented as mean±S.E.M*

4 Discussion

The function of the Ndr2 kinase in the mouse brain on morphology and behavior underwent investigation. To address this, several genetic models were used in an attempt to dissect the effect of knocking-out or over-expressing Ndr2 at different developmental stages and cell types. The germ line Ndr2-knockout (KO) mouse line was investigated for neuronal morphology and behavioral deficits, whereas the conditional Ndr2-knockout (cKO) lines and the Ndr2-overexpressing transgenic (TG) mouse lines were subjected to behavioral phenotyping.

4.1 Ndr2 expression and neuronal morphology

NDR kinases have been shown to regulate neurite outgrowth and branching in various species. The consequences of loss or gain of Ndr2 expression on neuronal morphology *in vivo* in mice was studied using genetic mouse models. The impact of constitutively knocking out Ndr2 was investigated using adult KO mice. Through immunohistochemical stainings against the β-galactosidase reporter in the KO mice, a prominent expression of Ndr2 in the hippocampus, especially in the CA3 pyramidal neurons was observed. This result has also confirmed the previously shown Ndr2 mRNA expression via *in situ* hybridization done in mouse brain tissue (Stork et al. 2004). Observing the Ndr2 expression in the CA3 pyramidal neurons, as a next step I investigated the dendritic branching of the CA3-pyramidal neurons using the Golgi-Cox staining method. A particular property of this method is that a low number of neurons are randomly filled (1-3%) thus enabling observation and tracing of single neurons' axons and dendrites. Horizontal sections obtained from KO and littermate WT adult mice were used to trace the dendrites of CA3 pyramidal neurons, followed by Sholl analysis in order to compare the total length of branches of the basal and apical dendrites. Whereas no difference in the dendritic complexity in the basal dendrites was observed, the apical dendrite complexity was shifted toward the soma of the KO neurons. When the length of the first order branch of the apical dendrites was investigated it was observed that the KO dendrites were shorter thus causing the premature branching phenotype. In addition, the spine density of CA1 and CA3 pyramidal neurons were measured from the samples stained using the Golgi-Cox method (work done by Dr. Atsuhiro Tsutiya). Even though there was no change in the basal and apical dendrite spine density in the CA3 pyramidal neurons, the CA1 basal and apical dendrite spine density was reduced in the KO neurons (unpublished data). Previously it has been shown that Ndr2, through regulating actin cytoskeleton rearrangement (Stork et al. 2004) and inside-out

activation and trafficking of β1-integrin (Rehberg et al. 2014) controls cells adhesion and neurite outgrowth. Furthermore, it has been recently shown that Ndr2 regulates the α1β1-integrin distribution on the cell surface and activity, regulating neurite outgrowth in PC12 cells (Demiray et al. 2018). In the Ndr2-KO CA3 pyramidal neurons, it is likely that the premature branching of the apical dendrite is a result of an impairment in the β1-integrin signaling regulating, which regulates dendritic growth and branching through extracellular cues. A similar phenotype was also observed in Semaphorin 3A (Sema3A) knockout mice, where an abnormal neuronal morphology in the CA1 pyramidal neurons were evident (Schlomann et al. 2009). In these mice, first order apical dendrites branched earlier disrupting the branching organization, which has in turn been shown to be β1-integrin signaling and FAK (focal adhesion kinase) activation dependent. In the Ndr2-KO mice, the experiments indicating a change in the dendritic morphology in CA3 and in the spine density in CA1 were accompanied by LTP recordings in dorsal CA1 (work done by Hussam Hayani). In hippocampal slices, after LTP induction with high frequency stimulation (HFS), it has been shown that there was a reduction in the late phase of the LTP with the KO mice. The observed phenotype was rescued by introducing RGD (Arginylglycylaspartic acid) peptides to the slices to activate the surface integrins (unpublished data). This data also suggests that Ndr2 regulates the surface β1-integrin activation and trafficking. On the other hand, a previous study had shown that Ndr1 and Ndr2 together negatively regulate dendritic growth and branching in the rat hippocampus, yet knocking-down Ndr2 individually did not affect the dendritic length (Ultanir et al. 2012). In the mouse brain, Ndr1 expression on the protein level is not observed neither during postnatal development (Rehberg et al. 2014) nor in adulthood. The opposing results observed in these different circumstances might be due to the differential expression profile between species and function of Ndr1 in the brain of the rat.

In primary hippocampal cultures prepared from WT and KO mice, immunocytochemical staining against PSD95 has shown that clusters positive for PSD95 on the dendrites are significantly reduced in the KO cells and this could be rescued when cells are transfected with Ndr2 (work done by Dr. Atsuhiro Tsutiya, unpublished data). Furthermore, TTX (tetrodotoxin) treatment (by blocking the voltage gated sodium channels, it inhibits the propagation of action potentials) decreased the PSD95 intensity in WT cells while KO cells were not affected. This might suggest that Ndr2 plays a role in spine development and neuronal activity. To validate the observed difference in PSD95 *in vivo*, synaptosome fractionation was performed with hippocampal tissue from both WT and KO mice, and the PSD95 expression in the synaptosome

was compared between genotypes. Western blot analysis revealed that there was no significant difference between genotypes in PSD95 expression in the synaptosomes. The difference in the results between *in vitro* and *in vivo* might be a consequence of the difference in the resolution between different quantification methods. Moreover, in the hippocampal synaptosome fractions, the whole hippocampus was present. Since there is an Ndr2 expression difference in the hippocampal subregions, the small molecular changes might be shadowed.

Besides the expression profile of Ndr2 in the hippocampus, a prominent expression was observed in the Purkinje cells in the cerebellum and also in the red nucleus (one of the structures that control body movement). Tests done with the KO mice however, did not reveal any motor function impairments. The behavioral tests performed rely on the motor skills of the mice and the performance between the WT and KO mice was not different.

In contrast to the Ndr2-knockout, axonal morphology was investigated in the Ndr2-TG mice overexpressing Ndr2 under the CamKIIalpha promoter (work done by Dr. Kati Rehberg, Dr. Iris Müller, and Dr. Jorge Bergado-Acosta, unpublished data). High expression of the Ndr2-transgene was observed in the mossy fibers (MF) in the TG-camKII mice (Fig. 4.1A). The MF terminals in both suprapyramidal and infrapyramidal bands underwent investigation in dorsal and ventral hippocampus via TIMM staining (Fig. 4.1B). A significant reduction in the ventral suprapyramidal layer was evident in the TG-camKII mice (Fig. 4.1C; Ventral: N(WT)=5, N(TG-camKII)=9; Student's t-test, suprapyramidal: $t(12)=2.505$, $p=0.0276$, infrapyramidal: $t(12)=1.454$, $p=0.1716$. Dorsal: N(WT)=6, N(TG-camKII)=10; Student's t-test, suprapyramidal: $t(14)=0.5639$, $p=0.5817$, infrapyramidal: $t(14)=0.9991$, $p=0.3347$). Since the CamKIIalpha allows a late postnatal induction of the transgene (Minichiello et al. 1999), Ndr2 overexpression might have interfered with the maturation of the MF terminals rather than the formation of the mossy fiber system (Gaarskjaer 1985). It has been previously shown that Ndr2 regulates axonal and dendritic growth *in vitro*; its knockdown with shRNA reduces the growth significantly, and its overexpression increases it (Rehberg et al. 2014). The enhancement in the growth both in axons and dendrites was prevented when echistatin (an RGD disintegrin, inhibiting β1- and β3-integrin function) was applied indicating that the overgrowth is β1-integrin dependent, since β3-integrin mRNA levels were very low in cultured hippocampal neurons and β1-integrin knockdown displayed a similar phenotype with the Ndr2-knockdown. Interestingly, axonal growth is affected differentially in both experimental setups, *in vitro* and *in vivo*, when Ndr2 is overexpressed. It has been previously suggested that in developing MF

fascicles, β1-integrins are not expressed (Schuster et al. 2001), yet in the *in vitro* study, it has been demonstrated that Ndr2 regulates the neurite outgrowth through β1-integrin activation (Rehberg et al. 2014). The interaction of Ndr2 with the actin cytoskeleton was also shown in outgrowing neurites (Stork et al. 2004). On the other hand, actin cytoskeleton rearrangement during MF development and activity-dependent MF terminal modulation were also displayed (Knöll et al. 2006; Owe et al. 2009; Zhao et al. 2012; Zhang et al. 2014). The phenotype observed upon the late overexpression of Ndr2 in the MF *in vivo* might suggest that Ndr2 modulates mature MF stability and function through the actin cytoskeleton, whereas *in vitro* Ndr2 promotes outgrowth that is dependent on β1-integrin activation. It is noteworthy to mention that MF terminals were also stained with the TIMM method used on Ndr2-KO mice tissue, yet no genotype difference was observed in the MF terminals (unpublished data). Even though the knockdown or knockout of Ndr2 *in vitro* reduced the axonal branching (Rehberg et al. 2014), *in vivo* this observation was not confirmed. Endogenous Ndr2 expression in the mossy fibers has not been observed, thus not affecting the MF terminal morphology.

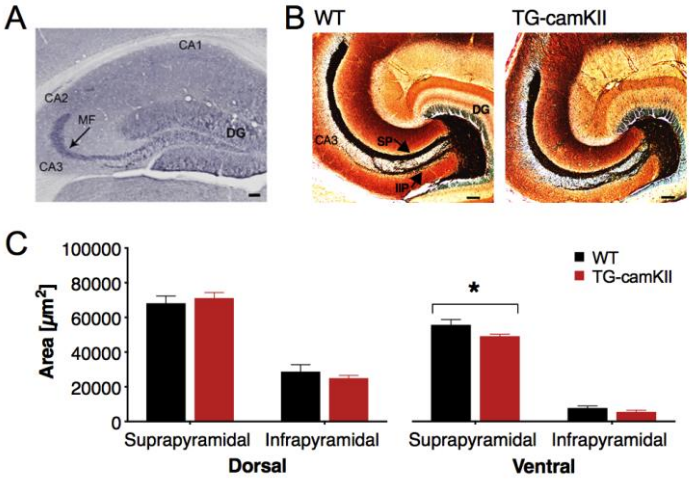

Figure 4.1: Ndr2 transgene expression in the hippocampus and Mossy fiber terminal reduction in the ventral hippocampus.

A. *Immunohistochemistry staining revealed the overexpressed Ndr2 in the hippocampus, especially in the mossy fibers (MF, indicated with an arrow). Scale bar: 500 µm.* ***B.*** *Representative images of WT and TG-camKII ventral hippocampus stained with the TIMM method (SP: suprapyramidal, IIP: infra/intrapyramidal). Scale bar: 100 µm.* ***C.*** *Mossy fiber terminals were reduced in the TG ventral suprapyramidal layer in the hippocampus of TG-camKII mice (N(WT)=5, N(TG-camKII)=9). No change was observed in the ventral infrapyramidal band or in either bands in the dorsal hippocampus (N(WT)=6, N(TG-camKII)=10). Data shown as mean±S.E.M. *p<0.05.*

4.2 The impact of Ndr2 on behavior

Previous research has addressed the role of Ndr2 at the cellular level, yet its implications on animal behavior especially on learning and memory has not been investigated. When new genetically modified mice are generated, behavioral tests can provide general information about

a gene and its impact on specific phenotypes. Even though my main focus was on learning and memory, other behavioral phenotypes were also investigated to have an overview and exclude any interference from other outcomes that may affect behavior due to the genetic manipulation.

Several different genetic approaches were used to examine the pleiotropic function of Ndr2 on behavior. For this purpose, constitutive-knockout (KO), conditional-knockout (cKO), and a conditional overexpressing (TG) mouse lines were tested. An overview of tests performed, and significant differences observed in at least one parameter of the test is summarized in Table 4.1. Each mouse line exhibited a specific phenotype pointing out to the importance of the timing of the genetic manipulation in development and the cell and region specificity.

Table 4.1: A summary table of the behavioral results for five tested Ndr2-mutant mouse lines.
All behavioral tests performed with the mice are summarized and significant outcomes in at least one parameter of the test evaluated were labeled with a "". B.P.: behavioral paradigm, HCA: home cage activity, EPM: elevated plus maze, FC: fear conditioning, OF: open field, L/D: light/dark transition test, NOR: novel object recognition, AA: active avoidance, WCM: water cross maze, ASR: acoustic startle response, PPI: pre-pulse inhibition, SI: social interaction, n.s.: not significant, #: experiments performed by Dr. Jorge Bergado-Acosta, $: data not significant, data obtained, analyzed, and discussed in the master's thesis from Deniz A. Madencioglu.*

B.P. / Ndr2	HCA	EPM	EPM after FC	OF	L/D	Y-maze	NOR	AA	FC	WCM	ASR, PPI	SI
KO	n.s.	n.s.	*	n.s.	n.s.	n.s.	n.s.	n.s.	*	n.s.	n.s.	$
cKO-emx	n.s.		*	*	n.s.			n.s.	n.s.	n.s.		
cKO-camKII	*		*	*	*			n.s.	*			
TG-emx	n.s.	n.s.		*				n.s.	n.s.	n.s.		n.s.
TG-camKII	n.s.	n.s. #		* #	n.s. #			* #	n.s. #	n.s.		

The behavioral phenotyping of different Ndr2-mutant mice has revealed several main findings:

1- The KO mice exhibit an increase in fear response to unconditioned fear stimuli, yet do not have an anxiety-like phenotype nor a deficit in conditioned fear learning or memory. On the other hand, the KO mice show a tendency towards a possible spatial learning deficiency.

2- Both cKO mice lines show a moderate anxiety-like phenotype. The cKO-camKII mice in addition have an impaired remote fear memory.

3- The TG-camKII mice display an impaired avoidance learning accompanied by higher exploratory behavior.

4.2.1 The effects of germline-knockout of Ndr2 on behavior

The KO mice were extensively tested for behavioral deficits, including hippocampus-dependent behavioral tasks. In general, the KO mice did not show an impairment neither in anxiety-like behavior, learning and memory, nor in sensorimotor gaiting and startle behavior. Behavioral paradigms dependent on hippocampal function including the Y-maze, novel object recognition, active avoidance, cued-fear conditioning, and water cross maze did not reveal a phenotype for the KO mice at the learning and memory level. Even though morphological and physiological differences were observed in the hippocampus, this did not translate into a strong behavioral impairment. A decrease in spine density in the CA1 accompanied by a reduction in the CA1-LTP and a reduction in the length of the first order apical dendrites in CA3 have been observed. The CA3 region has been implicated to play a crucial role in encoding spatial information within short term memory, novelty detection, and tasks requiring multiple trials to learn (reviewed in Kesner 2007; Rebola, Carta, and Mulle 2017) where as CA1 has been implicated in NMDA dependent spatial learning (McHugh et al. 1996). The KO mice were tested in various behavioral paradigms that are hippocampus-dependent, such as the water corss maze for spatial learning, the Y-maze for short-term memory, and the novel object memory test for novelty detection. No significant difference between genotypes was observed in either task in spite of the aforementioned changes in physiology and morphology, bringing up the question of the sensitivity of the behavioral tests performed. For instance, in the water cross maze, as the WT mice display a “learning jump” (accuracy above chance levels) during the training session on the third day, the KO mice show a one-day delay, eventually coming to similar learning levels on the fifth day. This translates into a significant difference in platform finding accuracy observed on the fourth day only and might indicate an impairment in the hippocampal function that could have easily gone undetected given the limited sensitivity of the test used. In contrast to the lack of obvious spatial learning deficits in Ndr2 knockout mice, the knockdown or knockout of Kibra, a Hippo pathway upstream activator, impairs spatial memory performance in rats and mice respectively (Vogt-Eisele et al. 2014). Kibra has also been indicated to play a role in human episodic memory performance (Papassotiropoulos et al. 2006). The water cross maze can be considered an easier spatial memory task when compared to the Morris-water-maze since mice have only two arm choices and are not dependent on the spatial cues only. It is important also to point out to the fact that a subpopulation of the CA3 pyramidal neurons of the KO mice exhibits shorter first order apical dendrites. This significant yet minor

morphological change might not be enough to give rise to an obvious behavioral phenotype that our tests can uncover. For this reason, a more fine-tuned spatial memory task that can reveal the possible behavioral deficit in the KO mice needs to be performed. Mice can be tested with the Morris-water-maze where finding the platform is solely dependent on spatial cues or with the radial arm or Barnes maze.

Even though an evident deficit in memory consolidation and remote memory was not present in the KO mice per se, an interesting phenotype was observed during the learning stage of the cued-fear conditioning test. Mice receive foot shocks paired to a tone (cue, CS+) and have 20 seconds in between these three foot-shock-tone pairs. WT mice displayed a normal learning behavior, after each pairing the freezing level increased and stayed at a high level at the end of the test. On the contrary, KO mice showed significantly higher freezing behavior during the first 20 second pause after the first foot shock, later on equalizing to the freezing levels of the WT mice at the end of the pairings. This extreme freezing response to an unexpected stimulus might be due to a disturbance to the innate fear circuitry activated via a painful stimulus (Silva, Gross, and Gräff 2016). To eliminate the possibility of the observed difference rising from altered pain perception due to the genetic manipulation, a hot plate test was performed, and no differences were observed. Nociceptive information is processed in the periaqueductal gray (PAG) and parabrachial nucleus (PB). The PAG through midline thalamic nuclei (MTN) project to the basolateral amygdala complex (BLA). PB projects the information to the central nucleus of the amygdala (CEA). The CEA also receives information through the BLA. CEA projects back to the ventrolateral PAG (vlPAG) mediating a passive response, in this case freezing behavior. An increase in freezing behavior when the local GABAergic vlPAG neurons were inhibited that in turn leads to the activation of glutamatergic neurons has been recently demonstrated (Tovote et al. 2016). It has been also suggested that the inhibitory input coming from CEA activates a disynaptic GABAergic local microcircuit that disinhibits the vlPAG to Mc (magnocellular nucleus) pathway and results in freezing behavior. High levels of Ndr2 expression is observed in the PAG accompanied by moderate expression in the amygdala. A GABAergic sub-cellular population in the amygdala that is known to project to the PAG, such as PKCδ+ (Protein kinase C delta) cells, using optogenetics was shown to induce freezing behavior when activated, by inhibiting CEA output neurons projecting to PAG (Haubensak et al. 2010). The loss of Ndr2 in the PAG and amygdala might have disrupted the excitation/inhibition balance within the innate fear circuitry, resulting in an over-freezing phenotype to an unpredicted fear stimulus as described above.

Fear-potentiated behavior on the elevated-plus maze was also investigated with the KO mice. Mice were trained using the cued-fear conditioning and one day after the 24-hour retrieval session were tested on the elevated plus maze. The KO mice exhibited significantly high immobility in the maze, yet no differences in the open and closed arm exploration were observed. These readouts point out to a phenotype that can be categorized as stress induced fear/anxiety. In rats, it has been previously shown that inescapable stress enhances the anxiety levels and when this is tested with the elevated plus maze, it results in a decrease in open arm exploration (S. Mechiel Korte, De Boer, and Bohus 1999). This type of behavior has been linked to mechanisms related to the gamma-aminobutyric acid receptor (GABAR), corticotropin releasing factor (CRF) receptors, glucocorticoid, and serotonin (Korte and De Boer 2003). Another rodent study has demonstrated that inescapable foot shock stress increased anxiety-like behavior on the EPM (Pliota et al. 2018). This phenotype was observed to be strongest when tested 10 minutes after the stress induction and coupled with an increase in activity in the lPAG and paraventricular thalamus (PVT) as well as in the recruitment of CRF. Moreover, in response to acute stress, PVT to CEA projections were shown to activate anxiogenic neuronal populations in the CEA and the release CRF. Amygdala is known to regulate fear and anxiety through (CRF) and its receptor CRF1 (Potter et al. 1994). It might be worthwhile to investigate the fear potentiated anxiety phenotype observed in the KO mice further by examining amygdala and PVT activation during the task and by using pharmacological interventions to dissect the circuitry underlying the phenotype.

4.2.2 The effects of the conditional knockout of Ndr2 on behavior

A phenotype particular to the cKO-camKII mice that is in contrast not observed in the other Ndr2-knockout mouse lines is a remote cue and context memory deficiency, which is dependent on an auditory cue reminder. For this type of behavior mice were trained with 3-foot shock-tone pairings and were tested for the cue memory 24 hours after the training. 14 days after the reminder, mice were re-tested for the cue memory and the following day for the shock-context memory. The cKO-camKII mice exhibited less freezing behavior to the conditioned cue (CS+) as well as to the shock-context indicating a remote memory deficiency. This phenotype was not evident when mice were trained and were tested the first time for the cue and context memory two weeks after the training. These results may indicate that stabilization of a memory trace is regulated by the Ndr2 kinase upon the recall of the original memory. This interesting phenotype might be further explained by investigating the circuitry underlying the activation of immediately early genes, such as c-fos and zif268, and signaling cascades that are related to

memory consolidation and synaptic plasticity. In line with my observations, a similar phenotype has been reported in mice heterozygous for Zif268 (zinc finger protein, also known as Egr1-early growth response protein 1) when mice were trained and tested with the contextual-fear conditioning (Besnard, Caboche, and Laroche 2013). Zif268 previously has been suggested to play a role in synaptic plasticity (Cole et al. 1989) and memory consolidation (Wisden et al. 1990) and is known to be regulated through the ERK1/2 (extracellular signal-regulated kinase) signaling cascade. The ERK1/2 pathway is activated upon contextual and cued-fear memory recall in hippocampus and amygdala (Duvarci, Nader, and LeDoux 2005; Besnard, Laroche, and Caboche 2014). The reconsolidation deficit observed in the Zif268-heterozygous mice after memory recall has been shown to be dependent on the reactivation of the original memory. This was demonstrated by inhibiting MEK (mitogen-activated kinase kinase, also known as MAP2K), an ERK1/2 pathway upstream kinase, before the recall and preventing the reactivation of the memory. It is noteworthy to mention that it has been shown that Ndr2 regulates ERK activation upon NGF (nerve growth factor) stimulation in PC12 cells (work done by Daniel Lang, unpublished data). In the cKO-camKII mice it might be the case that the ERK signaling pathway is not activated during the reactivation of the memory. Furthermore, the effects of Ndr2 on memory stabilization seen in the cKO-camKII mice, but not in the other knockout lines, might be explained by the timing of the gene knockout. The knockout depending on the camKIIalpha promoter is initiated postnatally and is confined to postmigratory forebrain neurons. The neural circuits by then are mostly formed and any modification after this time point might not be compensated for by other factors, whereas some sort of compensation might possibly take place in the still developing brains of the KO or cKO-emx lines.

A behavioral phenotype observed that is unique to both of the cKO lines but not seen in the KO mice is an anxiety-like behavior. In the open field paradigm, on the second day when mice were tested under light conditions, both the cKO-emx and the cKO-camKII mice spent significantly less time in the center and more in the corners. In the light/dark transition test, only the cKO-camKII mice were less active in the lit compartment, yet the time spent in each compartment was not significantly different. The significant difference observed in the home cage activity from the cKO-camKII mice also was not reflected in the open field paradigm, or in the other tests, as the exploration in the apparatus was not different between genotypes. Also, it is important to mention the anxiety phenotype observed in naïve cKO-camKII mice was not evident anymore after the fear-potentiated anxiety, which was measured on the elevated plus

maze. This might be the consequence of testing the same mice in several behavioral tests, where mice become more acquainted to handling and being tested. For this reason, naïve cKO-camKII mice should be tested to confirm whether a possible fear potentiated anxiety phenotype is masked by other behavioral tests.

The cKO-emx mice displayed a behavioral phenotype not seen with the cKO-camKII mice, yet similar to what has already been observed with the KO mice; in the fear-potentiated elevated plus maze. cKO-emx mice entered the open arms significantly less, and closed arms significantly more indicating a stress induced anxiety. The cKO-camKII mice did not show a similar phenotype, even though they entered the center compartment of the elevated plus maze significantly less.

4.2.3 The effects of overexpressing Ndr2 on behavior

Mice overexpressing Ndr2 dependent on the Emx1 promoter were tested with various behavioral protocols. A distinct behavioral phenotype was not evident in any domain of behavior: learning and memory, anxiety, spatial memory, and social behavior. The only difference detected was in the open field paradigm where on the second day of the test TG-emx mice preferred the rim of the apparatus significantly less yet there was no difference in the center time and maze exploration. These results did not point out to neither an anxiety-like phenotype nor to an exploratory deficiency.

On the other hand, TG-camKII mice displayed an interesting phenotype related to the morphological differences observed in the MF terminals. Mice did not show anxiety-like behavior, deficiency in cued-fear conditioning (experiments performed by Dr. Jorge Bergado-Acosta), and spatial learning deficiencies, whereas genotype differences were evident in active avoidance and open field. In the active avoidance task TG-camKII mice displayed a learning deficiency (Fig. 4.2A; N(WT)=7, N(TG-camKII)=7; repeated measures two-way-ANOVA: $F(1,12)=7.129$, $p=0.0204$) and in the open field, over the two days they were tested, they showed higher exploratory behavior (Fig. 4.2B; N(WT)=7, N(TG-camKII)=9; repeated measures two-way-ANOVA: day1: $F(1,14)=5.117$, $p=0.0401$, day 2: $F(1,14)=6.062$, $p=0.0274$).

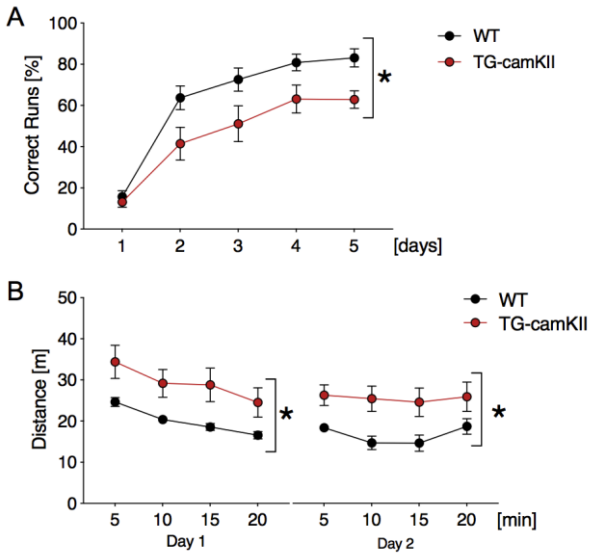

Figure 4.2: Active avoidance and open field with TG-camKII mice.
A. *A learning deficiency was observed in the TG-camKII mice in the active avoidance test (N(WT)=7, N(TG-camKII)=7).* ***B.*** *Higher exploration was observed with the TG-camKII mice over two days of the test (N(WT)=7, N(TG-camKII)=9). Data shown as mean±S.E.M. *p<0.05.*

Previous studies, which focused on the infra-/intrapyramidal band, illustrated a negative correlation between MF density and open field exploratory behavior (Crusio, Schwegler, and van Abeelen 1989) and active avoidance (Schwegler et al. 1981). In the TG-camKII mice the reduction of the MF terminals in the suprapyramidal band of the ventral hippocampus might be determining the behavioral outcome. An altered hippocampal network activity pattern was shown in the TG-camKII mice; decreased capacity for generation of SWs (sharp waves) and associated ripples in the hippocampus, reduction in the gamma oscillations in the CA1 (work done by Dr. Gürsel Çalışkan), and reduction in the MF-LTP (long term potentiation) (work done by Dr. Pingan Yuanxiang). This reduced hippocampal network activity might explain the reduced cognitive capacity and higher exploratory behavior. The decrease in the SWR (sharp wave ripples), spontaneously occurring off-line oscillations involved in memory consolidation (Wilson and McNaughton 1994; Buzsáki 2015; Çaliskan et al. 2016), can be associated with the poor memory consolidation since the active avoidance task depends on the information learned on the previous day. Furthermore, the higher exploratory behavior might be correlated with the observed reduction in the gamma oscillations in the CA1 since previously acquired spatial location memory has been correlated with gamma oscillations (Lu et al. 2011).

4.3 Differences between Ndr2-mutants mouse models

Overall, when the Ndr2-mutant mice are examined at the behavioral level as knockout and overexpressing, a discrepancy between the mouse lines is evident. Differences observed at the

behavioral level might be a consequence of a compensatory network starting from the germline maturation or embryonic development and resulting in the neural system adapting to the genetic alteration (reviewed in El-Brolosy and Stainier 2017).

Despite the advantage of using a germline knockout as a genetic model, such that it better relates in its timing to the human disorders, it also has its disadvantages. Ndr kinases are also expressed in other organs, like in the spleen and thymus, and their importance for the immune system has been shown. An *in vivo* study in mice suggested that Ndr1 and Ndr2 mediate thymocyte egress and T-cell migration (Tang et al. 2015). It has been also shown that Ndr1 is crucial for the immune response upon inflammatory injury by limiting the inflammation by restraining cytokine secretion (Wen et al. 2015). Moreover, in human B-cell lymphoblastoids the expression of Ndr2 has been found to be downregulated (Lou et al. 2013). The crosstalk between the peripheral immune system and the CNS has been studied and has suggested having implications on many CNS disorders including psychiatric disorders. As evidence point out to the critical functions of Ndr kinases in the immune system, the possibility of creating an imbalance between the immune-CNS homeostasis in the germline knockout is suggestable. To avoid the secondary effects of the possible developmental effects of the periphery on the brain development, studying Ndr2 in conditional mouse models might be considered as a better solution.

In addition to the germline knockout mice, conditional knockout mice were generated to knockout Ndr2 in a brain specific manner at two different developmental stages. Overexpressing mice were also generated using the same driver mouse lines. The Emx1-Cre expression starts during embryonic development, around e9.5, and is confined to the neurons in the cerebral cortex including the hippocampus (Gulisano et al. 1996). Furthermore, the CamKII-alpha-Cre is expression starts postnatally, around p20, and is expressed in neurons in the neocortex and hippocampus (Minichiello et al. 1999). The differences in the timing and the brain region of the knockout or overexpression of Ndr2 indeed had a measurable effect on the behavioral outcome. During the embryonic development, it is highly likely though not yet proven that compensatory mechanisms are in action to overcome the effects associated with the loss or overexpression of Ndr2, whereas this is not possible for when a gene manipulation is introduced at postnatal ages. The reason of having stronger phenotypes in the mice generated with the CamKII-alpha driver might be a result of the diminished capacity of the further developed postnatal brain to counteract the expression changes in Ndr2.

5 Concluding remarks and future perspectives

Genetic disorders in the human population, including deletions or increased copy numbers of the *NDR2* gene have been associated with neurological symptoms. Even though Ndr2 has not been found to cause a disorder in humans single handedly, evidence points out to the possibility of *NDR2* being in a hotspot for genetic mutations resulting in CNVs and disease. To have a better understanding, it is important to study individual genes and if possible the interaction with the neighboring genes that are also affected. Non-human studies in eukaryotic organisms also support the importance of the function of Ndr2 in various cell types, perhaps most importantly in neurons. Its already shown role in axonal and dendritic growth and branching *in vitro* and *in vivo* in various experimental setups has been a starting point to investigate Ndr2 in the context of behavior. During my thesis work I tried to unveil the behavioral consequences of different types of genetic modifications of the *NDR2* gene and possible morphological changes accompanied by these mannipulations using genetically modified mouse models.

Knocking-out Ndr2 in the germline altered the CA3 pyramidal neurons morphology in the hippocampus yet mice did not display a hippocampal-dependent behavioral change. To find a behavioral readout of this morphological change, a more challenging fine-tuned behavioral paradigm should be found, and mice should be further tested. On the other hand, the KO mice displayed an innate fear-like phenotype, which needs further investigation.

The conditional knockout mouse lines exhibited anxiety-like behavior regardless of the gene knockout time in development. The cKO-camKII mice displayed a distinctive phenotype, which was not observed in the other knockout lines: A remote memory deficiency dependent on a reminder of the original memory. This exciting finding needs further investigation to shed light on the circuitry and molecular mechanisms that Ndr2 is involved in the memory stabilization.

Even though the TG-emx mouse line did not present a behavioral phenotype, the TG-camKII mice were found to have a disrupted hippocampal network originating from MF terminal reduction giving rise to learning impairment and higher exploratory behavior.

Comparing the phenotypes that these mouse models displayed to the human patients with deletion or multiplication of *NDR2*, phenotypic similarities were observed only in the mouse model overexpressing Ndr2 dependent on camKII-alpha. Patients with the gene duplication present intellectual disabilities, learning impairments, and autism. The data on TG-camKII mice suggests that in these patients, *NDR2* might be contributing to an altered hippocampal network activity and to the intellectual disabilities observed.

As final words on Ndr2 and its role on behavior and morphology *in vivo*, I would like to conclude that the function of Ndr2 is highly sensitive to changes in expression in relation to the cell type and maturity. As Ndr kinases are evolutionarily conserved, it is highly likely that for the organism to survive, genetic changes are compensated as much as possible especially during early development, thus resulting in less dramatic phenotypes or disorders.

Bibliography

"A Novel Gene Containing a Trinucleotide Repeat That Is Expanded and Unstable on Huntington's Disease Chromosomes. The Huntington's Disease Collaborative Research Group." 1993. *Cell* 72 (6): 971–83. doi:10.1016/0092-8674(93)90585-E.

Albrecht, Anne, and Oliver Stork. 2012. "Are NCAM Deficient Mice an Animal Model for Schizophrenia?" *Frontiers in Behavioral Neuroscience* 6 (July). Frontiers: 43. doi:10.3389/fnbeh.2012.00043.

Albrecht, Anne, Marlen Thiere, Jorge Ricardo Bergado-Acosta, Janine Poranzke, Bettina Muller, and Oliver Stork. 2013. "Circadian Modulation of Anxiety: A Role for Somatostatin in the Amygdala." *PloS One* 8 (12). United States: e84668. doi:10.1371/journal.pone.0084668.

Bae, Sung Jun, and Xuelian Luo. 2018. "Activation Mechanisms of the Hippo Kinase Signaling Cascade." *Bioscience Reports* 38 (4). Portland Press Limited: BSR20171469. doi:10.1042/BSR20171469.

Bailey, Kathleen R, Nathan R Rustay, and Jacqueline N Crawley. 2006. "Behavioral Phenotyping of Transgenic and Knockout Mice: Practical Concerns and Potential Pitfalls." *ILAR Journal / National Research Council, Institute of Laboratory Animal Resources* 47 (2): 124–31. http://www.ncbi.nlm.nih.gov/pubmed/16547369.

Bannerman, D M, J N P Rawlins, S B McHugh, R M J Deacon, B K Yee, T Bast, W-N Zhang, H H J Pothuizen, and J Feldon. 2004. "Regional Dissociations within the Hippocampus-Memory and Anxiety." *Neuroscience and Biobehavioral Reviews* 28 (3): 273–83. doi:10.1016/j.neubiorev.2004.03.004.

Bannon, A.W, J Seda, M Carmouche, J.M Francis, M.H Norman, B Karbon, and M.L McCaleb. 2000. "Behavioral Characterization of Neuropeptide Y Knockout Mice." *Brain Research* 868 (1): 79–87. doi:10.1016/S0006-8993(00)02285-X.

Berta, Ágnes I., Kathleen Boesze-Battaglia, Sem Genini, Orly Goldstein, Paul J. O'Brien, Ágoston Szél, Gregory M. Acland, William A. Beltran, and Gustavo D. Aguirre. 2011. "Photoreceptor Cell Death, Proliferation and Formation of Hybrid Rod/S-Cone Photoreceptors in the Degenerating STK38L Mutant Retina." Edited by Rafael Linden. *PLoS ONE* 6 (9). Public Library of Science: e24074. doi:10.1371/journal.pone.0024074.

Besnard, Antoine, Jocelyne Caboche, and Serge Laroche. 2013. "Recall and Reconsolidation of Contextual Fear Memory: Differential Control by ERK and Zif268 Expression Dosage." *PLoS ONE* 8 (8): 1–8. doi:10.1371/journal.pone.0072006.

Besnard, Antoine, Serge Laroche, and Jocelyne Caboche. 2014. "Comparative Dynamics of MAPK/ERK Signalling Components and Immediate Early Genes in the Hippocampus and Amygdala Following Contextual Fear Conditioning and Retrieval." *Brain Structure and Function* 219 (1): 415–30. doi:10.1007/s00429-013-0505-y.

Bichsel, Samuel J, Rastislav Tamaskovic, Mario R Stegert, and Brian a Hemmings. 2004. "Mechanism of Activation of NDR (Nuclear Dbf2-Related) Protein Kinase by the HMOB1 Protein." *The Journal of Biological Chemistry* 279 (34): 35228–35. doi:10.1074/jbc.M404542200.

Bliss, T V, and T Lomo. 1973. "Long-Lasting Potentiation of Synaptic Transmission in the Dentate Area of the Anaesthetized Rabbit Following Stimulation of the Perforant Path." *The Journal of Physiology* 232 (2): 331–56. http://www.pubmedcentral.nih.gov/articlerender.fcgi?artid=1350458&tool=pmcentrez&rendertype=abstract.

Butterly, Dan A, Maurice A Petroccione, and David M Smith. 2012. "Hippocampal Context

Processing Is Critical for Interference Free Recall of Odor Memories in Rats." *Hippocampus* 22 (4). NIH Public Access: 906–13. doi:10.1002/hipo.20953.

Buzsáki, György. 2015. "Hippocampal Sharp Wave-Ripple: A Cognitive Biomarker for Episodic Memory and Planning." *Hippocampus* 25 (10). Wiley-Blackwell: 1073–1188. doi:10.1002/hipo.22488.

Çaliskan, Gürsel, Iris Müller, Marcus Semtner, Aline Winkelmann, Ahsan S Raza, Jan O Hollnagel, Anton Rösler, Uwe Heinemann, Oliver Stork, and Jochen C Meier. 2016. "Identification of Parvalbumin Interneurons as Cellular Substrate of Fear Memory Persistence." *Cerebral Cortex (New York, N.Y. : 1991)* 26 (5). Oxford University Press: 2325–40. doi:10.1093/cercor/bhw001.

Carlstrom, Lucas P, Jacob H Hines, Steven J Henle, and John R Henley. 2011. "Bidirectional Remodeling of B1-Integrin Adhesions during Chemotropic Regulation of Nerve Growth." *BMC Biology* 9 (1). BioMed Central: 82. doi:10.1186/1741-7007-9-82.

Chiba, Shuhei, Masanori Ikeda, Kokichi Katsunuma, Kazumasa Ohashi, and Kensaku Mizuno. 2009. "MST2- and Furry-Mediated Activation of NDR1 Kinase Is Critical for Precise Alignment of Mitotic Chromosomes." *Current Biology* 19 (8). Cell Press: 675–81. doi:10.1016/J.CUB.2009.02.054.

Cole, Andrew J., David W. Saffen, Jay M. Baraban, and Paul F. Worley. 1989. "Rapid Increase of an Immediate Early Gene Messenger RNA in Hippocampal Neurons by Synaptic NMDA Receptor Activation." *Nature* 340 (6233): 474–76. doi:10.1038/340474a0.

Crawley, J N, J K Belknap, a Collins, J C Crabbe, W Frankel, N Henderson, R J Hitzemann, et al. 1997. "Behavioral Phenotypes of Inbred Mouse Strains: Implications and Recommendations for Molecular Studies." *Psychopharmacology* 132 (2): 107–24. http://www.ncbi.nlm.nih.gov/pubmed/9266608.

Crusio, W.E., H. Schwegler, and J.H.F. van Abeelen. 1989. "Behavioral Responses to Novelty and Structural Variation of the Hippocampus in Mice. I. Quantitative-Genetic Analysis of Behavior in the Open-Field." *Behavioural Brain Research* 32 (1). Elsevier: 75–80. doi:10.1016/S0166-4328(89)80074-9.

Demiray, Yunus E., Kati Rehberg, Stefanie Kliche, and Oliver Stork. 2018. "Ndr2 Kinase Controls Neurite Outgrowth and Dendritic Branching Through A1 Integrin Expression." *Frontiers in Molecular Neuroscience* 11 (March). Frontiers: 66. doi:10.3389/fnmol.2018.00066.

Doetschman, Thomas. 2009. "Influence of Genetic Background on Genetically Engineered Mouse Phenotypes." *Methods in Molecular Biology (Clifton, N.J.)* 530. NIH Public Access: 423–33. doi:10.1007/978-1-59745-471-1_23.

Duvarci, Sevil, Karim Nader, and Joseph E. LeDoux. 2005. "Activation of Extracellular Signal-Regulated Kinase-Mitogen-Activated Protein Kinase Cascade in the Amygdala Is Required for Memory Reconsolidation of Auditory Fear Conditioning." *European Journal of Neuroscience* 21 (1): 283–89. doi:10.1111/j.1460-9568.2004.03824.x.

Eacott, Madeline J., and Gillian Norman. 2004. "Integrated Memory for Object, Place, and Context in Rats: A Possible Model of Episodic-like Memory?" *The Journal of Neuroscience : The Official Journal of the Society for Neuroscience* 24 (8). Society for Neuroscience: 1948–53. doi:10.1523/JNEUROSCI.2975-03.2004.

Ehrnhoefer, Dagmar E, Stefanie L Butland, Mahmoud A Pouladi, and Michael R Hayden. 2009. "Mouse Models of Huntington Disease: Variations on a Theme." *Disease Models & Mechanisms* 2 (3–4). Company of Biologists: 123–29. doi:10.1242/dmm.002451.

El-Brolosy, Mohamed A, and Didier Y R Stainier. 2017. "Genetic Compensation: A Phenomenon in Search of Mechanisms." *PLoS Genetics* 13 (7). Public Library of Science:

e1006780. doi:10.1371/journal.pgen.1006780.
Emoto, Kazuo, Ying He, Bing Ye, Wesley B Grueber, Paul N Adler, Lily Yeh Jan, and Yuh-Nung Jan. 2004. “Control of Dendritic Branching and Tiling by the Tricornered-Kinase/Furry Signaling Pathway in Drosophila Sensory Neurons.” *Cell* 119 (2): 245–56. doi:10.1016/j.cell.2004.09.036.
Fanciulli, Manuela, Penny J Norsworthy, Enrico Petretto, Rong Dong, Lorraine Harper, Lavanya Kamesh, Joanne M Heward, et al. 2007. “FCGR3B Copy Number Variation Is Associated with Susceptibility to Systemic, but Not Organ-Specific, Autoimmunity.” *Nature Genetics* 39 (6). Europe PMC Funders: 721–23. doi:10.1038/ng2046.
Fang, Xiaolan, and Paul N. Adler. 2010. “Regulation of Cell Shape, Wing Hair Initiation and the Actin Cytoskeleton by Trc/Fry and Wts/Mats Complexes.” *Developmental Biology* 341 (2). Academic Press: 360–74. doi:10.1016/j.ydbio.2010.02.029.
Firth, Helen V, Shola M Richards, A Paul Bevan, Stephen Clayton, Manuel Corpas, Diana Rajan, Steven Van Vooren, Yves Moreau, Roger M Pettett, and Nigel P Carter. 2009. “DECIPHER: Database of Chromosomal Imbalance and Phenotype in Humans Using Ensembl Resources.” *American Journal of Human Genetics* 84 (4). Elsevier: 524–33. doi:10.1016/j.ajhg.2009.03.010.
Fuchs, Helmut, Valérie Gailus-Durner, Thure Adler, Juan Antonio Aguilar-Pimentel, Lore Becker, Julia Calzada-Wack, Patricia Da Silva-Buttkus, et al. 2011. “Mouse Phenotyping.” *Methods* 53 (2). Academic Press: 120–35. doi:10.1016/j.ymeth.2010.08.006.
Gaarskjaer, Frank B. 1985. “The Development of the Dentate Area and the Hippocampal Mossy Fiber Projection of the Rat.” *Journal of Comparative Neurology* 241 (2): 154–70. doi:10.1002/cne.902410204.
Gallegos, Maria E, and Cornelia I Bargmann. 2004. “Mechanosensory Neurite Termination and Tiling Depend on SAX-2 and the SAX-1 Kinase.” *Neuron* 44 (2): 239–49. doi:10.1016/j.neuron.2004.09.021.
Geng, W, B He, M Wang, and P N Adler. 2000. “The Tricornered Gene, Which Is Required for the Integrity of Epidermal Cell Extensions, Encodes the Drosophila Nuclear DBF2-Related Kinase.” *Genetics* 156 (4): 1817–28. http://www.pubmedcentral.nih.gov/articlerender.fcgi?artid=1461384&tool=pmcentrez&rendertype=abstract.
Goldstein, Orly, Anna V Kukekova, Gustavo D Aguirre, and Gregory M Acland. 2010. “Exonic SINE Insertion in STK38L Causes Canine Early Retinal Degeneration (Erd).” *Genomics* 96 (6): 362–68. doi:10.1016/j.ygeno.2010.09.003.
Gonzalez, Enrique, Hemant Kulkarni, Hector Bolivar, Andrea Mangano, Racquel Sanchez, Gabriel Catano, Robert J. Nibbs, et al. 2005. “The Influence of CCL3L1 Gene-Containing Segmental Duplications on HIV-1/AIDS Susceptibility.” *Science* 307 (5714): 1434–40. doi:10.1126/science.1101160.
Grueber, Wesley B, Lily Y Jan, and Yuh Nung Jan. 2002. “Tiling of the Drosophila Epidermis by Multidendritic Sensory Neurons.” *Development (Cambridge, England)* 129 (12). The Company of Biologists Ltd: 2867–78. http://dev.biologists.org/content/129/12/2867.long.
Gulisano, Massimo, Vania Broccoli, Celia Pardini, and Edoardo Boncinelli. 1996. “Emx1 and Emx2 Show Different Patterns of Expression During Proliferation and Differentiation of the Developing Cerebral Cortex in the Mouse.” *European Journal of Neuroscience* 8 (5): 1037–50. doi:10.1111/j.1460-9568.1996.tb01590.x.
Guo, Cai, Xiaoying Zhang, and Gerd P Pfeifer. 2011. “The Tumor Suppressor RASSF1A Prevents Dephosphorylation of the Mammalian STE20-like Kinases MST1 and MST2.”

The Journal of Biological Chemistry 286 (8). American Society for Biochemistry and Molecular Biology: 6253–61. doi:10.1074/jbc.M110.178210.

Halder, Georg, and Randy L Johnson. 2011. "Hippo Signaling: Growth Control and Beyond." *Development* 138 (1). Oxford University Press for The Company of Biologists Limited: 9–22. doi:10.1242/dev.045500.

Hama, Hiroshi, Chikako Hara, Kazuhiko Yamaguchi, and Atsushi Miyawaki. 2004. "PKC Signaling Mediates Global Enhancement of Excitatory Synaptogenesis in Neurons Triggered by Local Contact with Astrocytes." *Neuron* 41 (3). Elsevier: 405–15. doi:10.1016/S0896-6273(04)00007-8.

Haubensak, Wulf, Prabhat S. Kunwar, Haijiang Cai, Stephane Ciocchi, Nicholas R. Wall, Ravikumar Ponnusamy, Jonathan Biag, et al. 2010. "Genetic Dissection of an Amygdala Microcircuit That Gates Conditioned Fear." *Nature* 468 (7321): 270–76. doi:10.1038/nature09553.

Hergovich, Alexander, Stefan Lamla, Erich A Nigg, and Brian A Hemmings. 2007. "Centrosome-Associated NDR Kinase Regulates Centrosome Duplication." *Molecular Cell* 25 (4). Elsevier: 625–34. doi:10.1016/j.molcel.2007.01.020.

Hirata, D., N Kishimoto, M Suda, Y Sogabe, S Nakagawa, Y Yoshida, K Sakai, et al. 2002. "Fission Yeast Mor2/Cps12, a Protein Similar to Drosophila Furry, Is Essential for Cell Morphogenesis and Its Mutation Induces Wee1-Dependent G2 Delay." *The EMBO Journal* 21 (18). EMBO Press: 4863–74. doi:10.1093/emboj/cdf495.

Joffre, Carine, Nicolas Dupont, Lily Hoa, Valenti Gomez, Raul Pardo, Catarina Gonçalves-Pimentel, Pauline Achard, et al. 2015. "The Pro-Apoptotic STK38 Kinase Is a New Beclin1 Partner Positively Regulating Autophagy." *Current Biology* 25 (19): 2479–92. doi:10.1016/j.cub.2015.08.031.

Kesner, Raymond P. 2007. "Behavioral Functions of the CA3 Subregion of the Hippocampus." *Learning & Memory (Cold Spring Harbor, N.Y.)* 14 (11). Cold Spring Harbor Laboratory Press: 771–81. doi:10.1101/lm.688207.

Kleinknecht, Karl R, Benedikt T Bedenk, Sebastian F Kaltwasser, Barbara Grünecker, Yi-Chun Yen, Michael Czisch, and Carsten T Wotjak. 2012. "Hippocampus-Dependent Place Learning Enables Spatial Flexibility in C57BL6/N Mice." *Frontiers in Behavioral Neuroscience* 6 (January): 87. doi:10.3389/fnbeh.2012.00087.

Knöll, Bernd, Oliver Kretz, Christine Fiedler, Siegfried Alberti, Günther Schütz, Michael Frotscher, and Alfred Nordheim. 2006. "Serum Response Factor Controls Neuronal Circuit Assembly in the Hippocampus." *Nature Neuroscience* 9 (2). Nature Publishing Group: 195–204. doi:10.1038/nn1627.

Koike-Kumagai, Makiko, Kei-ichiro Yasunaga, Rei Morikawa, Takahiro Kanamori, and Kazuo Emoto. 2009. "The Target of Rapamycin Complex 2 Controls Dendritic Tiling of Drosophila Sensory Neurons through the Tricornered Kinase Signalling Pathway." *The EMBO Journal* 28 (24). European Molecular Biology Organization: 3879–92. doi:10.1038/emboj.2009.312.

Korte, S. M., and Sietse F. De Boer. 2003. "A Robust Animal Model of State Anxiety: Fear-Potentiated Behaviour in the Elevated plus-Maze." *European Journal of Pharmacology* 463 (1–3): 163–75. doi:10.1016/S0014-2999(03)01279-2.

Korte, S. Mechiel, Sietse F. De Boer, and Béla Bohus. 1999. "Fear-Potentiation in the Elevated Plus-Maze Test Depends on Stressor Controllability and Fear Conditioning." *Stress* 3 (1): 27–40. doi:10.3109/10253899909001110.

Krishnan, Harini C, and Lisa C Lyons. 2015. "Synchrony and Desynchrony in Circadian Clocks: Impacts on Learning and Memory." *Learning & Memory (Cold Spring Harbor, N.Y.)* 22

(9). Cold Spring Harbor Laboratory Press: 426–37. doi:10.1101/lm.038877.115.
Laxmi, T Rao, Oliver Stork, and Hans-Christian Pape. 2003. “Generalisation of Conditioned Fear and Its Behavioural Expression in Mice.” *Behavioural Brain Research* 145 (1–2). Netherlands: 89–98.
Léger, Hélène, Evelyn Santana, N. Adrian Leu, Eliot T. Smith, William A. Beltran, Gustavo D. Aguirre, and Francis C. Luca. 2018. “Ndr Kinases Regulate Retinal Interneuron Proliferation and Homeostasis.” *Scientific Reports* 8 (1). Nature Publishing Group: 12544. doi:10.1038/s41598-018-30492-9.
Lilja, Johanna, and Johanna Ivaska. 2018. “Integrin Activity in Neuronal Connectivity.” *Journal of Cell Science* 131 (12). The Company of Biologists Ltd: jcs212803. doi:10.1242/jcs.212803.
Lou, Jianlin, Nanxiang Wu, Peng Song, Lingzhi Jin, Ming Gao, Yang Song, Yufeng Tan, and Kecheng Liu. 2013. “Chemokine (C-C Motif) Ligand 22 Is down-Regulated in a Human B Lymphoblastoid Cell Line by PCB153 and in Residents from PCBs-Contaminated Areas.” *Mutation Research - Genetic Toxicology and Environmental Mutagenesis* 752 (1–2). Elsevier B.V.: 21–27. doi:10.1016/j.mrgentox.2012.12.007.
Lu, Cheng B., John G R Jefferys, Emil C. Toescu, and Martin Vreugdenhil. 2011. “In Vitro Hippocampal Gamma Oscillation Power as an Index of in Vivo CA3 Gamma Oscillation Strength and Spatial Reference Memory.” *Neurobiology of Learning and Memory* 95 (3). Elsevier Inc.: 221–30. doi:10.1016/j.nlm.2010.11.008.
McHugh, T J, K I Blum, J Z Tsien, S Tonegawa, and M A Wilson. 1996. “Impaired Hippocampal Representation of Space in CA1-Specific NMDAR1 Knockout Mice.” *Cell* 87 (7). Elsevier: 1339–49. doi:10.1016/S0092-8674(00)81828-0.
Miedel, Christian J, Jennifer M Patton, Andrew N Miedel, Edward S Miedel, and Jonathan M Levenson. 2017. “Assessment of Spontaneous Alternation, Novel Object Recognition and Limb Clasping in Transgenic Mouse Models of Amyloid-β and Tau Neuropathology.” *Journal of Visualized Experiments : JoVE*, no. 123. MyJoVE Corporation. doi:10.3791/55523.
Millward, T, P Cron, and B a Hemmings. 1995. “Molecular Cloning and Characterization of a Conserved Nuclear Serine(Threonine) Protein Kinase.” *Proceedings of the National Academy of Sciences of the United States of America* 92 (11): 5022–26. http://www.pubmedcentral.nih.gov/articlerender.fcgi?artid=41840&tool=pmcentrez&rendertype=abstract.
Minichiello, Liliana, Martin Korte, David Wolfer, Ralf Kühn, Klaus Unsicker, Vincenzo Cestari, Clelia Rossi-Arnaud, Hans Peter Lipp, Tobias Bonhoeffer, and Rüdiger Klein. 1999. “Essential Role for TrkB Receptors in Hippocampus-Mediated Learning.” *Neuron* 24 (2): 401–14. doi:10.1016/S0896-6273(00)80853-3.
Mouse Genome Sequencing Consortium, Robert H Waterston, Kerstin Lindblad-Toh, Ewan Birney, Jane Rogers, Josep F Abril, Pankaj Agarwal, et al. 2002. “Initial Sequencing and Comparative Analysis of the Mouse Genome.” *Nature* 420 (6915). Nature Publishing Group: 520–62. doi:10.1038/nature01262.
Muller, Iris, Kunihiko Obata, Gal Richter-Levin, and Oliver Stork. 2014. “GAD65 Haplodeficiency Conveys Resilience in Animal Models of Stress-Induced Psychopathology.” *Frontiers in Behavioral Neuroscience* 8. Switzerland: 265. doi:10.3389/fnbeh.2014.00265.
Owe, Simen G, Vidar Jensen, Emma Evergren, Arnaud Ruiz, Oleg Shupliakov, Dimitri M Kullmann, Jon Storm-Mathisen, S Ivar Walaas, Øivind Hvalby, and Linda H Bergersen. 2009. “Synapsin- and Actin-Dependent Frequency Enhancement in Mouse Hippocampal

Mossy Fiber Synapses." *Cerebral Cortex* 19 (3). Oxford University Press: 511–23. doi:10.1093/cercor/bhn101.

Pallister, P D, L F Meisner, B R Elejalde, U Francke, J Herrmann, J Spranger, W Tiddy, S L Inhorn, and J M Opitz. 1977. "The Pallister Mosaic Syndrome." *Birth Defects Original Article Series* 13 (3B): 103–10. http://www.ncbi.nlm.nih.gov/pubmed/890087.

Pan, Duojia. 2010. "The Hippo Signaling Pathway in Development and Cancer." *Developmental Cell* 19 (4). Elsevier: 491–505. doi:10.1016/j.devcel.2010.09.011.

Papassotiropoulos, Andreas, Dietrich A. Stephan, Matthew J. Huentelman, Frederic J. Hoerndli, David W. Craig, John V. Pearson, Kim Dung Huynh, et al. 2006. "Common Kibra Alleles Are Associated with Human Memory Performance." *Science* 314 (5798): 475–78. doi:10.1126/science.1129837.

Park, Yun Kyung, and Yukiko Goda. 2016. "Integrins in Synapse Regulation." *Nature Reviews Neuroscience* 17 (12). Nature Publishing Group: 745–56. doi:10.1038/nrn.2016.138.

Paylor, Richard, and Jacqueline N. Crawley. 1997. "Inbred Strain Differences in Prepulse Inhibition of the Mouse Startle Response." *Psychopharmacology* 132 (2): 169–80. doi:10.1007/s002130050333.

Peltomäki, P., S. Knuutila, A. Ritvanen, I. Kaitila, and A. DE LA Chapelle. 1987. "Pallister-Killian Syndrome: Cytogenetic and Molecular Studies." *Clinical Genetics* 31 (6): 399–405. doi:10.1111/j.1399-0004.1987.tb02832.x.

Pliota, Pinelopi, Vincent Böhm, Florian Grössl, Johannes Griessner, Ornella Valenti, Klaus Kraitsy, Joanna Kaczanowska, et al. 2018. "Stress Peptides Sensitize Fear Circuitry to Promote Passive Coping." *Molecular Psychiatry*, June. Nature Publishing Group, 1. doi:10.1038/s41380-018-0089-2.

Potter, E, S Sutton, C Donaldson, R Chen, M Perrin, K Lewis, P E Sawchenko, and W Vale. 1994. "Distribution of Corticotropin-Releasing Factor Receptor MRNA Expression in the Rat Brain and Pituitary." *Proceedings of the National Academy of Sciences* 91 (19). National Academy of Sciences: 8777–81. doi:10.1073/PNAS.91.19.8777.

Praskova, Maria, Andrei Khoklatchev, Sara Ortiz-Vega, and Joseph Avruch. 2004. "Regulation of the MST1 Kinase by Autophosphorylation, by the Growth Inhibitory Proteins, RASSF1 and NORE1, and by Ras." *The Biochemical Journal* 381 (Pt 2). Portland Press Ltd: 453–62. doi:10.1042/BJ20040025.

Rebola, Nelson, Mario Carta, and Christophe Mulle. 2017. "Operation and Plasticity of Hippocampal CA3 Circuits: Implications for Memory Encoding." *Nature Reviews Neuroscience* 18 (4). Nature Publishing Group: 208–20. doi:10.1038/nrn.2017.10.

Rehberg, Kati, Jorge R Bergado-Acosta, Jeannette C Koch, and Oliver Stork. 2010. "Disruption of Fear Memory Consolidation and Reconsolidation by Actin Filament Arrest in the Basolateral Amygdala." *Neurobiology of Learning and Memory* 94 (2). United States: 117–26. doi:10.1016/j.nlm.2010.04.007.

Rehberg, Kati, Stefanie Kliche, Deniz A. Madencioglu, Marlen Thiere, Bettina Müller, Bernhard Manuel Meineke, Christian Freund, Eike Budinger, and Oliver Stork. 2014. "The Serine/Threonine Kinase Ndr2 Controls Integrin Trafficking and Integrin-Dependent Neurite Growth." *The Journal of Neuroscience : The Official Journal of the Society for Neuroscience* 34 (15): 5342–54. doi:10.1523/JNEUROSCI.2728-13.2014.

Schinzel, A. 1991. "Tetrasomy 12p (Pallister-Killian Syndrome)." *Journal of Medical Genetics* 28 (2): 122–25. doi:10.1136/jmg.28.2.122.

Schlomann, Uwe, Jens C Schwamborn, Myriam Müller, Reinhard Fässler, and Andreas W Püschel. 2009. "The Stimulation of Dendrite Growth by Sema3A Requires Integrin Engagement and Focal Adhesion Kinase." *Journal of Cell Science* 122 (Pt 12): 2034–42.

doi:10.1242/jcs.038232.
Schuster, Thomas, Manfred Krug, Martina Stalder, Natalie Hackel, Rita Gerardy-Schahn, and Melitta Schachner. 2001. “Immunoelectron Microscopic Localization of the Neural Recognition Molecules L1, NCAM, and Its Isoform NCAM180, the NCAM-Associated Polysialic Acid, Beta1 Integrin and the Extracellular Matrix Molecule Tenascin-R in Synapses of the Adult Rat Hippocampus.” *Journal of Neurobiology* 49 (2): 142–58. doi:10.1002/neu.1071.
Schwegler, H, H. Lipp, H Van der Loos, and W Buselmaier. 1981. “Individual Hippocampal Mossy Fiber Distribution in Mice Correlates with Two-Way Avoidance Performance.” *Science* 214 (4522): 817–19. doi:10.1126/science.7292015.
Scoville, W B, and B Milner. 1957. “Loss of Recent Memory after Bilateral Hippocampal Lesions.” *Journal of Neurology, Neurosurgery, and Psychiatry* 20 (1): 11–21. doi:10.1136/jnnp.20.1.11.
Sebat, Jonathan, B Lakshmi, Dheeraj Malhotra, Jennifer Troge, Christa Lese-Martin, Tom Walsh, Boris Yamrom, et al. 2007. “Strong Association of de Novo Copy Number Mutations with Autism.” *Science (New York, N.Y.)* 316 (5823). NIH Public Access: 445–49. doi:10.1126/science.1138659.
Silva, Bianca A, Cornelius T Gross, and Johannes Gräff. 2016. “The Neural Circuits of Innate Fear: Detection, Integration, Action, and Memorization.” *Learning & Memory (Cold Spring Harbor, N.Y.)* 23 (10). Cold Spring Harbor Laboratory Press: 544–55. doi:10.1101/lm.042812.116.
Sparkman, Nathan L, Rachel a Kohman, Anya K Garcia, and Gary W Boehm. 2005. “Peripheral Lipopolysaccharide Administration Impairs Two-Way Active Avoidance Conditioning in C57BL/6J Mice.” *Physiology & Behavior* 85 (3): 278–88. doi:10.1016/j.physbeh.2005.04.015.
Stäubli, U, D Chun, and G Lynch. 1998. “Time-Dependent Reversal of Long-Term Potentiation by an Integrin Antagonist.” *The Journal of Neuroscience : The Official Journal of the Society for Neuroscience* 18 (9). Society for Neuroscience: 3460–69. doi:10.1523/JNEUROSCI.18-09-03460.1998.
Staubli, U, P Vanderklish, and G Lynch. 1990. “An Inhibitor of Integrin Receptors Blocks Long-Term Potentiation.” *BEHAVIORAL AND NEURAL BIOLOGY*. Vol. 53. https://escholarship.org/uc/item/22r1x6rj.
Stegert, Mario R, Rastislav Tamaskovic, Samuel J Bichsel, Alexander Hergovich, and Brian a Hemmings. 2004. “Regulation of NDR2 Protein Kinase by Multi-Site Phosphorylation and the S100B Calcium-Binding Protein.” *The Journal of Biological Chemistry* 279 (22): 23806–12. doi:10.1074/jbc.M402472200.
Stork, Oliver, Alexander Zhdanov, Alexei Kudersky, Takeo Yoshikawa, Kunihiko Obata, and Hans-Christian Pape. 2004. “Neuronal Functions of the Novel Serine/Threonine Kinase Ndr2.” *The Journal of Biological Chemistry* 279 (44): 45773–81. doi:10.1074/jbc.M403552200.
Stryke, Doug, Michiko Kawamoto, Conrad C Huang, Susan J Johns, Leslie A King, Courtney A Harper, Elaine C Meng, et al. 2003. “BayGenomics: A Resource of Insertional Mutations in Mouse Embryonic Stem Cells.” *Nucleic Acids Research* 31 (1). Oxford University Press: 278–81. http://www.ncbi.nlm.nih.gov/pubmed/12520002.
Sugimura, Kaoru, Misato Yamamoto, Ryusuke Niwa, Daisuke Satoh, Satoshi Goto, Misako Taniguchi, Shigeo Hayashi, and Tadashi Uemura. 2003. “Distinct Developmental Modes and Lesion-Induced Reactions of Dendrites of Two Classes of Drosophila Sensory Neurons.” *Journal of Neuroscience* 23 (9). Society for Neuroscience: 3752–60.

doi:10.1523/JNEUROSCI.23-09-03752.2003.
Sukoff Rizzo, Stacey J., and Jacqueline N. Crawley. 2017. “Behavioral Phenotyping Assays for Genetic Mouse Models of Neurodevelopmental, Neurodegenerative, and Psychiatric Disorders.” *Annual Review of Animal Biosciences* 5 (1). Annual Reviews: 371–89. doi:10.1146/annurev-animal-022516-022754.
Tamaskovic, Rastislav, Samuel J Bichsel, Helene Rogniaux, Mario R Stegert, and Brian A Hemmings. 2003. “Mechanism of Ca2+-Mediated Regulation of NDR Protein Kinase through Autophosphorylation and Phosphorylation by an Upstream Kinase.” *The Journal of Biological Chemistry* 278 (9). American Society for Biochemistry and Molecular Biology: 6710–18. doi:10.1074/jbc.M210590200.
Tang, Fengyuan, Jason Gill, Xenia Ficht, Thomas Barthlott, Hauke Cornils, Debora Schmitz-Rohmer, Debby Hynx, et al. 2015. “The Kinases NDR1/2 Act Downstream of the Hippo HomologMST1 Tomediate Both Egress of Thymocytes from the Thymus and Lymphocyte Motility.” *Science Signaling* 8 (397): 1–13. doi:10.1126/scisignal.aab2425.
Teschler-Nicola, M, and W Killian. 1981. “Case Report 72: Mental Retardation, Unusual Facial Appearance, Abnormal Hair.” *Synd Ident* 7: 6–7.
Toji, Shingo, Norikazu Yabuta, Toshiya Hosomi, Souichi Nishihara, Toshiko Kobayashi, Susumu Suzuki, Katsuyuki Tamai, and Hiroshi Nojima. 2004. “The Centrosomal Protein Lats2 Is a Phosphorylation Target of Aurora-A Kinase.” *Genes to Cells* 9 (5). John Wiley & Sons, Ltd (10.1111): 383–97. doi:10.1111/j.1356-9597.2004.00732.x.
Tovote, Philip, Maria Soledad Esposito, Paolo Botta, Fabrice Chaudun, Jonathan P. Fadok, Milica Markovic, Steffen B.E. Wolff, et al. 2016. “Midbrain Circuits for Defensive Behaviour.” *Nature* 534 (7606). Nature Publishing Group: 206–12. doi:10.1038/nature17996.
Ultanir, Sila K, Nicholas T Hertz, Guangnan Li, Woo-Ping Ge, Alma L Burlingame, Samuel J Pleasure, Kevan M Shokat, Lily Yeh Jan, and Yuh-Nung Jan. 2012. “Chemical Genetic Identification of NDR1/2 Kinase Substrates AAK1 and Rabin8 Uncovers Their Roles in Dendrite Arborization and Spine Development.” *Neuron* 73 (6). Elsevier Inc.: 1127–42. doi:10.1016/j.neuron.2012.01.019.
Valsamis, Bridget, and Susanne Schmid. 2011. “Habituation and Prepulse Inhibition of Acoustic Startle in Rodents.” *Journal of Visualized Experiments : JoVE*, no. 55 (September). MyJoVE Corporation: e3446. doi:10.3791/3446.
Verde, F, D J Wiley, and P Nurse. 1998. “Fission Yeast Orb6, a Ser/Thr Protein Kinase Related to Mammalian Rho Kinase and Myotonic Dystrophy Kinase, Is Required for Maintenance of Cell Polarity and Coordinates Cell Morphogenesis with the Cell Cycle.” *Proceedings of the National Academy of Sciences of the United States of America* 95 (13). National Academy of Sciences: 7526–31. doi:10.1073/PNAS.95.13.7526.
Vogt-Eisele, Angela, Carola Krüger, Kerstin Duning, Daniela Weber, Robert Spoelgen, Claudia Pitzer, Christian Plaas, et al. 2014. “KIBRA (KIdney/BRAin Protein) Regulates Learning and Memory and Stabilizes Protein Kinase Mζ.” *Journal of Neurochemistry* 128 (5). NIH Public Access: 686–700. doi:10.1111/jnc.12480.
Walsh, Tom, Jon M. McClellan, Shane E. McCarthy, Anjené M. Addington, Sarah B. Pierce, Greg M. Cooper, Alex S. Nord, et al. 2008. “Rare Structural Variants Disrupt Multiple Genes in Neurodevelopmental Pathways in Schizophrenia.” *Science* 320 (5875): 539–43. doi:10.1126/science.1155174.
Wang, Xinjun, Chunzhao Zhang, Gábor Szábo, and Qian-Quan Sun. 2013. “Distribution of CaMKIIα Expression in the Brain in Vivo, Studied by CaMKIIα-GFP Mice.” *Brain Research* 1518 (June). NIH Public Access: 9–25. doi:10.1016/j.brainres.2013.04.042.

Wen, Mingyue, Xianwei Ma, Hong Cheng, Wei Jiang, Xiongfei Xu, Yi Zhang, Yan Zhang, et al. 2015. “Stk38 Protein Kinase Preferentially Inhibits TLR9-Activated Inflammatory Responses by Promoting MEKK2 Ubiquitination in Macrophages.” *Nature Communications* 6 (1). Nature Publishing Group: 7167. doi:10.1038/ncomms8167.

Wilson, M., and B. McNaughton. 1994. “Reactivation of Hippocampal Ensemble Memories during Sleep.” *Science* 265 (5172): 676–79. doi:10.1126/science.8036517.

Wisden, W., M.L. Errington, S. Williams, S.B. Dunnett, C. Waters, D. Hitchcock, G. Evan, T.V.P. Bliss, and S.P Hunt. 1990. “Differential Expression of Immediate Early Genes in the Hippocampus and Spinal Cord.” *Neuron* 4 (4): 603–14. doi:10.1016/0896-6273(90)90118-Y.

Wu, Shian, Jianbin Huang, Jixin Dong, and Duojia Pan. 2003. “Hippo Encodes a Ste-20 Family Protein Kinase That Restricts Cell Proliferation and Promotes Apoptosis in Conjunction with Salvador and Warts.” *Cell* 114 (4). Elsevier: 445–56. doi:10.1016/S0092-8674(03)00549-X.

Yin, Feng, Jianzhong Yu, Yonggang Zheng, Qian Chen, Nailing Zhang, and Duojia Pan. 2013. “Spatial Organization of Hippo Signaling at the Plasma Membrane Mediated by the Tumor Suppressor Merlin/NF2.” *Cell* 154 (6). Elsevier: 1342–55. doi:10.1016/j.cell.2013.08.025.

Yu, F.-X., and K.-L. Guan. 2013. “The Hippo Pathway: Regulators and Regulations.” *Genes & Development* 27 (4). Cold Spring Harbor Laboratory Press: 355–71. doi:10.1101/gad.210773.112.

Yu, Fa-Xing, Bin Zhao, and Kun-Liang Guan. 2015. “Hippo Pathway in Organ Size Control, Tissue Homeostasis, and Cancer.” *Cell* 163 (4). Elsevier: 811–28. doi:10.1016/j.cell.2015.10.044.

Zhang, Yan-Feng, Shu-Lei Li, Tian-Qing Xiong, Li-Bin Yang, Yong-Nan Li, Bai-Hong Tan, Qun Liu, and Yan-Chao li. 2014. “The Rearrangement of Filamentous Actin in Mossy Fiber Synapses in Pentylenetetrazol-Kindled C57BL/6 Mice.” *Epilepsy Research* 108 (1). Elsevier: 20–28. doi:10.1016/J.EPLEPSYRES.2013.10.019.

Zhao, Shanting, Daniel Studer, Xuejun Chai, Werner Graber, Nils Brose, Sigrun Nestel, Christina Young, E Patricia Rodriguez, Kurt Saetzler, and Michael Frotscher. 2012. “Structural Plasticity of Spines at Giant Mossy Fiber Synapses.” *Frontiers in Neural Circuits* 6. Frontiers Media SA: 103. doi:10.3389/fncir.2012.00103.

Declaration of Honor

I hereby declare that I prepared this thesis without impermissible help of third parties and that none other than the indicated tools have been used; all sources of information are clearly marked, including my own publications.

In particular I have not consciously:
• Fabricated data or rejected undesired results
• Misused statistical methods with the aim of drawing other conclusions than those warranted by the available data
• Plagiarized external data or publications
• Presented the results of other researchers in a distorted way

I am aware that violations of copyright may lead to injunction and damage claims of the author and also to prosecution by the law enforcement authorities.
I hereby agree that the thesis may be reviewed for plagiarism by mean of electronic data processing.

This work has not yet been submitted as a doctoral thesis in the same or a similar form in Germany or in any other country. It has not yet been published as a whole.

Magdeburg, 28.01.2019

Deniz Ashan Madencioglu Kul